The relevance of the silica metabolizing enzyme silicatein-α to biomineralization and the formation of biogenic silica in siliceous sponges

Dissertation
zur Erlangung des Grades
"Doktor der Naturwissenschaften"
am Fachbereich Biologie
der Johannes Gutenberg-Universität
in Mainz

vorgelegt von
Ute Schloßmacher

Mainz, 2012

Dekan:

Erster Berichterstatter:

Zweiter Berichterstatter:

Tag der mündlichen Prüfung: 18.07.2012

This thesis is based on the following 4 research articles, which are presented as chapters 2 to 5.

Müller W.E.G., Boreiko A., Schloßmacher U., Wang X.H., Tahir M.N., Tremel W., Brandt D., Kaandorp J.A. & Schröder H.C. (2007a) Fractal-related assembly of the axial filament in the demosponge *Suberites domuncula*: relevance to biomineralization and the formation of biogenic silica. *Biomaterials* 28: 4501-4511

Müller W.E.G., Boreiko A., Schloßmacher U., Wang X.H., Eckert C., Kropf K., Li J. & Schröder H.C. (2008b) Identification of a silicatein(-related) protease in the giant spicules of the deep-sea hexactinellid Monorhaphis chuni. *J Exp Biol* 211, 300-309.

Müller W.E.G., Schloßmacher U., Wang X.H., Boreiko A., Brandt D., Wolf S.E., Tremel W. & Schröder H.C. (2008g) Poly(silicate)-metabolizing silicatein in siliceous spicules and silicasomes of demosponges comprises dual enzymatic activities (silica-polymerase and silica-esterase). *FEBS J* 275, 362–370.

Schloßmacher U., Wiens M., Schröder H.C., Wang X.H., Jochum K.P. & Müller W.E.G. (2011) Silintaphin-1: Interaction with silicatein during structure guiding biosilica formation. *FEBS J* 278, 1145-1155.

Chapter 1

1.1 Porifera

Der Tierstamm der Schwämme (Porifera) wurde aufgrund seiner sessilen Lebensweise und des relativ ungegliederten, „schwammigen“ Körpers lange Zeit für Pflanzen gehalten und erst 1766 als Tiere erkannt (Wehner und Gehring, 1995).
Ihr Ursprung wurde aufgrund paläontologischer, morphologischer und embryologischer Studien auf einen Zeitpunkt vor 550 Millionen Jahren zurückdatiert (Westheide und Rieger, 1996). Fortschritte in der Evolutionsforschung durch molekularbiologische Untersuchungen lassen sogar auf ein Alter von 800 Millionen Jahren schließen (Müller et al., 2003a). Zunächst wurden sie als Parazoa den Metazoa gegenübergestellt (Müller, 2001) oder zu den Protozoa gezählt (Spencer, 1864) bevor Haeckel sie auf Grund ontogenetischer Untersuchungen 1896 den Metazoa zuordnete. Mittels diverser molekularbiologischer Techniken war es möglich, die Porifera phylogenetisch den Metazoa zuzuordnen und nachzuweisen, dass sie monophyletischen Ursprungs sind (Reitner und Mehl, 1995; Cavalier-Smith et al., 1996; Borchiellini et al., 2001; Müller, 1995) und damit auf einen gemeinsamen Vorfahren (Urmetazoa) zurückgehen (Müller et al., 2001). Paläontologische Untersuchungen der Porifera zeigten, dass sie die ältesten multizellularen Organismen sind und damit die ursprünglichsten Metazoen darstellen (Wiens et al., 2004), weswegen sie auch als „lebende Fossilien“ bezeichnet werden (Müller et al., 1998). Neue Gene entstehen hauptsächlich durch Genduplikationen, die in phylogenetisch älteren Taxa als Vorstufen oder Teilstücke wiederzufinden sind. Dies macht die Porifera zu äußerst interessanten Forschungsobjekten im Bereich der Aufklärung molekularbiologischer und biochemischer Vorgänge. Heute sind ca. 8000 rezente Arten bekannt, von denen nur rund 150 (Spongillidae) in limnischen Biotopen vorkommen (Müller et al., 2003a). Die Mehrzahl der Schwämme ist marin und weltweit verbreitet, sowohl im Flachwasser als auch in den tiefsten Ozeangräben anzutreffen (Westheide und Rieger, 1996; Campbell, 2005). Sie weisen ein hohes Maß an Diversität in Größe (1cm bis 3m), Morphologie und Farbgebung auf (Storch und Welsch, 1994).
Schwämme sind sessile Strudler, die mit Hilfe von begeißelten Choanozyten einen Wasserstrom erzeugen, der Wasser durch mikroskopisch kleine Öffnungen, die sogenannten Ostien, einstrudeln lässt, welches weiter über Känale und

Geißelkammern fließt und letztlich den Schwamm durch das Osculum verlässt (Westheide und Rieger, 1996). Die Filtrieraktivität liefert dem Schwamm Nahrungspartikel, Plankton und organische Makromoleküle, welche über Phagozytose aufgenommen und intrazellulär verdaut werden. Der ständige Wasserstrom liefert dem Schwamm neben Nahrung auch Sauerstoff und dient der Defäkation, die als Exocytose an den Kanalwänden durchgeführt wird. Zusätzlich besitzen viele Schwämme lebende Mikrosymbionten (Bakterien, Cyanobakterien, einzellige Grünalgen), die zur Ernährung beitragen. Im Gegensatz zu den Schwämmen nehmen diese keine partikulären, sondern gelöste Stoffe auf. Außerdem beliefern photoautotrophe Symbionten wie Cyanobakterien und Grünalgen den Schwamm mit photosynthetisch hergestellten organischen Makromolekülen. Die Geschwindigkeit des Wasserdurchstroms wird durch die kontraktilen Pinacozyten regulierbar, die den Kanaldurchmesser verändern können. Außerdem beeinflusst wesentlich der mechanische Strömungsdruck des Außenmediums den Transport des Wassers durch den Schwammkörper. Die Filtrierleistung von Schwämmen ist beachtlich, es wurden Durchflussraten von mehr als 1 Tonne Wasser pro Tag und kg Schwamm berechnet (Müller et al., 2004a).

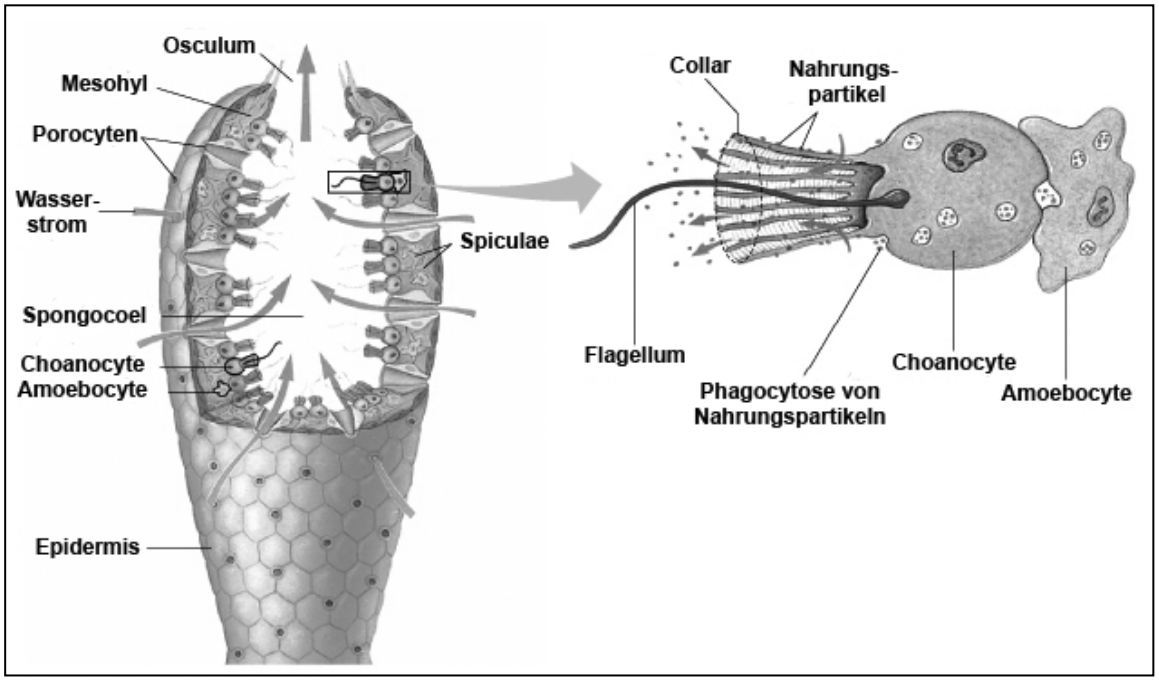

Abb. 1.1.: Anatomie eines Schwammes. Verändert nach Campbell, N. A., Reece, J. B., "Biology" 7th edition 2005

1.2 Aufbau der Porifera

Die Porifera besitzen zwei Zellschichten, das äußere Pinacoderm und das innere Choanoderm, welche durch eine bindegewebsartige von Poren durchzogene Zellschicht, das Mesohyl, voneinander getrennt werden. Das Pinacoderm besteht aus einer sehr dünnen Schicht (ca. 1 µm) aus flachen, plattenförmigen Pinacocyten. Je nach Lage im Schwammkörper unterscheidet man drei Typen von Pinacocyten. Die Exopinacocyten bilden das äußere Exopinacoderm, die Basopinacocyten setzen sich zum Basopinacoderm zusammen, das dem Schwamm zur Anheftung an das Substrat dient, und die Endopinacocyten bilden das Endopinacoderm, das die Kanäle auskleidet (Müller et al., 2004d). Das aus Choanocyten gebildete, innen gelegene Choanoderm ermöglicht dem Schwamm eine gerichtete Bewegung des Wassers durch den Körper. Choanocyten oder Kragengeißelzellen sind mit einer langen Geißel ausgestattet, die jeweils zwei flügelartige Anhängsel tragen und an der Basis von einem trichterförmigen Mikrovilli-Kragen umgeben sind. Alle Zellen sind über ein sehr komplexes Zell-Zell-Adhäsionssystem miteinander verbunden (Schütze et al., 2001), in manchen Spezies stehen sie zusätzlich durch so genannte „less complex junctions“ miteinander in Verbindung (Simpson et al., 1984). Im Mesohyl, das den Hauptteil des Schwammkörpers ausmacht, sind mehrere Zelltypen mit unterschiedlichen Funktionen anzutreffen. Ein Großteil der Zellen ist in der Lage sich mittels Ausbildung von Pseudopodien aktiv zu bewegen (Amoebocyten) und ihre Position im Zellverbund zu verändern. Diese großen undifferenzierten Archaeocyten sind totipotente Zellen, die zahlreiche Mitosen durchlaufen und sich zu jedem anderen Zelltyp differenzieren können. Sie sind zur Phagocytose und dem Transport von Nahrungspartikeln, die sie von den Choanocyten aufnehmen, befähigt. Die intrazelluläre Verdauung ist einer der größten Unterschiede zwischen Porifera und Eumetazoa. Neben den Archaeocyten lassen sich drei Zellgruppen im Mesohyl unterscheiden: Zellen, die das Stützskelett produzieren, kontraktile Zellen und Zellen mit Einschlüssen. An der Ausbildung skelettartiger Strukturen sind Lophocyten, Spongio- und Sklerocyten beteiligt. Der Bildungsort der Spicula sind die Sklerocyten, eine abgewandelte Form von Amoebocyten.

Fast alle Schwämme bilden ein hartes Skelett, bestehend aus vielen, einzelnen oder verbundenen Nadeln, den sogenannten Spiculae. Deren Form, Material und Lokalisation im Schwamm sind artspezifisch und teilen die Schwämme

in drei Gruppen ein; die Calcerea (Kalkschwämme), die Demospongiae (Hornkieselschwämme) und die Hexactinellida (Glasschwämme).

Bereits 1825 beschrieb J.E. Gray, dass die Spiculae einiger Schwämme aus Silikat bestehen. 1885 teilte Schulze die silikatbildenden Schwämme in die zwei Klassen Hexactinellida und Demospongiae ein. Die Demospongiae besitzen ein- oder vierachsige Spiculae, während die Hexactinelliden immer drei- oder sechsachsige Spiculae aufweisen. Die Spiculae beider Klassen besitzen einen zentralen Axialkanal in dem sich das sogenannte Axialfilament befindet. Im Spiculaquerschnitt findet man in den Demospongiae ein drei- bzw. sechseckiges Axialfilament, während das der Hexactinelliden quadratisch ist. Der Querschnitt des Axialfilaments weist eine Größe von ca. 1 µm auf, während die Länge abhängig von der Größe der Spicula ist. Die Spiculae werden traditionell in Megaskleren, die eine Größe von mehr als 10 µm haben und Mikroskleren, deren Länge unter 10 µm liegt, eingeteilt (Uriz et al., 2006). Die Silikatschicht um den Axialkanal herum ist im phylogenetisch ältesten Taxon (Kruse et al., 1998), den Hexactinellida, lamellar aufgebaut (Abb. 1.2 F,G), während die Silikatschicht in den Demospongiae (Abb. 1.2 B,C) aus einem Block zu bestehen scheint (Minchin, 1909). Im Gegensatz zu den pflanzlichen Phytolithen oder zu den Frusteln (Zellhüllen) der Diatomeen, die Biosilikat aus einer supergesättigten Lösung an einer organischen Matrize ausscheiden und dadurch dreidimensionale komplexe Nano- und Mikrostrukturen bilden können (Müller et al., 2003a), werden die silikathaltigen Spiculae der Schwämme in einem Silikat untersättigten Zellmilieu gebildet. Diese Eigenschaft erlaubt es den Schwämmen in den heutigen silikatarmen aquatischen Systemen, die nur noch ca. 5 µM Silikat (Maldonado et al., 2005) enthalten, Strukturen aus Silikat zu bilden.

Bereits Schulze (1904) erkannte, dass die Spiculae der Hexactinelliden neben dem anorganischen Silikat auch organische Komponenten beinhalten. Um das von Organismen hergestellte Silikat vom amorphen anorganischen Silikat (Sandford et al., 2003), welches durch Präzipitation aus silikathaltigen Lösungen oder kolloidalen Suspensionen in Abwesenheit organischer Komponenten entsteht, zu unterscheiden, wird das biologisch entstandene Silikat als Biosilikat bezeichnet. Schon vor 100 Jahren wurde festgestellt, dass die Nadeln in spezialisierten Zellen, den Sklerocyten synthetisiert werden (Minchin et al., 1909) (Abb. 1.2 D). Die Nadelbildung startet intrazellulär und wird nach dem Ausschleusen der Spicula in den extrazellulären Raum (Imsiecke et al., 1995; Müller et al., 2005a), in das Mesohyl, abgeschlossen.

Während angenommen wurde, dass das Axialfilament der Nadel die entscheidende Struktur der Anfangsphase der Spiculabildung ist (Uriz et al., 2006), blieb es unklar, wie die Nadel ihre endgültige Form und Größe im Mesohyl erreicht.

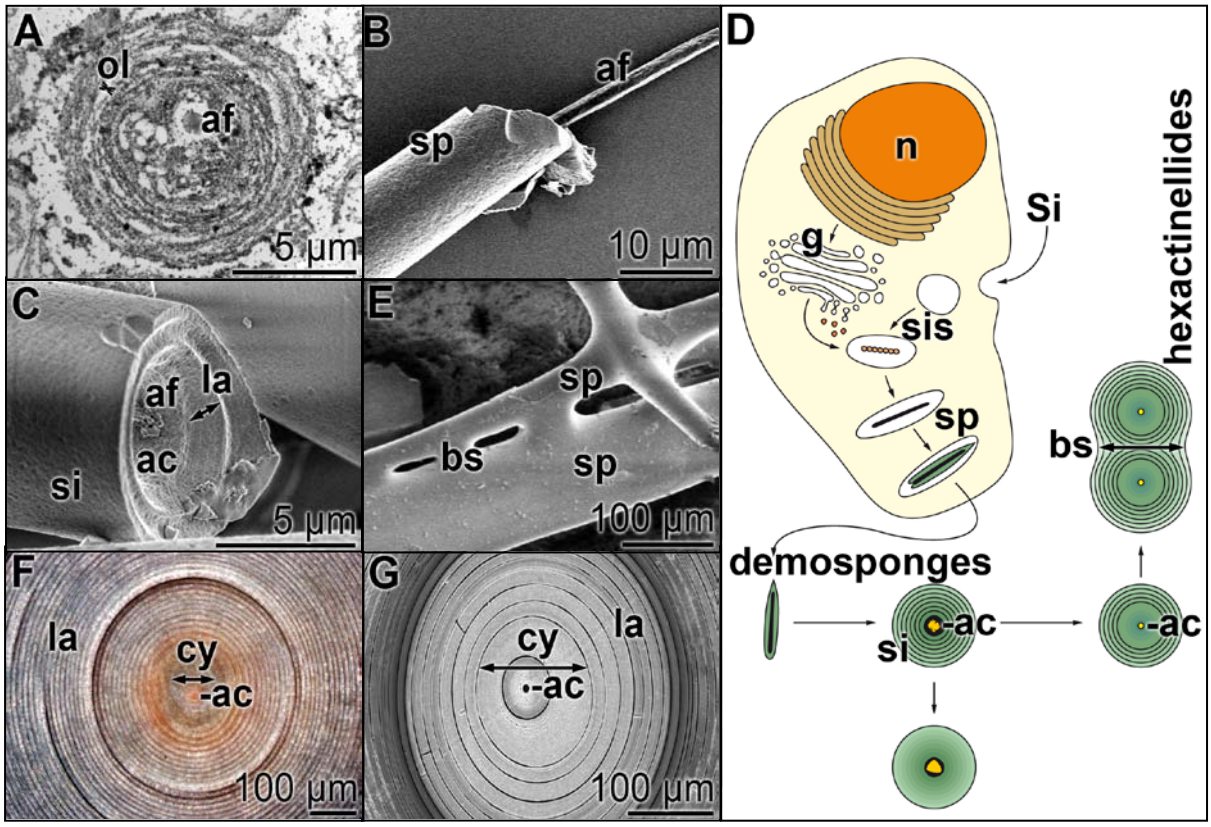

Abb. 1.2: Demospongien und Hexactinelliden Spiculae. (**A**-**C**) *S. domuncula* Spiculae. (A) Eine junge sich entwickelnde Spicula, um deren Axialfilament (af) organische Schichten (ol) konzentrisch angeordnet sind; TEM. Diese treten durch Immunogoldfäbung mit Antikörpern gegen Silicatein und Galektin hervor. (B) Bruch durch eine Spicula (sp), deren Axialfilament (af) aus dem Axialkanal herausschaut; SEM. (C) Blick auf einen Spicula-bruch; SEM. In der Mitte des Axialkanals (ac) befindet sich das Axialfilament (af). Der Axialkanal (ac) ist von einer Silikathülle umgeben (si). Durch Behandlung der Spiculae mit HF-Dampf, wird das Silikat teilweise aufgelöst und einzelne Lamellen (la) werden sichtbar. (**D**) Schematische Darstellung der Nadelbildung in Demospongien und Hexactinelliden. Silikat (si) wird über einen $Na^{+}/HCO3^{-}[Si(OH)_4]$ Co-Transporter in die Zellen aufgenommen und in den Silikasomen (sis) gespeichert. Nachdem die erste Silikatschicht gebildet ist, wird die Spicula in den extrazellulären Raum geschleust. In Demospongien wachsen die Nadeln durch appositionelles Wachstum. Die einzelnen Lamellen (la) fusionieren (biosintern; bs) zu einer Silikathülle. In Hexactinelliden fusionieren nur die inneren Lamellen zum Axialzylinder, während die äußeren Lamellen separiert bleiben. Bei einigen Hexactinelliden-Familien fusionieren (bs) individuelle Nadeln miteinander. (**E**) Bio-sintern (bs) zwischen zwei Spicula (sp) (*Euplectella aspergillum*); SEM. (**F** und **G**) Querschnitt durch eine Pfahlnadel von *Monoraphis chuni*. Um den Axialkanal (ac) herum befindet sich der Axialzylinder (cy), der wiederum von einzelnen Lamellen (la) umgeben ist.

1.3 Potentielle Funktion der Nadeln: ein einzigartiges Nervensystem?

Die Organisation der Nadeln innerhalb des Schwammorganismus ist genetisch fixiert. Das Spiculaskelett der Schwämme ist architektonisch komplex und in einer funktionellen Weise effizient organisiert. Wie bereits im Challenger Report (Ridley und Dendy, 1887) beschrieben, gibt es im Wesentlichen zwei Arten von genetisch determinierten Organisationen der Nadeln in Demospongien. Es gibt netzförmig und strahlenförmig angelegte Muster. In Hexactinelliden, z. B. in *Euplectella aspergillum,* ist die Interaktion zwischen den Nadeln noch deutlicher zu sehen, da hier die einzelnen Nadeln zu einer kontinuierlichen Gitterstruktur mit mehreren Ebenen (Müller et al., 2009c) verschmelzen. Dieses enge Zusammenspiel der Nadeln bietet dem Schwamm nicht nur die biologische Funktion als Stützsklett und Fraßschutz, sondern könnte im Idealfall auch eine Lichtleiterfunktion übernehmen (Cattaneo-Vietti et al., 1996; Aizenberg et al., 2004) Da Schwämme kein Nervensystem besitzen, könnten die Spiculae als Nervensystemersatz dienen (Müller et al., 2004).
Für die ersten Untersuchungen wurden die Schwammarten *Hyalonema siebold* und später *Monoraphis chuni* (Hexactinellida) (Wang et al., 2009c) gewählt, die durch ihre extrem lange Nadel, die den Stiel der Tiere bildet, charakterisiert sind. Das erste überraschende Ergebnis war, dass Licht von 400 nm bis 1600 nm durch die Nadeln übertragen werden kann. Licht unter 600 nm und über 1310 nm wurde nicht geleitet, was von der Filterleistung eines kombinierten Hoch / Tiefpassfilters bekannt ist. Es ist erstaunlich, dass die fast 3 m lange basale Nadel von *M. chuni* Licht über diese Distanz übertragen kann, ohne einen erheblichen Verlust an Lichtintensität einzubüßen (Abb. 1.3).

1.3.1 Licht erzeugender Komplex: Luciferase-Luciferin:

Biolumineszenz ist ein weit verbreitetes Phänomen in der Natur, eine Reaktion, bei der die freiwerdende Energie in Form von Licht (Emission) abgeben wird. Am besten untersucht ist bisher das Biolumineszenzsystem des Glühwürmchens *Photinus pyralis* (Strehler und McElroy, 1949), welches mit einem Luciferin-Luciferase-Komplex ausgestattet ist, dessen Spektrum in einem Bereich von 520 nm bis 620 nm liegt (Müller et al., 2009h). Die Luciferase kann neben der Lichtreaktion auch effizient Coenzym-A an das Luciferinmolekül kondensieren und erfüllt damit die Funktion einer klassischen Fettsäure-CoA-Synthetase.

Die EST-Datenbank des Schwammes *S. domuncula* wurde nach Polypeptiden mit den charakteristischen Domänen der Luciferase, z.B. Acetyl-Coenzym-A-Synthetase (Müller et al., 2009h) durchsucht und die klonierte cDNA zeigte die höchste Sequenzähnlichkeit mit der Luciferase aus Photinus pyralis (Müller et al, 2009h). Es konnte gezeigt werden, dass sowohl der Gewebeextrakt als auch die rekombinante Luciferase bioaktiv ist und *in vitro* Biolumineszenzaktivität zeigt. Das Expressionsniveau des Luciferase-Gens wird stark herunterreguliert, wenn Primmorphe von *S. domuncula* unter Lichteinfluß gehalten werden. Das Emissionsspektrum der *S. domuncula* Luciferase zeigte ein Maximum bei 548 nm und einen kleineren Peak bei 590 nm (pH 8,0). Dieses Biolumineszenz-Emissionsspektrum überschneidet sich mit dem Transmissionsspektrum der Hexactinellidennadeln. Ebenso sind in *S. domuncula* die Spiculae unmittelbar unter der Oberflächenzellschicht in einem Palisadenmuster angeordnet (Müller et al., 2010). Die spitzen Enden der Tylostylen zeigen in die Mitte der Tiere, während die Köpfe zur Oberfläche hin gerichtet sind. Dies könnte darauf hindeuten, dass die Nadeln in Schwämmen auch *in vivo* als Lichtleiter für biogenes Licht dienen. Diese These kann durch die vorherrschenden Lichtverhältnisse des Lebensraums von *S. domuncula* unterstützt werden. Die Tiere sind ausschließlich in seichtem Wasser (20-30 m) zu finden. Im Gegensatz zur offenen See wird das Licht in diesen Küstengewässern bevorzugt innerhalb eines kürzeren Wellenlängenbereiches (etwa 500 nm) übertragen, was wiederum dem Biolumineszenz-Emissionsspektrum der *S. domuncula* Luciferase entspricht. Zu berücksichtigten sind auch die kugeligen Köpfe der *S. domuncula* Spiculae, die das Licht wie konvexe Linsen konzentrieren könnten, und das durch Carotinoide (Spektrummaxima 400 nm und 430 nm) roteingefärbte Gewebe. Damit lässt sich ableiten, dass die Nadeln an der Oberfläche des Schwammes das schwache Licht der Umgebung sammeln und über die Nadeln zu einem möglichen photorezeptorischen System im Inneren des Tieres leiten.

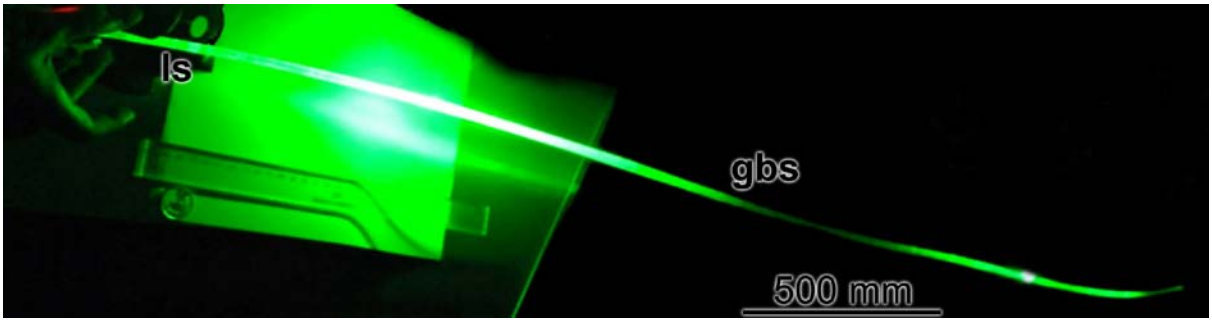

Abb. 1.3: Die Pfahlnadel (gbs) von *M. chuni* agiert als Lichtwellenleiter. Das Licht der Laserquelle (Ls) wird über die gesamte Nadel (3m) geleitet.

1.3.2 *Lichtdetektionssystem: Cryptochrom*

Überraschend war die Beobachtung, dass *S. domuncula* Lichtblitze generieren kann (Wiens et al, 2010h.). Dazu wurde ein Schwamm ohne Einsiedlerkrebs in einem Becherglas mit Meerwasser unter ständiger Belüftung dunkel-adaptiert. Nach der Ablation der kortikalen Zellschichten begannen die Schwammproben mit einer Lag-Phase von 23-33 Stunden Licht zu emittieren. Derzeit ist es nur möglich, über die Funktion des Blinkens während der Regeneration von beschädigten Geweben zu spekulieren. In Korallen, die auf Licht reagieren, scheint z.B. ein Cryptochrom-System an der Synchronisation der Laichzeit beteiligt zu sein (Levy et al., 2007), was gleichzeitig darauf hindeutet, dass das Cryptochrom-System der Korallen deren zirkadianen Rhythmus steuern könnte. Nach Entdeckung des Cryptochroms in Korallen (Levy et al., 2007) wurden die cDNA-Banken von Demospongien (*S. domuncula*) und Hexactinelliden (*C. meyeri*) nach homologen Schwammproteinen durchsucht (Müller et al., 2010h). Wie im Korallen-Modell (Levy et al., 2007) wird auch die Cryptochromexpression in Schwämmen durch Lichteinfluß gesteuert (Müller et al., 2010). Dabei zeigte sich, dass sich die Cryptochromexpression nach Belichtung (Lichtquellenbereich 330-900 nm und 700-1100 nm, Müller et al., 2010h) des Schwammes auf die Oberflächenzone des Tieres beschränkt. Man geht davon aus, dass das photoaktive Protein in Kompartimenten im Cortex (äußere Gewebeschicht) des Tieres vorliegt und dessen Genexpression lichtabhängig ist. RNA-Expression-Analysen zeigen, dass Schwammproben nach Belichtung mit einer bis zu 3,5-fach erhöhten Expression von Cryptochrom reagieren. Ebenso wie die

Schwammluciferase ist auch das Schwammcryptochrom helladaptiert (Müller et al., 2009h).

Im Gegensatz zu Korallen (Levy et al., 2007) erfolgt die lichtinduzierte Reaktion in Schwämmen unabhängig vom Spektralbereich. Da das Cryptochrom vor allem rund um die Nadeln lokalisiert ist, können die Skelettelemente als Wellenleiter des Umgebungslichtes dienen. So könnten Nadeln an der Oberfläche des Tieres als Sammler das Licht an Cryptochrom, als vermeintlichen photosensorischen Rezeptor senden. Gleichzeitig könnte intrazellulär erzeugtes Licht (Luziferase-vermittelte) über das gleiche optische System gesammelt und übermittelt werden. In beiden Fällen ist das Cryptochrom der Lichtphotorezeptor.

1.4 Biosilikat: Schwammenzyme und ihre assoziierten Proteine

1.4.1 Silicateine

Ein großer Durchbruch des Verständnisses der Spiculabildung erfolgte durch die Entdeckung, dass die Axialfilamente der Spicula von Demospongien (Cha et al., 1999) und Hexactinelliden (Müller et al., 2008d) hauptsächlich aus einem Enzym bestehen, dem sogenannten Silicatein. Der Name des Proteins wird zusammengesetzt aus den Begriffen „silica“ und „proteins“, da es die Biosilikatbildung während des Axial- und Radialwachstums katalysiert. Nach dieser ersten wichtigen Entdeckung wurde Schritt für Schritt herausgearbeitet, dass Silicatein das Schlüsselmolekül der Biosilikatbildung in Schwämmen ist (Morse 1999; Brutchey and Morse, 2008; Müller et al., 2009d). Dies konnte sowohl *in vitro* (Shimizu et al., 1998; Müller et al., 2008g) wie auch *in vivo* (Schloßmacher et al., 2011) unter physiologischen Bedingungen dargestellt werden.

Die Silicateine wurden zuerst aus dem Axialfilament des Schwammes *Tethya aurantium* isoliert und durch proteinbiochemische und molekularbiologische Methoden wie SDS-Page und Edmann-Abbau mit anschließender Klonierung und Analyse der Sequenz charakterisiert (Shimizu et al., 1998). Die Axialfilamente bei *Tethya aurantium* sind aus drei ähnlichen Protein-Untereinheiten, genannt Silicatein-α (29 kDa), -β (28 kDa) und -γ (27 kDa), in regelmäßiger, sich wiederholender Struktur im Verhältnis α:β:γ = 12:6:1 zusammengesetzt (Shimizu et al.; 1998), wobei Silicatein-α mengenmäßig den größten Ante il darstellt. Im Schwamm *Suberites domuncula* besitzen die Silicateine der Spiculae eine molekulare Masse von 24 –

29 kDa (Krasko et al., 2000; Müller et al., 2005a). Mittels Western Blot mit anti-Silicatein-Antikörpern konnte gezeigt werden, dass außer den 24/29 kDa Silicateinen noch eine 33 kDa Form im *Suberites domuncula* Gewebeextrakt existiert (Müller et al., 2005a). Während man im Axialkanal nur das reife Silicatein (24-29 kDa) nachweisen kann, findet man das 33 kDa große Pro-Silicatein-α im extrazellulären Raum (Müller et al., 2005a). Dort findet das appositionelle, radiale Wachstum der Nadeln statt, welches durch Silicatein-α katalysiert wird. Nach einer Modellvorstellung bindet das pro-Silicatein-α im extrazellulären Raum an die Oberfläche der wachsenden Nadel an und wird dort zum reifen Enzym prozessiert (Müller et al., 2005a).

In den marinen Schwämmen *Tethya aurantium* (Shimizu et al., 1998) und *Suberites domuncula* (Krasko et al., 2000; Schröder et al., 2005a) konnten bisher nur zwei Isoformen, die α- und β- Silicatein-Isoform identifiziert und kloniert werden. Süßwasserschwämme scheinen nur Isoformen der Silicatein-α -Gruppe auszubilden (Wiens et al., 2009a). Die Silicateine sind Mitglieder der papainähnlichen Cysteinprotease-Superfamilie und sind am nächsten verwandt mit der Familie der Cathepsine (Shimizu et al., 1998; Weaver und Morse, 2003). Das erste Schwammcathepsin wurde in dem Demosponge *Geodia cydonium* identifiziert und kloniert (Krasko et al., 1997).

Zur Analyse der Silicateinsequenz können mittlerweile über 85 Silicatein cDNA Sequenzen aus der Schwamm-cDNA-Bank herangezogen werden. Da es sich hier meist um vollständig sequenzierte Silicateine handelt, konnte gezeigt werden, dass die abgeleiteten Proteine eine hohe Sequenzähnlichkeit aufweisen (Wiens et al., 2009a). Die Silicateine durchlaufen posttranslationale Modifikationen, die bisher am Silicatein-α von *Suberites domuncula* (Krasko et al., 2000; Müller et al., 2005a; Abb. 1.4) am besten untersucht wurden.

Strukturell besteht das Silicatein-α bei *Suberites domuncula* aus 331 Aminosäuren, mit einem Signalpeptid am N-terminalen Ende, das sich von Aminosäure$(As)_{1\text{-}17}$ der Proteinsequenz erstreckt. Das errechnete Molekulargewicht des primären Translationsproduktes besitzt eine Größe von 34,6 kDa und einen isoelektrischen Punkt (pI) von 5.95. Zunächst durch Sequenzvergleich und anschließende experimentelle Analyse wurde die Prozessierungsschnittstelle zwischen dem Propeptidsegment (AS_{18}-AS_{112}) und dem reifen Protein (AS_{113}-As_{330}) des Silicateins von *Petrosia ficiformis* (Pozzolini et al., 2004) als

ProLeuGln↓AspTyrPro identifiziert. Das Propeptid wird weiter zum reifen Protein mit 23 kDa prozessiert und dabei schrittweise phosphoryliert (Müller et al., 2005). Das reife Enzym, ohne das Propeptid, hat ein Molekulargewicht von 18,466 kDa mit einem isoelektrischen Punkt von 4,97. Ebenso wie die Cathepsine enthält Silicatein-α sechs Cysteinreste, die an der Bildung intramolekularer Disulfidbrücken beteiligt sind (Krasko et al., 2000; Armirotti et al., 2009). Das katalytische Zentrum der Silicateine entspricht dem der Cathepsine und unterscheidet sich nur in einer Position (Shimizu et al., 1998). Die katalytische Triade der Silicateine besteht aus den drei Aminosäuren Serin (in *S. domuncula* As_{138}), Histidin (As_{277}) und Asparaginsäure (As_{350}). Die Aminosäure Serin ist bei den Cathepsinen gegen Cystein ausgetauscht. Zhou et al. (1999) konnte experimentell zeigen, dass die Aminosäuren Serin und Histidin eine zentrale Rolle in der silicateinvermittelten Polykondensation spielen.

Im reifen Silicatein-α wurden fünf Phosphorylierungsstellen, zwei potentielle Proteinkinase C– (As_{227} und As_{267}) und drei Caseinkinase-Phosphorylierungsstellen (As_{160}, As_{230} und As_{232}) zunächst vorhergesagt (Krasko et al., 2000) und anschließend bewiesen (Müller et al., 2005a) (Abb. 1.4). 2-D - Gelelektrophorese mit vorausgegangener isoelektrischer Fokussierung des Axialfilamentextraktes ergab, dass Silicatein-α in 5 Phosphorylierungsformen mit den folgenden pI-Werten: 5.5, 4.8, 4.6, 4.5 und 4.3 vorkommt. Die Verschiebung von ca. 0,2 pH-Wert-Einheiten entspricht jeweils einer Phosphorylierungsstelle.

Im Vergleich zu den Cathepsinen besitzen die Silicatein-α-Moleküle eine Anhäufung der polaren Aminosäure Serin, sogenannte Serin-Cluster. In den Demospongien *T. aurantium* und *S. domuncula* dehnt sich diese Region über 8 Aminosäuren (6 Serine) aus, während in Hexactinelliden z.B. in *C. meyeri* sich dieses Serinsegment über 13 Aminosäuren ($As_{145-158}$) erstreckt (Abb. 1.4). Verblüffenderweise besitzen die Hexactinelliden ein zweites “Hexactinelliden-spezifisches“ Serincluster zwischen As_{169} und As_{173} (Müller et al., 2008c). Diese beiden Cluster flankieren den Histidinrest des aktiven Zentrums in *C. meyeri*. Man nimmt an, dass die Serin-Cluster an der Bindung des Silikatsubstrates beteiligt sind (Lobel et al., 1996; Müller et al., 2008c).

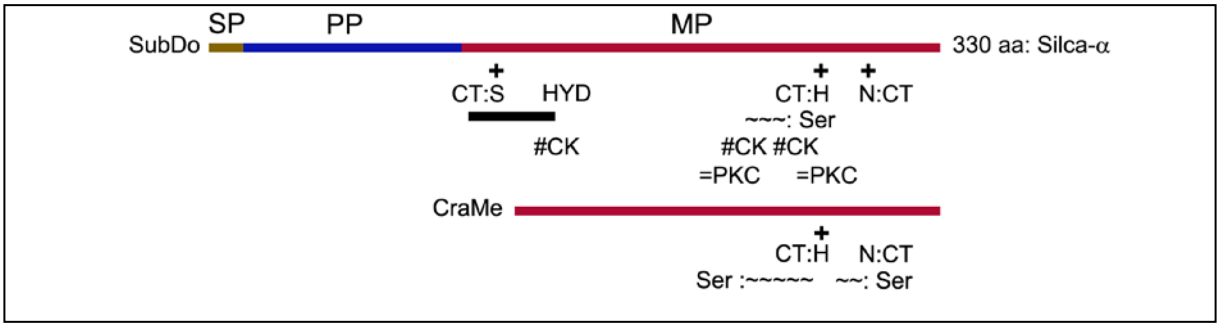

Abb. 1.4: Die Silicateinsequenz in *S. domuncula* (SubDo) umfasst das Signalpeptid (SP), das Pro-Peptid (PP) und das reife, enzymatisch aktive Silicatein (MP). Das katalytische Zentrum (CT) besteht aus den drei Aminosäuren Serin (CT:S), Histidin (CT:H) und Asparagin (CT:N). Vor dem Histidin erstreckt sich ein Serin-reicher Abschnitt (Ser~~). Darüber hinaus besitzt die Sequenz fünf Phosphorylierungsstellen, drei Caseinkinase- [CK] und zwei Proteinkinase C [PKC] -Phosphorylierungsstellen. Nach Prozessierung zum reifen Enzym liegt ein hydrophober Aminosäureabschnitt (HYD) exponiert vor. Vom Hexactinellid *C. meyeri* (CraMe) konnte bisher nur ein Fragment der cDNA kloniert werden, das die beiden Aminosäuren Histidin (CT:H) und Asparagin (CT:N) des aktiven Zentrums umfasst. Das Histidin wird hier von zwei Serin-reichen Abschnitten umgeben (Ser~~).

Um das Serin des katalytischen Zentrums herum befindet sich eine hydrophobe Region (zwischen $As_{135-150}$), die in Cathepsinen nicht zu finden ist. Hier liegt auch die Prozessierungsschnittstelle, um aus dem pre-Silicatein-α durch Abspaltung der Signalsequenz ein reifes Protein zu falten (Krasko et al., 2000). Neuere Studien gehen davon aus, dass diese hydrophobe Region des Proteins ein Grund für die schlechte Löslichkeit des rekominant hergestellten Silicateins ist. Modelberechnungen zeigten, dass dieser hydrophobe Aminosäureabschnitt im Pro-Silicatein-α durch das Propeptid (Abb. 1.5 a) verdeckt wird und im reifen Enzym zusammen mit dem aktiven Zentrum exponiert an der Molekülоberfläche positioniert ist (Abb. 1.5 b, Abb. 1.5 c).

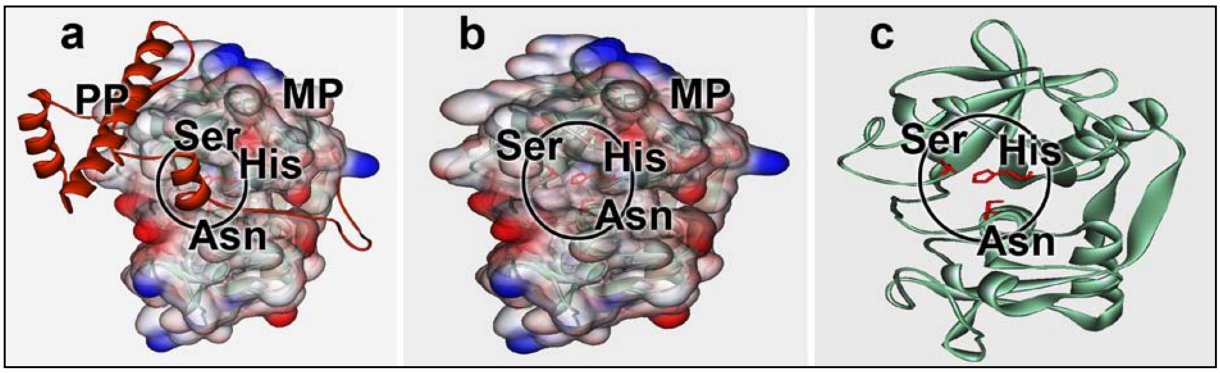

Abb. 1.5: Van der Waals Oberflächenillustration des Silicatein-α-modells **(a**) 3-D-Modell der Ladungsverteilungen am Pro-Silicatein- α und am reifen Silicatein-α (**b**) (positive Ladung: rot; negative Ladung: blau; hydrophobe Bereiche: weiß). Das Propeptid (PP), das das aktive Zentrum (Kreis) blockiert, ist als rote Helix dargestellt. (**c**). Das aktive Zentrum des reifen Enzyms liegt exponiert an der Moleküloberfläche vor.

Im Vergleich mit den Proteinen der Datenbank zeigt Silicatein die höchste Sequenzähnlichkeit mit den Cathepsinen. Der Anteil der identischen oder ähnlichen Sequenzabschnitte des reifen Silicatein-α von *S. domuncula* im Vergleich zum humanen Procathepsin S (Müller et al., 2007h) liegt bei 48,9% bzw. 62,6%. Die Kristallstruktur der Cys25→Ser Mutante des humanen Catepsin S (2.2Å Auflösung) wurde bereits veröffentlicht (Turkenburg et al., 2002). Basierend auf dieser Kristallstruktur (PDB108 database: www.PDB.org / at http://swissmodel.expasy.org) wurde die Struktur des reifen Silicatein-α-Moleküls vorhergesagt.

Die Strukturvorhersage des Silicateinmoleküls zeigte, dass sowohl Kieselsäuremoleküle sowie synthetische Organosilikate z.B. TEOS in das aktive Zentrum des *S. domuncula* Silicatein-α-Moleküls hineinpassen (Schröder et al., 2011) (Abb. 1.5). Der Abstand der drei Aminosäuren, Ser, His und Asn im katalytischen Zentrum wurden auf 7,8 Å vom C-α Atom des Serin zum C-α des Histidin, 9,6° Å bis zur Asparaginsäure und 9,77 Å zurück zum Serin berechnet. Der errechnete Abstand der Hydroxylgruppe des Serins zum TEOS-Molekül liegt bei 2,93 Å. Die Serinhydroxylgruppe spielt eine Schlüsselrolle während des nukleophilen Angriffes an das Siliziumatom des Substrates. Diese ist kürzer als die gemessene Wasserstoffbrückenbindung (3,6 Å) und erlaubt damit die enzymatische Spaltung des TEOS-Substrates. Kalkulationen zeigen, dass bis zu acht Moleküle des natürlichen

Substrates gleichzeitig in die Substrattasche des Enzyms passen (Schröder et al., 2011).

1.4.1.1 Silikatchemie

Die lösliche Form von Silikat ist die schwach saure (pKa 9,8) monomere Orthokieselsäure (Iler, 1979). Sie liegt im wässrigen Milieu bei neutralem pH-Wert nur in niedrigen Konzentrationen (< 1 mM) gelöst vor. Sobald die Konzentration die Löslichkeitsgrenze überschreitet, findet eine Polykondensationsreaktion statt. Zwei Monokieselsäuremoleküle, je nach pH-Wert ionisiert oder nicht-ionisiert, formen unter Ausbildung einer Siloxanbindung (Si-O-Si) Dimere (Greenberg and Sinclair, 1955), die wiederum über Trimere und Oligomere Polymere bilden (Perry et al., 2000). Das Reaktionsprodukt besitzt dabei in der Regel eine maximale Anzahl an Siloxanbindungen und eine minimale Anzahl an nicht kondensierten Si(OH)-Gruppen (Iler, 1979; Perry, 2000). Die Polykondensation ist stark pH-Wert abhängig. Je nach pH-Wert, Konzentration und ionischen Bedingungen bilden sich verschiedene Kondensationsprodukte. Die Reaktion bei neutralem pH-Wert ist langsam, kann aber durch geladene Moleküle ($Si\text{-}O^-$) beschleunigt werden (Coradin und Lopez, 2003). Bei einem pH-Wert unter 7 herrscht eine geringe elektrostatische Abstoßung zwischen den Partikeln. Es bilden sich Bindungen zwischen den einzelnen Partikeln aus und diese wachsen von den Enden her zu fibrillären Silikataggregaten zusammen. Als Endprodukt entsteht ein Gel, ein dreidimensionales Netzwerk mit großen wassergefüllten Hohlräumen. Im Gegensatz dazu limitieren elektrostatische Kräfte das fibrilläre Wachstum im basischen (>7) Milieu. Es bilden sich wenige, aber dafür größere Polymere, die durch die sogenannte Oswald Reifung zu einem monodispersen Sol heran wachsen (Coradin, 2003). Dabei lagern sich die Kieselsäuremoleküle aus kleineren löslicheren Partikeln an die größeren schlechter löslichen Partikel (10 – 100 nm) an (Hildebrand, 2003b; Iler, 1979).

1.4.1.2 Reaktionsmechanismus des Silicateins

Der erste Reaktionsmechanismus des Silicateins wurde von Cha et al. (1999) mittels Polykondensation von Organo-Silikaten wie z.B Tetraethylorthosilikat (TEOS) dargestellt. Die Autoren gingen von einem 2-Schritt-Mechanismus der Silicatein

vermittelten Silikatbildung aus. Neben TEOS können aber auch Orthokieselsäure (Schröder et al., 2011) oder Alkoxysilane (Wolf et al., 2010) als Substrat dienen.

Der geschwindigkeitsbestimmende erste Schritt der Reaktion ist die Hydrolyse des Substrates, welche zur Ausbildung von Silanolgruppen führt. Im zweiten Schritt kondensieren die Silanolgruppen zu Polymeren. Dieser Mechanismus impliziert, dass Silicatein ähnlich den Cathepsinen durch Spaltung einer Esterbindung wirkt. Die Polykondensation der Substrate zu einem Silikatpolymer ist hier nicht ausreichend aufgeklärt. Mittels molekularbiologischer Methoden konnten Cathepsin-L-Chimären, kombiniert mit den spezifischen Sequenzmerkmalen des Silicatein-α, hergestellt werden (Fairhead et al., 2008). Diese Studie konnte die Bildung eines Dikieselsäuredimers erklären, ließ aber keinen Schluss zur Bildung des Substrat-Enzym-Komplexes zu. Erst Schröder et al (2011) erklärte sowohl die initiale Kondensation und Dimerbildung sowie den anschließendem Polymerisationsprozess (Abb. 1.6).

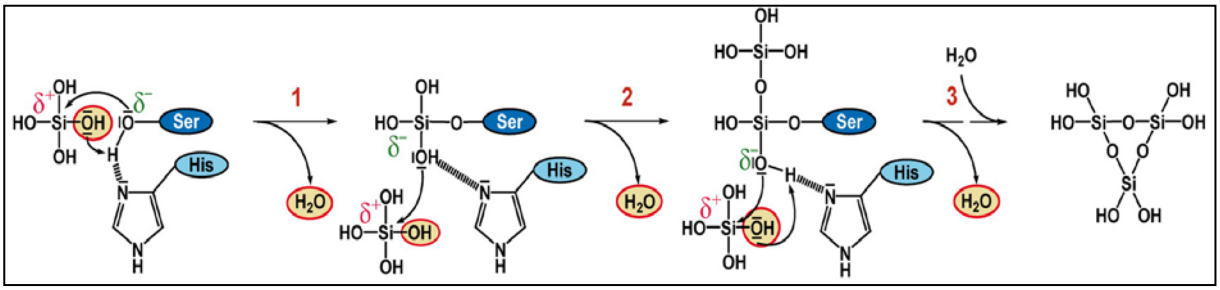

Abb. 1.6: Vorgeschlagener Reaktionsmechanismus der Silicatein-vermittelten Polykondensation der Kieselsäure. *Schritt 1:* Nukleophiler Angriff des Serin-Sauerstoffatoms an das Siliziumatom der Kieselsäure und Transfer eines Protons vom Imidazol-Stickstoff des Histidins zur Hydroxylgruppe der Kieselsäure. Die Wasserabspaltung vom pentavalenten Intermediat erlaubt einen weiteren nukleophilen Angriff an einem zweiten Kieselsäuremolekül durch das Sauerstoffatom einer Hydroxylgruppe der bereits kovalent gebundenen Kieselsäure. *Schritt 2:* Abspaltung eines zweiten Wassermoleküls durch Protonentransfer von der Imidazolgruppe. Die Rotation der Si-O-C Bindung am Serinrest leitet einen nukleophilen Angriff der zweiten Hydroxylgruppe des ersten Kieselsäuremoleküls an einem dritten Kieselsäuremoleküls ein. *Schritt 3:* Mittels nukleophilen Angriffs der Hydroxylgruppe des dritten Kieselsäuremoleküls erfolgt eine Zyklisierung der Tri-Kieselsäure. Nach Hydrolyse der Si-O-C-Bindung wird ein Trisiloxanring abgespalten.

Beim ersten Schritt, der Bildung der Dimere, erfolgt ein nukleophiler Angriff (SN2) des elektronegativen Sauerstoffatoms der Hydroxylgruppe des Serins am

elektropositiven Siliziumatom des Kieselsäuremoleküls. Diese Reaktion findet im katalytischen Zentrum statt. Das Histidin wirkt hier unterstützend, indem es die Elektronegativität des Serinrestes erhöht. Es erfolgt ein Protonentransfer vom Stickstoffatom des Histidins zur Hydroxylgruppe des Siliziumatoms. In dieser Übergangphase bildet sich ein intermediäres pentavalentes Siliziumatom. Nach Abspaltung eines Wassermoleküls liegt die Kieselsäure kovalent gebunden am Serin des katalytischen Zentrums von Silicatein-α vor. Dieses Serin-gebundene Kieselsäuremolekül wiederum vollführt einen nukleophilen Angriff am Siliziumatom des zweiten Kieselsäuremoleküls, so dass auch dieses ins aktive Zentrum eintreten kann. Im Gegenzug kann das attackierende Sauerstoffatom die Bildung einer Wasserstoffbrückenbindung zum Stickstoff des Histidinimidazols im katalytischen Zentrum erhöhen. Diese Reaktion wurde bereits aufgrund molekularer Simulationsexperimente vorgeschlagen (Croce et al., 2004). Der Protonentransfer vom Imidazol des Histidins erleichtert die Abspaltung eines Wassermoleküls, sodass das Dimer, das über eine Esterbindung an Silicatein gebunden bleibt, gebildet werden kann. Durch Rotation der Esterbindung kann die nächste Hydroxylgruppe mit dem Stickstoff des Imidazols im katalytischen Zentrum in Kontakt treten, eine Wasserstoffbrückenbindung ausbilden, ein Wassermolekül abspalten und dadurch mittels nukleophilen Angriffs das Dimer um ein drittes Kieselsäuremolekül erweitern. Durch Wiederholung dieser Reaktionsabfolge (nukleophiler Angriff, Protontransfer, Wasserabspaltung, Rotation) sollten Oligomere der Kieselsäure entstehen. Neu in diesem Modell ist die These, dass die Freisetzung der Silicatein gebundenen Kieselsäureoligomeren durch Zyklisierung der Oligomeren eingeleitet wird. Prozesse der zyklischen Siloxanpolymerbildung und ihrer Mechanismen wurde bereits 1966 etabliert (Flory und Semlyen, 1966). Die Polykondensationsreaktion kann durch Silintaphin-1 (Wiens et al., 2010), das mit Silicatein assoziiert vorliegt, gesteuert werden.

1.4.2 Biosilikatabbauendes Enzym: die Silicase

Neben den anabolen Polysilikat-bildenden Enzymen, den Silicateinen, wurde auch ein Silikat-abbauendes Enzym, die Silicase in *S. domuncula* entdeckt (Schröder et al., 2003). Die Silicase kann amorphe Kieselsäure depolymerisieren. Die entspechende cDNA konnte kloniert und in Bakterien exprimiert werden. Dieses von der cDNA abgeleitete Protein hat ein Molekulargewicht von 43 kDa.

Sequenzanalysen ergaben, dass die Silicase eines der Mitglieder der Familie der Carboanhydrasen ist, die die Hydratisierung von Kohlenstoffdioxid zu Hydrogencarbonat und umgekehrt katalysieren können. Die größte Ähnlichkeit ergab sich mit der humanen Carboanhydrase II. Carboanhydrasen besitzen als Cofaktor ein Zinkion, welches im aktiven Zentrum an die Imidazolreste der drei Histidine gebunden ist und dessen vierte Koordinationsstelle von einem Hydroxidion besetzt ist. Diese drei Histidine konnten auch in der Silicasesequenz an den folgenden Stellen As_{181}, As_{183} und As_{206} gefunden werden. Aktivitätstests zeigten, dass die rekombinante Silicase neben der Carboanhydrase-funktion auch in der Lage ist, amorphes Silikat unter Abspaltung von freier Kieselsäure aufzulösen (Schröder et al., 2003).

Die Hypothese des Wirkmechanismus der Depolymerisation amorphen Silikates durch die Silicase ähnelt der Reaktion anderer Zink-abhängiger Enzyme. In Wasser (Lewis-Base) wird ein an das Zink(II)ion, das als Lewissäure agiert, gebundenes Hydroxidanion gebildet. Die freien Elektronenpaare am Sauerstoffatom des Hydroxidions greifen nukleophil an einem der Siliziumatome an, die über Sauerstoffatome miteinander verknüpft sind. Im nächsten Schritt bindet der Zink-Komplex unter Spaltung der Sauerstoffbindung an das Siliziumatom an. Durch Bindung eines weiteren Wassermoleküls wird Kieselsäure freigesetzt und das initiale Zink(II)-gebundene Hydroxidanion wieder gebildet. Durch diese Regenerierung des aktiven Zentrums kann ein neuer Zyklus beginnen.

Die Expression des Silicase-Gens kann in Gegenwart erhöhter Silikat-Konzentrationen hochreguliert werden. Licht- und elektronenmikroskopische Techniken (Eckert et al., 2006) zeigten, dass die Enzyme Silicase und Silicatein sowohl an der Oberfläche wachsender Spiculae als auch im Axialfilament des Axialkanals kolokalisiert sind. Man geht davon aus, dass auch die Silicase an der Polysilikatabscheidung beteiligt ist, z.B. während der Reorganisation der neuen Silikatschicht der Nadeln. Die Silicase existiert ebenso wie Silicatein innerhalb wie auch außerhalb der wachsenden Nadel. Dies deutet darauf hin, dass die Spezies-spezifische Nadelbildung ein Netzwerk von regulatorischen Faktoren benötigt, um die enzymatische Silikatablagerung, d.h. die Form und Größe, zu kontrollieren.

1.4.3 Schwammspezifische Silicatein-assozierte Proteine: Die Silintaphine

Mittels eines „Yeast-two-Hybrid“-Screenings konnten Interaktionspartner des Silicateins identifiziert werden. Zwei Proteine wurden bisher isoliert, die keine deutliche Sequenzähnlichkeit zu einem der anderen gelisteten Proteine in den Datenbanken aufweisen.

1.4.3.1 Silintaphin-1

Als erstes Protein aus der Gruppe der Silicatein-α interagierender Proteine wurde Silintaphin-1 mittels two-hybrid-screening Technik durch direkten physischen Kontakt mit Silicatein-α als Interaktionspartner identifiziert (Wiens et al., 2009b). Die cDNA ist 1608 Nukleotide lang und der offene Leserahmen codiert für ein 42,5 kDa großes Polypeptid. Silintaphin-1 verfügt über eine signifikante Homologie zur Pleckstin-Homologiedomäne (PH-Domäne). Sie befindet sich zwischen den Aminosäuren 91 bis 197 der Polypeptidsequenz. Aus einer aktuellen Studie ist bekannt, daß Proteine mit einer PH-Domäne die enzymatische Funktion des Zielproteins nicht aufhebt sondern die Fähigkeit der Faserbildung fördert (Aittaleb et al., 2009). Die PH-Domäne ist in einer Vielzahl von eukaryotischen Proteinen, die in Signalreaktionen, besonders in Assoziation mit organischen Skelettelementen involviert sind, vorhanden. Am C-terminalen Ende befinden sich acht nahezu identische „Repeats“, die aus 10-12 Aminosäuren bestehen. Darüber hinaus gibt es mehrere PEST-Sequenzen, die darauf hindeuten, dass Silintaphin-1 selbst ein regulatorisches Protein oder ein in einer regulatorischen Signalkaskade involviertes Protein ist, das nur eine kurze Halbwertszeit besitzt. Bereits in den ersten Studien zeigte sich, das Silintaphin-1 sowohl innerhalb als auch außerhalb der Spiculae mit Silicatein-α kolokalisiert vorliegt. Die wahrscheinlichste Binde- oder Interaktionsregion der PH-Domäne des Silintaphin-1 ist eine hydrophobe Sequenz am N-Terminus des reifen Silicatein-α. Zusammen mit Silicatein-α formt es synthetische Nadeln aus Fe_2O_3 (Wiens et al., 2010) oder aus Silikatnanopartikeln (Müller et al., 2009d).

1.4.3.2 Silintaphin-2:

Erst vor kurzem konnte ein zweites Mitglied der Silintaphine mittels Zwei-Hybrid-Bibliothek-Screening und mittels eines neuen Pull-down-assays (Wiens et al., 2011a) identifiziert werden.

Silintaphin-2, dessen 0,7 kb große cDNA für ein 15,5 kDa großes Protein codiert, besitzt vier Ca^{2+}-Bindungsstellen und liegt nach Immunfluoreszenz mikroskopischen Untersuchungen mit Silicatein-α innerhalb des Axialfilamentes und auf der Nadeloberfläche kolokalisiert vor. Silintaphin-2 ähnelt strukturell den calciumbindenden sekretorischen Proteinen, zu deren Aufgabe die Mineralisierung der organischen Matrix im Metazoengewebe gehört. Somit könnte Silintaphin-2 im Schwamm eine ähnliche Rolle übernehmen. Die Funktion des Silicatein-assoziierten Silintaphin-2 Proteins ist bisher ungeklärt, es sind aber 2 Szenarien vorstellbar.
Erstens, Silintaphin-2 nimmt direkt an der Biosilikatsynthese teil, indem es durch Calciumbindung und anschließende Konformationsänderung die Bindung der Kieselsäure, die Silikatsynthese, durch Silicatein-α erleichtert. In diesem Fall würde das Kieselsäure beladene Silintaphin-2 während des Axialfilamentwachstums und des Längen- und Dickenwachstums der Nadeln den Transport der Kieselsäure zum aktiven Zentrum des Silicatein-α unterstützen. Damit würde es zu einer lokal begrenzten Kieselsäureanreicherung in der Nähe des aktiven Zentrums kommen. Die Silikatkonzentration im Meerwasser ist in der Regel gering (≤ 10 µM) (Fröhlich und Bartel, 1997), womit Silintaphin-2 die Spiculogenese deutlich verbessern könnte.
Im zweiten Fall würde Silintaphin-2 nur indirekt an der Mineralisierung beteiligt sein, indem es eine Hormon- oder Zytokin-ähnliche Rolle übernehmen würde und damit die Aktivität der mineralisierenden Zellen, den Sklerocyten, in den Schwämmen beeinflussen würde.

1.5 Nadelwachstum

Gibt man kleine Stücke eines Schwammes in Calcium- und Magnesium-freies Wasser, so löst sich der Zellverband auf und die entstehenden Einzelzellen können unter bestimmten Bedingungen aggregierte Zellhaufen (Primmorphe) bilden, die wiederum zu einem funktionsfähigen Schwamm auswachsen können. Durch die Etablierung dieser Primmorphen-Zellkultur stand erstmals ein Zellsystem zur Verfügung um die Spiculogenese der Schwämme näher zu untersuchen. Mittels TEM-Analysen der Primmorphe konnte zunächst in Süßwasserschwämmen (Imsiecke et al., 1995) und später in marinen Schwämmen (Müller et al., 2005a) gezeigt werden, dass die Nadelbildung intrazellulär beginnt. Die meisten

zellbiologischen und biochemischen Studien wurden am Schwamm *S. domuncula* durchgeführt.

Der Prozess der Nadelbildung kann in zwei Abschnitte, den initialen intrazellulären und den formgebenden extrazellulären Abschnitt eingeteilt werden. (Abb. 1.2 D):

In früheren Studien konnte bereits gezeigt werden, dass die nadelbildenden Schwammzellen (Sklerocyten) Kieselsäure aktiv über einen Na^{+}/HCO_3^{-} $[Si(OH)_4]$ Kotransporter (Schröder et al., 2004) aufnehmen können. Gleichzeitig wird das Silicatein über das endoplasmatische Retikulum und den Golgi-Apparat posttranslational modifiziert und zum reifen Silicatein prozessiert. Anschließend wird es zusammen mit der Kieselsäure in speziellen Organellen, den Silicasomen, deponiert. Innerhalb dieser Organellen assembliert Silicatein-α zum Axialfilament und scheidet die erste Silikatschicht ab. Diese unreifen Nadeln werden nun in den extrazellulären Raum freigesetzt, wo sie in der Länge (axial) und im Durchmesser (radial) durch appositionelles Wachstum zu ihrer endgültigen Größe und Form heranwachsen (Müller et al., 2005a). Das Silicatein-vermittelte Nadelwachstum verläuft in zwei Richtungen. Das axiale Längenwachstum erfolgt durch die Elongation des Biosilikatzylinders, welches von der 23 kDa Form des Silicateins gebildet wird. Das radiale Dickenwachstum erfolgt extrazellulär durch appositionelles Wachstum, d.h. das extrazelluläre Silicatein-α, 34,7 kDa vermittelt die schichtweise Ablagerung von Silikat auf der Oberfläche der wachsenden Spicula (Müller et al., 2005a; Schröder et al., 2006). Diese längere Silicatein-α Form unterscheidet sich von dem 23 kDa Silicatein-α durch die Anwesenheit der N-terminalen Propeptidsequenz, von welcher ausgegangen wird, dass sie zu Beginn der Biosilikatsynthese autokatalytisch abgespalten wird (Müller et al., 2005a).

Das radiale Dickenwachstum wurde früher verstanden (Müller et al., 2005a; Schröder et al., 2006) als der axiale Elongationsprozess (Wang et al., 2011). Die appositionelle Verdickung der Nadeln erfolgt im extrazellulären Raum. Mittels goldmarkierter Antikörper gegen Silicatein-α konnten elektronenmikroskopische Untersuchungen zeigen (Abb. 1.2 A), dass Silicatein-α dort in größeren Einheiten organisiert vorliegt. In Anwesenheit von Calciumionen oligomerisieren Galektine zusammen mit Silicateinen zu filamentösen Fäden, die sich konzentrisch um die Nadeloberfläche anordnen (Schröder et al., 2006; Abb. 1.8 A). Innerhalb dieses organischen Zylinders, der die wachsende Nadel umgibt, wächst der Silikat-Mantel schrittweise durch Schichtung neuer Silikatlamellen. In Hexactinelliden können bis zu

1000 Lamellen in einer Nadel unterschieden werden (Wang et al., 2009c, Abb. 1.2 F, G); während in Demospongien die einzelnen Lamellen zu einer soliden Silikat-Hülle fusionieren, die das Axialfilament umgibt (Abb 1.2 B, C). Die erhaltenen Daten deuten darauf hin, dass die Galektinfäden durch Kollagenfasern zu netzartigen Strukturen organisiert werden (Schröder et al., 2006). Spezielle Zellen, die Lophozyten/Collenzyten, synthetisieren die Kollagenfasern und geben sie in den extrazellulären Raum ab. Somit scheinen sie die Nadelmorphogenese zu steuern.

1.5.1 Axiales Nadelwachstum:

Der vorherrschende Spiculatyp im Gewebe und in Primmorphen von *S. domuncula* sind die Tylostylen (Abb. 1.8 B, C). Es handelt sich um 150 – 320 µm lange monoaxonale Nadeln, die einen stumpfen kugelförmigen Kopf (6,5 - 9,2 µm) und ein spitzes Ende besitzen. Jede Spicula besteht aus einem Axialkanal, in dem sich das organische Axialfilament befindet (Wang et al., 2010) (Abb. 1.2 C). In TEM-Aufnahmen stellt sich das Axialfilament als dichtgepackte Struktur, die in die granulierte Struktur des Axialkanals eingebettet ist, dar. Da die Spiculasynthese ein schneller Prozess ist und junge, sich entwickelnde Spiculae nur sehr selten im Gewebe von erwachsenen Tieren zu finden sind, kann das Primmorphen-Zellkultursystem erfolgreich zur Aufklärung der Nadelbildung eingesetzt werden.
In einer aktuellen Studie wurden zum ersten Mal experimentelle Beweise für die zelluläre Beteiligung/Kontrolle der Sklerocyten am Nadelwachstum anhand des Primmorphen-Zellkultursystems dargelegt. Die Spiculasynthese startet intrazellulär in den Sklerocyten und die initiale Spicula wird nach Fertigstellung der ersten Silikatschicht in den Extrazellulärenraum entlassen. Die Spicula bleibt jedoch mit der Sklerocyte verbunden, indem die Sklerocyte Zellausstülpungen in den wachsenden, sich verlängernden Axialkanal hinein ausbildet (Wang et al., 2011) (Abb. 1.7 G) .Die Sklerocyte transportiert Silicateinmolekülen und Silikatpräkursoren in den Axialkanal, die dort das Axialfilament verlängern und die Biosilikat-Abscheidung an der inneren Oberfläche des Silikatmantels katalysieren. Im extrazellulären Raum assoziiert sich die wachsende Nadel mit weiteren Sklerocyten, die mit Silicateinmolekülen und Silikatpräkursoren gefüllte Silicasome (Schröder et al., 2007b) zur Spiculaoberfläche transportieren. Somit wird deutlich, dass zur Fertigstellung einer kompletten Spicula zwei unabhängige Silikatablagerungsprozesse ablaufen müssen. Erstens die Biosilikatbildung, die zur Formierung des inneren Kerns der wachsenden Spicula

mittels des Silicateins des Axialfilamentes führt, und zweitens das lamellare Dickenwachstum der Spicula durch nacheinander folgende Ablagerung einzelner Biosilikatschichten auf der äußeren Oberfläche. In Demospongien fusionieren die einzelnen Silikatlamellen zu einem Zylinder (Biosintern) oder liegen wie bei den Hexactinellida als einzelne separierte Silikatschichten vor.

Einem solchen Wachstumsmechanismus liegt wahrscheinlich ein hoher Energieverbrauch zugrunde, der z.B. durch ATP-Spaltung mit Hilfe der Argininkinase im Schwamm gewährleistet werden kann. In *S. domuncula* konnte nachgewiesen werden, dass das Gen codierend für die Argininkinase mittels Silikat induziert werden kann (Perović-Ottstadt et al., 2005). Mittels Immunfluoreszenzfärbungen konnte zusätzlich zu Silicatein und Argininkinase ein drittes Protein, Aquaporin-8, im Axialkanal nachgewiesen werden (Müller et al., 2011g). Aquaporine bilden Kanäle in der Zellmembran, die die Strömung des Wassers entlang eines Wassergradienten erleichtern (Huang et al., 2001). Während der Polykondensationsreaktion des Silikates wird Reaktionswasser akkumuliert, welches über Aquaporine der umgebenden Zellen abgeführt wird. Somit wird dem Reaktionssystem Wasser entzogen, welches sich in einer beschleunigten Reaktionsgeschwindigkeit der Biosilikatsynthese und Reifung äußert.

Der Prozess der Zellausstülpungen in den Axialkanal hinein konnte mittels Längsschnitten durch die wachsende Nadel analysiert werden (Wang et al., 2011). Ein vollständiger Längsschnitt durch eine 50µm lange Nadel zeigte, dass der Axialkanal an einem Ende geschlossen ist, während das andere Ende offen und mit einer Sklerocyte verbunden ist (Abb. 1.7 G). Das offene Ende des axialen Kanals scheint die Wachstumsregion der Spicula zu sein. In der Mitte sind dicht gepackte Vesikel, die als Silicasome identifiziert wurden, von einer Membran, wahrscheinlich der Zellmembran, umgeben (Abb. 1.7 H). Am terminalen Ende des axialen Kanals sind neben dem Axialfilament keine zellulären Fragmente mehr auffindbar (Abb. 1.7 I). Querschnitte durch wachsende Nadeln zeigten Zellausstülpungen in der Nähe der Sklerocytenbindungestelle (Abb. 1.7J, K), während man in Richtung der Nadelspitze nur das Axialfilament im Axialkanal findet (Abb. 1.8L).

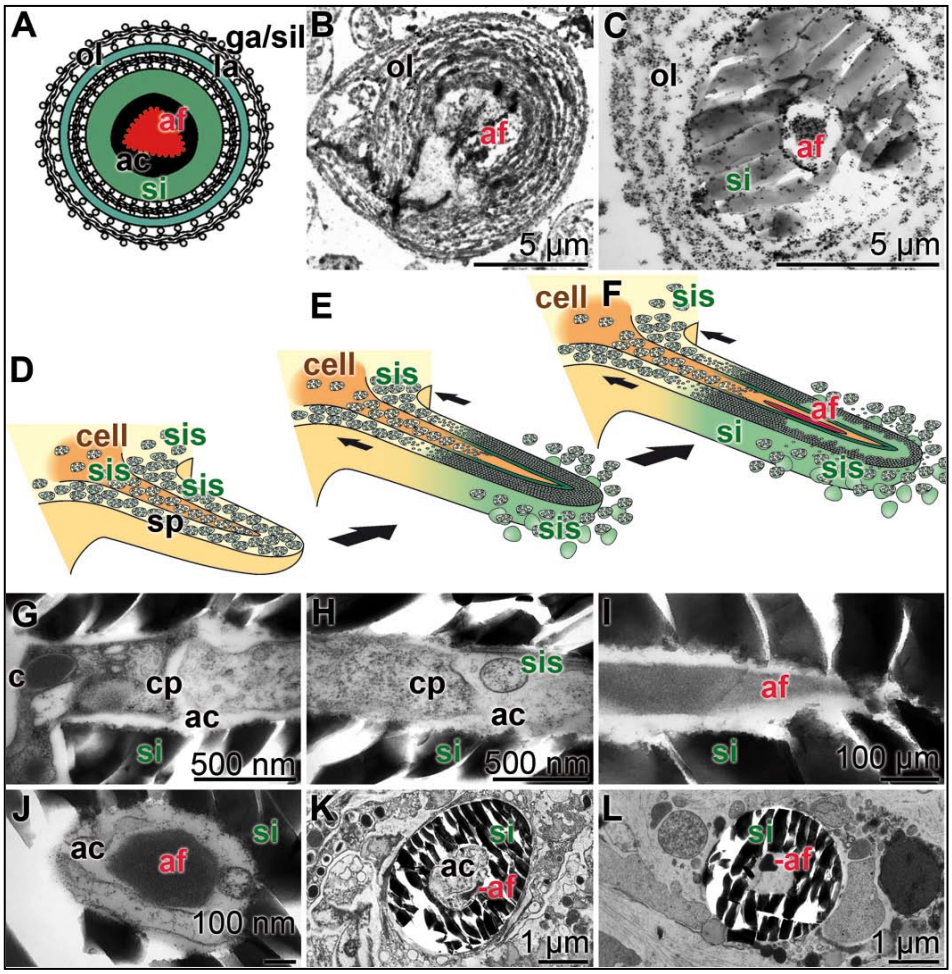

Abb. 1.7. Nadelwachstum im extrazellulären Raum. (**A**) Schematische Darstellung des appositionellen Nadelwachstums im Mesohyl. In der Gegenwart von Ca^{2+}-Ionen bilden sich Galektin-Silikatein-Stränge aus, die sich in Schichten (ol) konzentrisch um die wachsende Nadel herum anordnen und die Basis für die Silikatlamellen (la) bilden. Im Zentrum der Nadel befindet sich das Axialfilament (af) im Axialkanal (ac) liegend, um den sich die erste Silikatschicht (si) gebildet hat. (**B**, **C**) Wachsende Nadeln mit dem Axialfilament (af), die von organischen Lagen (ol) umgeben sind. Im fortgeschrittenen Stadium des Nadelwachstums ist bereits die erste Silkatschicht (si), die von organischen Schichten (ol) umgeben ist, zu erkennen; Immunogoldmarkierung gegen Silicatein (TEM). (**D** - **F**) Schematische Darstellung der Spiculabildung mittels Zell-Evagination und anorganischer Selbstorganisation. **(D)** Die Spiculabildung (sp) beginnt intrazellulär in einer Sklerocyte. Während der Verlängerung der Zellausstülpung in den Axialkanal hinein werden Silicasome (sis), die den inneren Silikatkern bilden, freigesetzt **(E)**. Während dieser Phase bewegt sich die Nadelspitze vom Zellkörper weg (Pfeile). **(F)** Während des fortschreitenden Nadelwachstums erfährt die Spitze und der mittlere Nadelteil eine zunehmende Silizifizierung (si; grün). Das Axialfilament (af) verlängert sich zur Nadelspitze hin durch Anlagerung der Silicateinmoleküle aus den Silicasomen. Silicasome sind nicht nur im Axialkanal (D) zu finden, sondern auch an der Oberfläche der wachsenden Nadel. **(G - I)** Longitudinaler Schnitt durch eine Spicula; TEM. (G) Die Zellausstülpung (cp) einer Zelle (c) reicht in den Axialkanal (ac) hinein. Der Axialkanal ist von einer Silikathülle (si) umgeben. (**H**) Im mittleren Teil der Nadel im Axialkanal (ac) befindet sich das Ende der Zellausstülpung (cp) in der Nähe eines Silicasomes (sis). (**I**) An der Nadelspitze ist nur das Axialfilament (af) zu erkennen. Nadelquerschnitte mit verschiedenen Reifungsgraden. (**J, H**) Nadelquerschnitte. Die Spicula ist mit einer Sklerocyte verbunden. Im Axialkanal (ac) befinden sich zelluläre Strukturen sowie das Axialfilament (af). (**L**) Im Nadelquerschnitt ist nur das Axialfilament (af) im Axialkanal (ac) zu finden.

Diese Daten deuten darauf hin, dass das axiale Wachstum der Nadeln durch die Erweiterungen der zellulären Prozesse in die axialen Kanäle hinein durch hydrodynamische Kräfte angetrieben wird. Evagination ist ein nicht selten auftretender Vorgang in Metazoen, die durch ein Zusammenspiel von Bewegung, Einlagerung und Teilung von Zellen sowie durch Veränderungen der Zellpolarität und Zellform (Philipp et al., 2009) erklärt werden kann. Auf der Gewebe-Ebene wird die Evagination in erster Linie durch morphogenetische Ereignisse, die von genetischen Prozessen angetrieben werden, kontrolliert. Ein berühmtes Beispiel ist der Wnt-Signalweg, der sowohl Entwicklungsprozesse wie auch Krankheiten kontrolliert (Davies, 2005). Dieser Signalweg, der auf einer sequentiellen Expression eines Genclusters basiert, ist an der Achsenbildung in Metazoen beteiligt. Dieser Signalweg wurde bereits bei der Achsenbildung in Primmorphen und Embryonen von *S. domuncula* beschrieben (Adell et al., 2003). Hierbei bewirkt die differentielle Genexpression eine kontrollierte Zell-Zell-Kommunikation, die für die Achsenbildung benötigt wird, und kontrolliert somit zellbasierte morphogenetische Ereignisse im Gewebe. Die Nadelsynthese wird durch eine genetisch gesteuerte Komponente und hydromechanische Prinzipien (Gierer, 1977), die während der chemischen Reaktionen auftreten, gesteuert. Mittels sequentieller Genexpression von Silicatein und Kollagen (Krasko et al. 2000) wird die Spiculasynthese gestartet. Die Selbstorganisation der Silicateine erfolgt unter Kontrolle und Zwang der fraktalen Polymerisationsparameter (Murr und Morse, 2005.; Müller et al., 2007h). Die initialen, intrazellulär gebildeten Nadeln werden mittels Evagination aus den Zellen extrudiert. Dieser Prozess, der vermutlich durch hydro-mechanische Kräfte angetrieben wird, erfolgt aufgrund der unterschiedlichen Widerstandskräfte der Zellmembran und dem osmotischen Druck. Schließlich, da auch anorganische Polykondensationsreaktionen beteiligt sind, sind Zugkräfte während der Biosilikatbildung vorhanden, die die Zelldehnung steuern und den Zellkörper wegbewegen.

1.5.2 Reifung und Härtung des Biosilikats

Synärese ist ein Prozess während der Reifung von Kieselgelen durch Sol-Gel-Synthese, in dem Schrumpfung und Wasserausscheidung durch eine Umlagerung und Erhöhung der Anzahl der Siloxanbindungen (Brinker und Scherer, 1990) stattfindet. Die Beeinträchtigung der Synärese, die durch Schrumpfung des

Kieselsäure-Netzwerkes charakterisiert ist, wurde in intakten Primmorphen, die mit Mangansulfat (Müller et al., 2011g) behandelt worden waren, untersucht.

Werden Primmorphe in Gegenwart von Mangansulfat kultiviert, kann eine Veränderung in der Morphologie bereits durch Augenuntersuchung wahrgenommen werden (Müller et al., 2011g). Die Mangansulfat-behandelten Aggregate weisen keine kugelige Morphologie wie die Kontrollen (Abb. 1.8 A) auf, sondern sind durch ihre flache Organisation charakterisiert (Ab. 1.8 E). Die Primmorphe zeigen ähnliche Entwicklungsfähigkeit, unabhängig davon ob sie mit Mangansulfat inkubiert wurden oder nicht. Allerdings waren die Nadeln, die in solchen Primmorphen gebildet wurden, sehr unterschiedlich. Während die Oberfläche der neu gebildeten Nadeln in den nicht-behandelten Primmorphen glatt war (Abb. 1.8 B, C), zeigten diejenigen, die sich mit Mangansulfat entwickelt hatten, eine ganz andere Textur. Auf den Nadeln bildeten sich Ablagerungen (Abb. 1.8 F, G), die rau und porös waren, und oft schienen die Nadeln miteinander fusioniert zu sein (Müller et al., 2011g) (Abb. 1.8 F). Während in Demospongien der Fusionierungsprozess (Biosintern) nur in Primmorphen, die mit Mn-Sulfat behandelt worden waren, induziert werden kann, ist diese Fusionsreaktion bei zwei einzelnen Nadeln in der Natur häufig bei Hexactinelliden (Leys et al., 2007) zu finden.

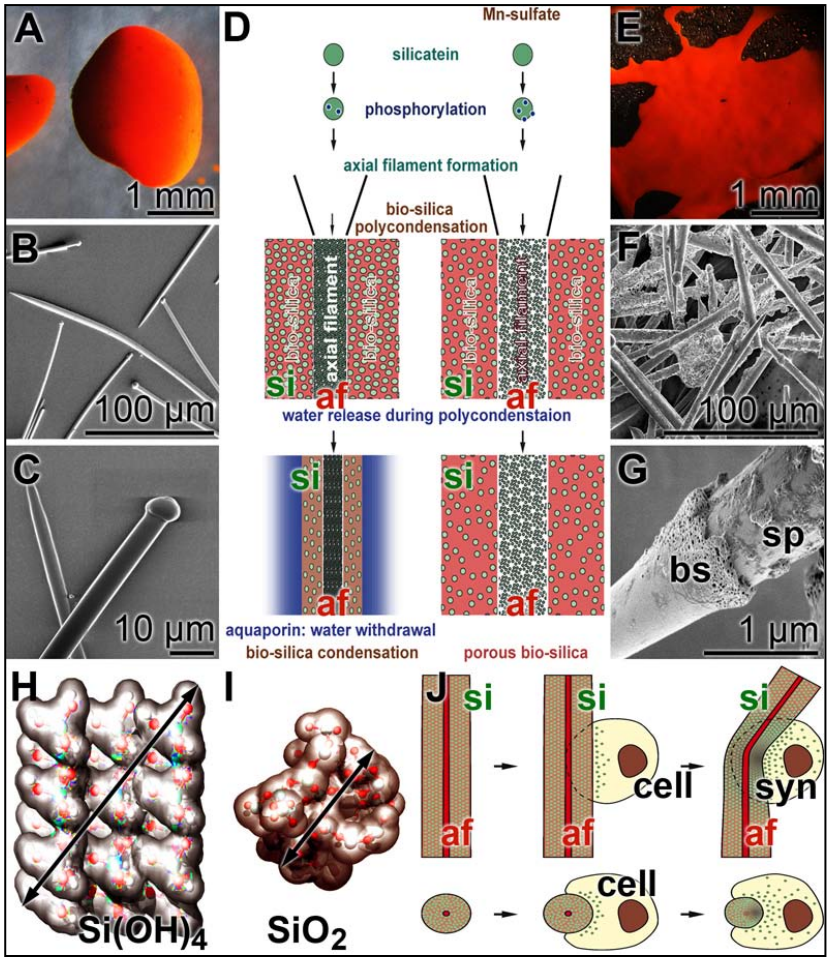

Abb. 1.8. Effekt von Mangansulfat auf die Biosilikathärtung und dessen Reifungsprozess. (**A**) 7 Tage alte Primmorphe in Medium ohne Mangansulfat (Kontrolle). (**B, C**) Isolierte Tylostylen aus unbehandelten Primmorphen (*S. domuncula*). (**D**) Schematische Darstellung der biochemischen Prozesse in unbehandelten (links) und Mangansulfat-behandelten Primmorphen (rechts). Die Mangansulfat-Exposition der Primmorphe führt zu einer erhöhten Phosphorylierung der Silicateinmoleküle, was wiederum in einer weniger kompakten Organisation der Silicateinmoleküle im Axialfilament der Spicula resultiert. Während der enzymatisch-kontrollierten Polykondensation entsteht Reaktionswasser, welches in den Kontrollen mittels Aquaporinkanälen an der Oberfläche der umgebenden Zellen vom Reaktionsort entfernt wird. Im Gegensatz dazu fehlen diese Kanäle in den Mangansulfat behandelten Zellen, damit verlangsamt sich die Reaktionsgeschwindigkeit der Polykondensation und führt zu porösen Biosilikat. (**E**) Mangansulfat behandelte Primmorphe nach 7 Tagen in Kultur. (**F**, **G**) Die Mangansulfat behandelten Spicula weisen poröse Biosilikatablagerungen auf. (**H**, **I**) Van-der-Waals-Oberflächendarstellung von monomerer Kieselsäure [$Si(OH)_4$] (H) und Silikat in seiner (fast) kondensierten Form [SiO_2] (I).
(**J**) Theorie zur Nadelkrümmung. Die Krümmung von Spiculae erfolgt als Konsequenz auf die lokale Entfernung des Reaktionswassers an neu synthetisierten Silikatablagerungen (si). Die assoziierten Zellen an der Oberfläche der wachsenden Spicula entfernen das Reaktionswasser (Synärese [syn]) und bewirken dadurch eine Krümmung der Nadel an dieser Stelle.

Die Bestimmung der Mikrohärte wurde durch Anwendung der Nanoindentierungs-Methode ermittelt (Müller et al., 2011g). Dabei wird ein harter Prüfkörper (üblicherweise eine Diamantspitze) in das zu untersuchende Material gedrückt. Während des Versuchs werden aufgebrachte Kraft und Eindringweg der Spitze simultan gemessen, woraus die Härte des Materials berechnet werden kann.

Im Gegensatz zu Nadeln, die in Primmorphen in der Abwesenheit von Mangansulfat wuchsen und die eine fast glatte Oberfläche aufweisen, erkennt man an Bruchstellen der Nadeln, die aus Mangansulfat-Kulturen isoliert wurden, ein körniges Aussehen der Oberfläche. Die durchschnittliche Härte Mangansulfat-freier Nadeln beträgt etwa 1,5 GPa, während die Nadeln aus Mangansulfat-Kulturen eine niedrigere Härte von 0,35 GPa aufweisen (Müller et al., 2011g). Auf biochemischer Ebene wurde festgestellt, dass der Grad der Phosphorylierung von Silicateinen während der Mangansulfat-Behandlung (Müller et al., 2011g) geändert vorliegt. Daten, die mit der zweidimensionalen Gelelektrophorese ermittelt wurden, ergaben, dass die Silicateine im Axialfilament aus nicht behandelten Primmorphen aus Isoformen bestehen. Neben dem isoelektrischen Punkt von 5,9 (nicht-modifizierte Protein) existieren fünf weitere Formen mit isoelektrischen Punkten von 4,8, 4,6, 4,5 und 4,3. Nadeln, die in den Mangansulfat Primmorphen gebildet wurden, weisen mindestens zwei weitere Isoformen mit einem isoelektrischen Punkt von 4,1 und 3,9 auf. Bedenkt man die neusten experimentellen Befunde wie die gestörte Nadelsynthese durch Mangansulfat-Inkubation, die erhöhte Phosphorylierung von Silicatein in Mangansulfat behandelten Primmorphen, die reduzierte Expression des Aquaporin-Gens in Primmorphen und die damit verminderte Bildung von Aquaporin-Kanälen, drängt sich ein funktionelles Zusammenspiel des Aquaporin-Wasser-Kanals mit der enzymatischen Polykondensation des Biosilikats auf (Müller et al., 2011g). Diese Daten wurden sowohl durch molekularbiologische als auch immunobiologische Studien gesammelt. In Abbildung 1.8 D ist die Beeinträchtigung der Biosilikatsynthese in Mangansulfat behandelten Primmorphen schematisch dargestellt. Die erhöhte Phosphorylierung der Silicateine führt vermutlich zu einer weniger kompakten Polymerisation der Silicateine zum Axialfilament. Der nachfolgende Schritt der enzymatischen Polykondensation zum Biosilikat führt zur Bildung eines dreidimensionalen Silikat-Netzwerks unter Verbrauch von Silikat und dem Abscheiden von Wassermolekülen (Hench, 1998). Der Entzug des freigesetzten Wassers aus dem Bereich der Biosilikatsynthese ist sicherlich kein schnelles

Verfahren angesichts der schnellen Wachstumsrate der Spiculae. Allerdings ist die Entfernung des Reaktionwassers während der Polykondensation essentiell für die Aufrechterhaltung und die Geschwindigkeit der Spiculabildung. Die Spicula-Umgebung ist relativ arm an Zellen, aber reich an Proteinen der extrazellulären Matrix, besonders an Galektinen als vorherrschendes Adhäsionsmolekül. Die Lektine bilden eine gelartige Matrix in Gegenwart von Ca^{2+} (Müller et al., 1997) und dienen als stabile dynamische Matrix für die "wandernden Zellen" um sowohl Metabolite wie auch das Reaktionswasser der Polykondensation rund um die Spicula abtransportieren zu können.

Die Entdeckung der Aquaporin-Kanal exprimierenden Zellen um die Nadeln herum war der erste überzeugende Hinweis darauf, dass der Wasserentzug aus der Umgebung einer rasch wachsenden Nadeln nötigt ist. Dies wurde bereits in vitro beobachtet (Imsiecke et al., 1995). Im Hinblick auf diese Daten wurde postuliert, dass im intakten Gewebe unter *in vivo* Bedingungen die Wassermoleküle, die während der Biosilikat-Synthese freigesetzt werden, in die umgebenden Zellen aufgenommen werden. Diese Zellen migrieren und transportieren das Wasser weiter weg, so dass das Wasser schneller der Reaktion entzogen werden kann und die Gleichgewichtskonstante auf die Seite des Produktes verschoben wird.

Während der Nadelbildung nimmt der Durchmesser des Biosilikatmantels ab. Der initiale Durchmesser der wachsenden Nadel im extrazellulären Raum liegt bei ca. 10 µm und schrumpft später auf ca. 2-3 µm (Müller et al., 2006; Schröder et al., 2006). Dieser Schrumpfungsprozess wird auch bei höheren Temperaturen während der anorganischen Sol-Gel-Silicat-Polykondensation beobachtet (Calamita et al., 2001). Diese empirisch bestimmte Schrumpfung der Spicula während des Wachstums kann auch durch theoretische Berechnungen bestätigt werden. Der Durchmesser eines Silikat-Monomers beträgt 4,48 Å, während die Größe eines Silikatmoleküls in einem vollständig polykondensierten Gelnetz nur 3,56 Å beträgt (Thompson et al., 1998). Damit nimmt der molekulare Durchmesser eines Silikatmoleküls um 21 % ab. Nimmt man an, dass 30 Silikatmonomere raumfüllend angeordnet sind (Abb. 1.8 H), nimmt die gleiche Anzahl an Kieselsäuremolekülen im Silikatnetzwerk einen 30 % kleineren Raum ein (Abb. 1.8I). Die Entfernung des Reaktionswassers hat ein Altern/ Verhärtung des Biosilikatproduktes zur Folge und trägt dazu bei, die Nadelbildung im Schwamm zu erklären. In beiden Klassen der Kieselschwämme existieren Nadelarten, die verziert, mit Haken oder Dornen

bewaffnet und fast immer in ihrer Längsachse gebogen sind (Uriz, 2006). Das Biegen von Nadeln könnte auf der Grundlage einer lokalen Entfernung des Reaktionswassers während der Silikatpolykondensation erklärt werden (Abb. 1.8 J). In Primmorphen sind die wachsenden Nadeln an der Biegungsstelle mit Zellen verbunden. Im Hinblick auf die diskutierte Schrumpfung des Biosilikats könnte eine regionale und differentiale Entfernung von Wasser die Grundlage für eine Änderung der Wachstumsrichtung der Nadeln sein (Abb. 1.8 J).

1.5.3 Zelluläres Zusammenspiel während der Nadelsynthese

Bis vor kurzem war es nicht möglich, Zelltypen in Schwämmen genau zu definieren. Nach Entdeckung molekularer Marker wurde es möglich, verschiedene Differenzierungstadien der Stammzellen zu Sklerocyten, die Zellen, die an der Nadelsynthese beteiligt sind, zu unterscheiden. Wie alle anderen Metazoen bilden sich auch die befruchteten Eier der Schwämme während einer Reihe von Zellteilungen zur Morula, Blastula und vielleicht sogar zu Gastrula um (Müller, 2006a). Mit dem Primmorphen-System konnte gezeigt werden, dass sich aus den totipotenten Stammzellen folgende differenzierte Zelltypen, die an der Skelettbildung beteiligt sind, ableiten: die Sklerocyten, die Archaeocyten, die Lophocytes und die Chromocyten. Die Charakterisierung dieser Zelltypen und die Aufklärung der Mechanismen der Nadelsynthese in Demospongien ermöglichen einen Überblick über dieses Netzwerk und die Kontrolle der Nadelbildung (Abb. 1.10). Die Chromocyten (Simpson, 1984) lagern Carotinoide ein, die von bakteriellen Symbionten des Schwammes (Biesalski et al., 1992) hergestellt werden. Diese Schwammzellen synthetisieren und setzen knochenmorphogenetisches Protein-1 [BMP-1] frei. BMP-1 ist eine Proteinase, die bei der Verarbeitung einer Reihe von extrazellulären Strukturproteinen, z. B. Kollagen oder Laminin (Amano et al., 2000) beteiligt ist und in *S. domuncula* Silintaphin-2 spaltet. Experimentell konnte gezeigt werden, dass Silintaphin-2, ein Ca^{2+}-bindendes Protein, in Sklerocyten (Wiens et al., 2011a) gebildet wird und die zur Galektinpolymerisation benötigten Ca^{2+}-Ionen in den extrazellulären Raum transportiert. Anschließend assoziiert das prozessierte Silintaphin-2 in Anwesenheit der gebundenen Ca^{2+}-Ionen mit Galektin und Silicatein. Die Galektinmoleküle bilden die Grundlage für die Silicateine, die wiederum einen organischen Zylinder formen, in den mit Hilfe der Sklerocyten Orthosilikat geleitet wird. Kollagen dirigiert die Galektin-Silicatein-Stränge um die

wachsende Nadel herum und ist damit am Aufbau des Biozylinders beteiligt (Schröder et al., 2006), aber ist nicht ursächlich an der Silicatein-vermittelten Biosilikatbildung. Die Galectin-Moleküle werden in Archaeocyten synthetisiert, während die Silicateine in Sklerocyten (Krasko et al., 2000; Krasko et al., 2002) hergestellt werden. Diese Daten implizieren, dass die Zellen, die die strukturellen und funktionellen Moleküle synthetisieren, sowohl die Synthese der Nadeln sowie die Wachstumsrichtung und die Spezies-spezifische Form und Größe über extrinsische (Silikat) und intrinsische Mediatoren (Myotrophin) kontrollieren. Dieses Zusammenspiel der Moleküle ist aber auch entscheidend abhängig von der Verfügbarkeit von Retinoiden, die von symbiotischen Bakterien gebildet werden. Sie kontrollieren die Prozessierung von Silintaphin-2, welches wiederum Ca^{2+}-Ionen liefert, die zur Bildung des organischen Zylinders benötigt werden.

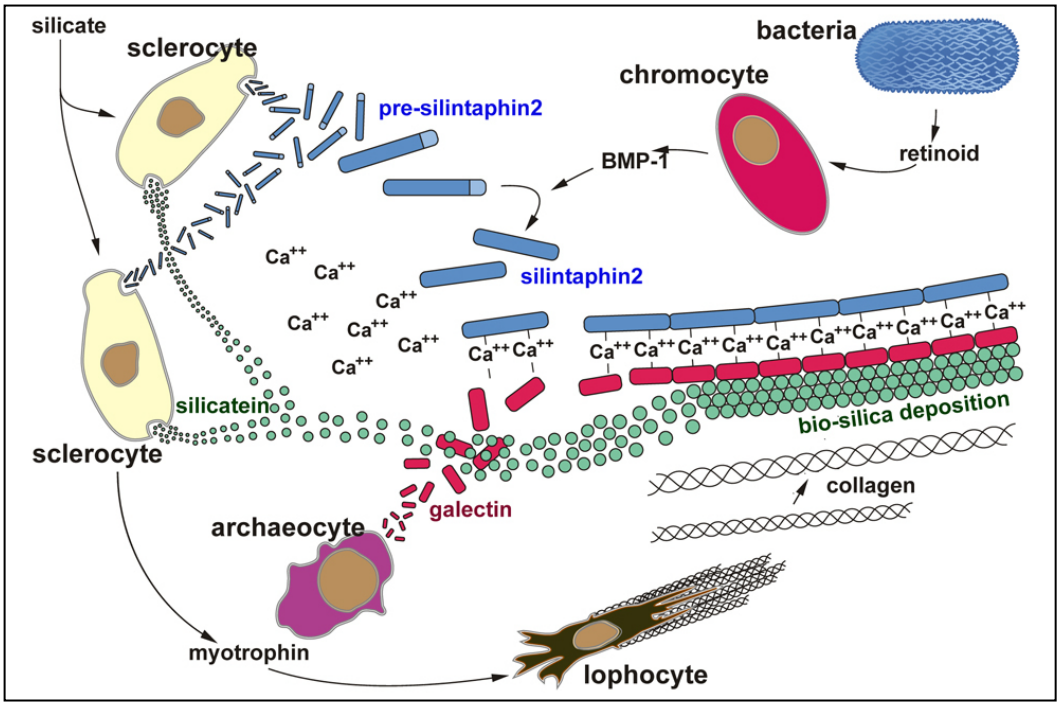

Abb. 1.9: Schematische Darstellung der in die Spiculasynthese involvierten Zelltypen und deren produzierten funktionellen und strukturellen Moleküle. Die drei Hauptkomponenten, die zur Bildung des organischen Zylinders mittels radialer und appositioneller Silikatablagerung erforderlich sind, werden in den Sklerocyten (Silicateine, Silintaphin-2) und in den Archaeocyten (Galektin) gebildet. Die Expression von Silicateinen und Silintaphin-2 wird durch Silikat aktiviert. Myotrophin, welches die Kollagensynthese in Lophocyten reguliert, wird von den Sklerocyten produziert. Das pre-Silintaphin-2 wird durch BMP-2 mittels Proteolyse zum funktionell aktiven Protein prozessiert. Die Bildung von BMP-2 wird durch Retinsäure reguliert, die aus bakteriellen Retinoid-Vorläufern in Chromocyten gebildet wird.

Referenzen

Adell T., Nefkens I. & Müller W.E.G. (2003). Polarity factor “frizzled” in the demosponge *Suberites domuncula*: Identification, expression and localization of the receptor in the epithelium/pinacoderm. *FEBS Lett* 554, 363-368.

Aittaleb M. Gao G. Evelyn C.R., Neubig R.R. & Tesmer J.J.G. (2009). A conserved hydrophobic surface of the LARG pleckstrin homology domain is critical for RhoA activation in cells. *Cell Signal* 21, 1569-1578.

Aizenberg J., Sundar V.C., Yablon A.D., Weaver J.C. & Chen G. (2004). Biological glass fibers: correlation between optical and structural properties. *Proc Natl Acad Sci USA* 101, 3358–3363.

Amano S., Scott I.C., Takahara K., Koch M., Champliaud M.F., Gerecke D.R., Keene D.R., Hudson D.L., Nishiyama T., Lee S., Greenspan D.S. & Burgeson R.E. (2000). Bone morphogenetic protein 1 is an extracellular processing enzyme of the laminin 5 gamma 2 chain. *J Biol Chem* 275**,** 22728–22735.

Armirotti A., Damonte G., Pozzolini M., Mussino F., Cerrano C., Salis A., Benatti U. & Giovine M. (2009). Primary Structure and Post-Translational Modifications of Silicatein Beta from the Marine Sponge Petrosia ficiformis (Poiret, 1789). *J Proteome Res* 8, 3995-4004.

Biesalski H.K., Doepner G., Tzimas G., Gamulin V., Schröder H.C., Batel R., Nau H. & Müller W.E.G. (1992). Modulation of *myb* gene expression in sponges by retinoic acid. *Oncogene* 7, 1765–1774.

Brinker C.J. & Scherer G.W. (1990). Sol-Gel Science: The Physics and Chemistry of Sol-Gel Processing. Boston: *Academic Press.*

Brutchey R.L. & Morse D.E. (2008). Silicatein and the Translation of its Molecular Mechanism of Biosilicification into Low Temperature Nanomaterial Synthesis. *Chem Rev* 108, 4915-4934.

Calamita G., Mazzone A., Bizzoca A., Cavalier A., Cassano G., Thomas D. & Svelto M. (2001). Expression and immunolocalization of the aquaporin-8 water channel in rat gastrointestinal tract. *Eur J Cell Biol* 80, 711-719.

Cattaneo-Vietti R., Bavestrello G., Cerrano C., Sarà A., Benatti U., Giovine M. & Gaino E. (1996). Optical fibres in an Antarctic sponge. *Nature* 383, 397–398.

Cha J.N., Shimizu K., Zhou Y., Christianssen S.C., Chmelka B.F., Stucky G.D. & Morse D.E. (1999). Silicatein filaments and subunits from a marine sponge direct the polymerization of silica and silicones in vitro. *Proc Natl Acad Sci USA* 96, 361-365.

Coradin T. & Lopez P.J. (2003**).** Biogenic silica patterning: simple chemistry or subtle biology? *ChemBiochem* 4, 251-259.

Croce G., Frache A., Milanesio M., Marchese L., Causà M., Viterbo D., Barbaglia A., Bolis V., Bavestrello G., Cerrano C., Benatti U., Pozzolini M., Giovine M. & Amenitsch H. (2004). Structural characterization of siliceous spicules from marine sponges. *Biophys J* 86, 526-534.

Davies J.A. (2005). Mechanisms of Morphogenesis. Amsterdam:*Elsevier-Academic Press.*

Eckert C., Schröder H.C., Brandt D., Perovic-Ottstadt S. & Müller W.E.G. (2006). A histochemical and electron microscopic analysis of the spiculogenesis in the demosponge *Suberites domuncula*. *J Histochem Cytochem* 54, 1031-1040.

Ehrlich H., Deutzmann R., Brunner E., Cappellini E., Koon H., Solazzo C., Yang Y, Ashford D., Thomas-Oates J., Lubeck M., Baessmann C., Langrock T., Hoffmann R., Wörheide G., Reitner J., Simon P., Tsurkan M., Ereskovsky A.V., Kurek D., Bazhenov V.V., Hunoldt S., Mertig M., Vyalikh D.V., Molodtsov S.L., Kummer K., Worch H., Smetacek V. & Collins M.J. (2010). Mineralization of the meter-long biosilica structures of glass sponges is templated on hydroxylated collagen. *Nature Chem* 2, 1084-1088.

Ellis J. (1796). The Natural History of Many Curious and Uncommon Zoophytes, Collection from Various Parts of the Globe. London:*Benjamin White*.

Fairhead M., Johnson K.A., Kowatz T., Mcmahon S.A., Carter L.G., Oke M., Liu H., Naismith J.H. & Van der Walle C.F. (2008). Crystal structure and silica condensing activities of silicatein α-cathepsin L chimeras. *Chem Commun* 21, 1765–1767.

Flory P.J. & Semlyen J.A. (1966). Macrocyclization equilibrium constants and the statistical configuration of poly (dimethylsiloxane) chains. *J Am Chem Soc* 88, 3209–3212.

Fröhlich H. & Bartel, D. (1997). Silica uptake of the *Halichondria panicea* in Kiel Bight. *Mar. Biol.* 128, 115–125.

Gehring W.J. & Ikeo K. (2009). Pax 6: mastering eye morphogenesis and eye evolution. *Trends Genet* 15, 371-377.

George M. (2005). Rigid biological systems as models for synthetic composites. *Science* 310, 1144-1147.

Gierer A. (1977). Physical aspects of tissue evagination and biological form. *Q Rev Biophy* 10, 529-93.

Gray J.E. (1825). On the chemical composition of sponges. *Ann Philos* NS9, 431–432.

Greenberg S.A. & Sinclair D. (1955). The polymerization of silicic acid. *J Phys Chem* 59*,* 435-440.

Hench L.L. (1998). Sol–gel Silica: Properties, Processing, and Technology Transfer, *Noyes Publications*, Westwood.

Huang P., Lazarowski E.R., Tarran R., Milgram S.L., Boucher R.C. & Stutts M.J. (2001). Compartmentalized autocrine signaling to cystic fibrosis transmembrane conductance regulator at the apical membrane of airway epithelial cells. *Proc Natl Acad Sci USA* 98, 14120-14125.

Imsiecke G., Steffen R., Custodio M., Borojevic R. & Müller W.E.G. (1995). Formation of spicules by sclerocytes from the freshwater sponge *Ephydatia muelleri* in short-term cultures *in vitro*. *In Vitro Cell Dev Biol* 31, 528-535.

Koopman P., Schepers G., Brenner S. & Venkatesh B. (2004). Origin and diversity of the Sox transcription factor gene family: genome-wide analysis in *Fugu rubripes*. *Gene* 328, 177-186.

Krasko A., Gamulin V., Seack J., Steffen R., Schröder H.C. & Müller W.E.G. (1997). Cathepsin, a major protease of the marine sponge *Geodia cydonium*: Purification of the enzyme and molecular cloning of cDNA. *Molec Marine Biol & Biotechnol* 6, 296-307.

Krasko A., Batel R., Schröder H.C., Müller I.M. & Müller W.E.G. (2000). Expression of silicatein and collagen genes in the marine sponge *Suberites domuncula* is controlled by silicate and myotrophin. *Eur J Biochem* 267, 4878-4887.

Krasko A., Schröder H.C., Batel R., Grebenjuk V.A., Steffen R., Müller I.M. & Müller W.E.G. (2002). Iron induces proliferation and morphogenesis in primmorphs from the marine sponge *Suberites domuncula*. *DNA & Cell Biol* 21, 67-80.

Kruse M., Leys S.P., Müller I.M. & Müller W.E.G. (1998). Phylogenetic position of Hexactinellida within the phylum Porifera based on amino acid sequence of the protein kinase C from *Rhabdocalyptus dawsoni. J Molec Evolution* 46, 721-728.

Levy O., Appelbaum L., Leggat W., Gothlif Y., Hayward D.C., Miller D.J. & Hoegh-Guldberg O. (2007). Light-responsive cryptochromes from a simple multicellular animal, the coral *Acropora millepora*. *Science* 318, 467-470.

Leys S.P., Mackie G.O. & Reiswig H.M. (2007). The biology of glass sponges. *Adv Mar Biol* 52, 1-145.

Lobel K.D., West J.K. & Hench L.L. (1996). Computational model for protein-mediated biomineralization of the diatom frustule. *Mar Biol* 126, 353-360.

Maldonado M., Carmona M.C., Velásquez Z., Puig M.A., Cruzado A., López A. & Young C.M. (2005). Siliceous sponges as a silicon sink: An overlooked aspect of benthopelagic coupling in the marine silicon cycle. *Limnol Oceanog* 50, 799-809.

Minchin E.A. (1909). Sponge-spicules. A summary of present knowledge. *Erg Fortschr Zool* 2, 171–274.

Morse D.E. (1999). Silicon biotechnology: harnessing biological silica production to construct new materials. *Trends Biotechnol* 17, 230–232.

Müller W.E.G., Blumbach B., Wagner-Hülsmann C. & Lessel U. (1997). Galectins in the phylogenetically oldest metazoa, the sponges [Porifera]. *Trends Glycosci Glycotechnol* 9, 123-130.

Müller W.E.G. (ed.) (2003a). Silicon Biomineralization: Biology-Biochemistry. Molecular Biology-Biotechnology. *Progress Molecular Subcellular Biology*. Vol. 33, Springer, Berlin.

Müller W.E.G., Wiens M., Adell T., Gamulin V., Schröder H.C. & Müller I.M. (2004). Bauplan of urmetazoa: Basis for genetic complexity of Metazoa. *Intern Review of Cytology* 235, 53-92.

Müller W.E.G., Rothenberger M., Boreiko A., Tremel W., Reiber A. & Schröder H.C. (2005a). Formation of siliceous spicules in the marine demosponge *Suberites domuncula. Cell Tissue Res* 321, 285-297.

Müller W.E.G. (2006a). The stem cell concept in sponges (Porifera): metazoan traits. *Seminars in Cell & Develop Biol* 17, 481–491.

Müller W.E.G., Belikov S.I., Tremel W., Perry C.C., **Gieskes W.W.C.**, **Boreiko A. & Schröder H.C. (2006b).** Siliceous spicules in marine demosponges (example *Suberites domuncula*). *Micron* 37, 107-120.

Müller W.E.G., Boreiko A., Schloßmacher U., Wang X.H., Tahir M.N., Tremel W., Brandt D., Kaandorp J.A. & Schröder H.C. (2007a). Fractal-related assembly of the axial filament in the demosponge *Suberites domuncula*: relevance to biomineralization and the formation of biogenic silica. *Biomaterials* 28, 4501-4511.

Müller W.E.G., Boreiko A., Wang X.H., Belikov S.I., Wiens M., Grebenjuk V.A., Schloßmacher U. & Schröder H.C. (2007h). Silicateins, the major biosilica forming enzymes present in demosponges: protein analysis and phylogenetic relationship. *Gene* 395, 62–71.

Müller W.E.G., Jochum K., Stoll B. & Wang X.H. (2008c). Formation of giant spicule from quartz glass by the deep sea sponge Monorhaphis. *Chem Mate*r 20, 4703–4711.

Müller W.E.G., Wang X.H., Kropf K., Boreiko A., Schloßmacher U., Brandt D., Schröder H.C. & Wiens M. (2008d). Silicatein expression in the hexactinellid *Crateromorpha meyeri*: the lead marker gene restricted to siliceous sponges. *Cell Tissue Res* 333, 339–351.

Müller W.E.G., Schloßmacher U., Wang X.H., Boreiko A., Brandt D., Wolf S.E., Tremel W. & Schröder H.C. (2008g). Poly(silicate)-metabolizing silicatein in siliceous spicules and silicasomes of demosponges comprises dual enzymatic activities (silica-polymerase and silica-esterase). *FEBS J* 275, 362–370.

Müller W.E.G., Wang X.H., Burghard Z., Bill J., Krasko A., Boreiko A., Schloßmacher U., Schröder H.C. & Wiens M. (2009c). Bio-sintering processes in hexactinellid sponges: Fusion of bio-silica in giant basal spicules from Monorhaphis chuni. *J Struct Biol* 168, 548–561.

Müller W.E.G., Wang X.H., Cui F.Z., Jochum K.P., Tremel W., Bill J., Schröder H.C., Natalio F., Schloßmacher U. & Wiens M. (2009d). Sponge spicules as blueprints for the biofabrication of inorganic-organic composites and biomaterials. *Appl Microbiol Biotechnol* 83, 397-413.

Müller W.E.G., Kasueske M., Wang X.H., Schröder H.C., Wang Y., Pisignano D. & Wiens M. (2009h). Luciferase a light source for the silica-based optical waveguides (spicules) in the demosponge *Suberites domuncula. Cell Mol Life Sci* 66, 537-552.

Müller W.E.G., Wang X.H., Schröder H.C., Korzhev M., Grebenjuk V.A., Markl J.S., Jochum K.P., Pisignano D. & Wiens M. (2010). A cryptochrome-based photosensory system in the siliceous sponge *Suberites domuncula* (Demospongiae). *FEBS J* 277, 1182-1201.

Müller W.E.G., Wang X.H., Sinha B., Wiens M., Schröder H.C. & Klaus Jochum P. (2010b). NanoSIMS: Insights into the organization of the proteinaceous scaffold within hexactinellid sponge spicules. *ChemBioChem* 11, 1077-1082.

Müller W.E.G., Wang X.H., Schröder H.C., Korzhev M., Grebenjuk V.A., Markl J. S., Jochum K.P., Pisignano D. & Wiens M. (2010h). A cryptochrome-based photosensory system in the siliceous sponge *Suberites domuncula* (Demospongiae). *FEBS J*: 277, 1182-1201.

Müller W.E.G., Wang X.H., Wiens M., Schloßmacher U., Jochum K.P. & Schröder H.C. (2011g). Hardening of bio-silica in sponge spicules involves an aging process after its enzymatic polycondensation: Evidence for an aquaporin-mediated water absorption. *Biochim. Biophys. Acta [General Subjects]* 1810, 713–726.

Murr M.M. & Morse D.E. (2005). Fractal intermediates in the self-assembly of silicatein filaments. *Proc Natl Acad Sci USA* 102, 11657-11662.

Nomura T., Fujishima A. & Fujisawa Y. (1996). Characterization and crystallization of recombinant human cathepsin L. *Biochem Biophys Res Commun* 228, 792-796.

Pasteur M.L. (1857). Mémoire sur la fermentation alcoolique. Comptes Rendue de L' Acad Scien 45, 1032-1036.

Perović-Ottstadt S., Schröder H.C., Batel R., Giovine M., Wiens M., Krasko A., Müller I.M. & Müller W.E.G. (2005). Arginine kinase in the demosponge *Suberites domuncula*: Regulation of its expression and catalytic activity by silicic acid. *J Exp Biol* 208, 637-646.

Perry C.C. (2003). Silicification: the processes by which organisms capture and mineralize silica. Rev. Miner. *Geochem* 54, 291-327.

Philipp I., Aufschnaiter R., Özbek S., Pontasch S., Jenewein M., Watanabe H., Rentzsch F, Holstein T.W. & Hobmayer B. (2009). Wnt/ß-Catenin and noncanonical Wnt signalling interact in tissue evagination in the simple eumetazoan *Hydra*. *Proc Natl Acad Sci USA* 106, 4290-4295.

Pozzolini M., Sturla L., Cerrano C., Bavestrello G., Camardella L., Parodi A.M., Raheli F., Benatti U., Müller W.E.G. & Giovine M. (2004). Molecular cloning of silicatein gene from the marine sponge *Petrosia ficiformis* (Porifera, Demospongiae) and development of primmorphs as a model for biosilicification studies. *Marine Biotechnol* 6, 594-603.

Sandford F. (2003). Physical and chemical analysis of the siliceous skeleton in six sponges of two groups (Demospongiae and Hexactinellida). *Microsc Res Tech* 62, 336–355.

Schloßmacher U., Wiens M., Schröder H.C., Wang X.H., Jochum K.P. & Müller W.E.G. (2011). Silintaphin-1: Interaction with silicatein during structure guiding biosilica formation. *FEBS J* 278, 1145-1155.

Schröder H.C., Krasko A., Le Pennec G., Adell T., Wiens M., Hassanein H., Müller I.M. & Müller W.E.G. (2003). Silicase, an enzyme which degrades biogenous amorphous silica: contribution to the metabolism of silica deposition in the demosponge *Suberites domuncula*. *Prog Mol Subcell Biol* 33, 250–268.

Schröder H.C., Perović-Ottstadt S., Rothenberger M., Wiens M., Schwertner H., Batel R., Korzhev M., Müller I.M. & Müller W.E.G. (2004). Silica transport in the demosponge *Suberites domuncula*: fluorescence emission analysis using the PDMPO probe and cloning of a potential transporter. *Biochem J* 381, 665–673.

Schröder H.C., Perović-Ottstadt S., Grebenjuk V.A., Engel S., Müller I.M. & Müller W.E.G. (2005a). Biosilica formation in spicules of the sponge *Suberites domuncula*: Synchronous expression of a gene cluster. *Genomics* 85, 666-678.

Schröder H.C., Boreiko A., Korzhev M., Tahir M.N., Tremel W., Eckert C., Ushijima H., Müller I.M. & Müller W.E.G. (2006). Co-Expression and functional interaction of silicatein with galectin: matrix-guided formation of siliceous spicules in the marine demosponge *Suberites domuncula*. *J Biol Chem* 281, 12001-12009.

Schröder H.C., Natalio F., Shukoor I., Tremel W., Schloßmacher U., Wang X.H. & Müller W.E.G. (2007b). Apposition of silica lamellae during growth of spicules in the demosponge *Suberites domuncula*: biological/biochemical studies and chemical/biomimetical confirmation. *J Struct Biol* 159, 325-334.

Schröder H.C., Wiens M., Schloßmacher U., Brandt D. & Müller W.E.G. (2011). Silicatein-mediated polycondensation of orthosilicic acid: Modeling of catalytic mechanism involving ring formation. *Silicon*; DOI: 10.1007/s12633-010-9057-4

Schulze, F.E. (1885). The Hexactinellida. Pp. 437–451. in T. H. Tizard, H. N. Moseley, J. Y. Buchanan and J. Murray, eds., Report on the Scientific Results of the Voyage of H.M.S. Challenger during the years 1873–1876, under the command of Captain George S. Nares, R.N., F.R.S. and the late Captain Frank Tourle Thomson, R.N. Narrative –Vol. I. *Longmans & Co.*, London.

Schulze F.E. (1904). Hexactinellida. Wissenschaftliche Ergebnisse der Deutschen Tiefsee–Expedition auf dem Dampfer "Valdivia" 1898–1899. *Fischer,* Stuttgart.

Shimizu K., Cha J., Stucky G.D. & Morse D.E. (1998). Silicatein alpha: cathepsin L-like protein in sponge biosilica. *Proc Natl Acad Sci* USA 95, 6234-6238.

Simpson T.L. (1984). The Cell Biology of Sponges, *Springer-Verlag*, Berlin, Heidelberg, New York, Tokyo.

Strehler B.L. & McElroy W.D. (1949). Purification of firefly luciferin. *J Cell Physiol* 34, 457-466.

Turkenburg J.P., Lamers M.B., Brzozowski A.M., Wright L.M., Hubbard R.E., Sturt S.L. & Williams D.H. (2002). Structure of a Cys25→Ser mutant of human cathepsin S. *Acta Crystallogr D Biol Crystallogr* 58, 451–455.

Uriz M.J. (2006). Mineral spiculogenesis in sponges. *Can J Zool* 84, 322-356.

Wang X.H., Boreiko A., Schloßmacher U., Brandt D., Schröder H.C., Li J., Kaandorp J.A., Götz H., Duschner H. & Müller W.E.G. (2008c). Axial growth of hexactinellid spicules: formation of cone-like structural units in the giant basal spicules of the hexactinellid *Monorhaphis. J Struct Biol* 164, 270–280.

Wang X.H. & Müller W.E.G. (2009). Marine biominerals: perspectives and challenges for polymetallic nodules and crusts. *Trends Biotechnol* 27, 375-383.

Wang X.H., Schröder H.C. & Müller W.E.G. (2009c). Giant siliceous spicules from the deep-sea glass sponge *Monorhaphis chuni*: morphology, biochemistry and molecular biology. *Int Rev Cell Mol Biol* 273, 69-115.

Wang X.H., Wiens M., Schröder H.C., Hu S., Mugnaioli E., Kolb U., Tremel W., Pisignano D. & Müller W.E.G. (2010). Morphology of sponge spicules: silicatein a structural protein for bio-silica formation. *Advanced Biomaterials/Advanced Engineering Mat* 12, B422- B437.

Wang X.H., Wiens M., Schröder H.C., Schloßmacher U., Pisignano D., Jochum K.P. & Müller W.E.G. (2011). Evagination of cells controls bio-silica formation and maturation during spicule formation in sponges. *PLoS ONE*; 6, e20523.

Wang X.H., Schlossmacher U., Wiens M.,Batel R., Schröder H.C. & Müller W.E.G. (2012). Silicateins, silicatein interactors and cellular interplay in sponge skeletogenesis: formation of glass fiber-like spicules. *FEBS J.* 279, 1721-1736.

Weiner S. & Dove P.M. (2003). An overview of biomineralization processes and the problem of the vital effect. *Rev. Mineral. Geochem*. 54, 1–29.

Wiens M., Wrede P., Grebenjuk V.A., Kaluzhnaya O.V., Belikov S.I., Schröder H.C. & Müller W.E.G. (2009a). Towards a molecular systematics of the Lake Baikal/Lake Tuva Sponges. In: WEG Müller and MA Grachev (eds) Biosilica in Evolution, Morphogenesis, and Nanobiotechnology. *Progress in Molecular and Subcellular* Biology [Marine Molecular Biotechnology] vol. 47, Berlin Heidelberg:Springer-Verlag. Pp. 111-144.

Wiens M., Bausen M., Natalio F., Link T., Schlossmacher U. & Müller W.E.G. (2009b). The role of the silicatein-a interactor silintaphin-1 in biomimetic biomineralization. *Biomaterials*. 30, 1648-56

Wiens M., Wang X.H., Schröder H.C., Kolb U., Schloßmacher U., Ushijima H. & Müller W.E.G. (2010). The role of biosilica in the osteoprotegerin/RANKL ratio in human osteoblast-like cells. *Biomaterials* 31, 7716-7725.

Wiens M., Wang X.H., Unger A., Schröder H.C., Grebenjuk V.A., Pisignano D., Jochum K.P. & Müller W.E.G. (2010h). Flashing light signaling circuit in sponges: endogenous light generation after tissue ablation in *Suberites domuncula*. *J Cell Biochem* 111, 1377–1389.

Wiens M., Schröder H.C., Wang X.H., Link T., Steindorf D. & Müller W.E.G. (2011a). Isolation of the silicatein-α interactor silintaphin-2 by a novel solid-phase pull-down assay. *Biochemistry* 50, 1981-1990.

Woesz A., Weaver J.C., Kazanci M., Dauphin Y., Aizenberg J., Morse D.E. & Fratzl P. (2006). Micromechanical properties of biological silica in skeletons of deep-sea sponges. *J Mater Res* 21, 2068-2078.

Wöhler F. (1828). Über künstliche Bildung des Harnstoffs. *Annalen der Physik und Chemie* 12, 253-256.

Wolf S.E., Schloßmacher U., Pietuch A., Mathiasch B., Schröder H.C., Müller W.E.G & Tremel W. (2010). Formation of silicones mediated by the sponge enzyme silicatein-α. *Dalton Trans* 39, 9245–9249.

Zhou Y., Shimizu K., Cha J.N., Stucky G.D. & Morse D.E. (1999). Efficient catalysis of polysiloxane synthesis by silicatein α requires specific hydroxy and imidazole functionalities. *Angew Chem Int Ed* 38, 780-782.

Chapter 2

Fractal-related assembly of the axial filament in the demosponge *Suberites domuncula*: relevance to bio-mineralization and the formation of biogenic silica

2.1 Introduction

The sponges as the phylogenetically oldest metazoan phylum (Müller, 1998 a; Müller, 1998 b) are characterized by a distinct body plan, which is organized – in contrast to that of most other, higher metazoan phyla – along only one body axis (reviewed in Müller, 2005). It runs in apical-basal direction, while most triploblastic metazoans are organized along an anteroposterior and a dorso-ventral axis. Surely the form and hence the body plan of sponges is genetically controlled, since the size and shape of a given species are defined; e.g. the morphology of the species *Tethya aurantium* is the same in the littoral of the Pacific Ocean around California and in the Mediterranean Sea – or, *Suberites domuncula* in the North Sea, Atlantic Ocean or in the Mediterranean Sea (Arndt 1935) are the same. In the last years a bulk of information became available about the genetic basis of cell-cell and cell-tissue interactions in sponges, e.g. about the integrin system (Pancer et al., 1997), the differentiation of cells, e.g. stem cells (Müller et al., 2004), the axis formation of the body, e.g. the Wnt pathway (Adell et al., 2003), or the immune system, e.g. cytokines or immunoglobulin (Müller et al., 1999). Most of the studies were performed with the demosponge *S. domuncula* (reviewed in Müller et al., 1999). However, one major morphogenetic process remained enigmatic (reviewed in Müller, 2005), it is the regulatory systems controlling the skeleton formation in sponges. It is well established that the skeletal elements of sponges in general and of the Demospongiae in particular, the siliceous spicules, have species-specific sizes, forms and shapes. The spicules are subdivided into megascleres [up to 400 µm], and microscleres [≤ 10 µm] (Uriz et al., 2003). In *S. domuncula* only two types of spicules (megascleres) can be distinguished, monactinal tylostyles and a smaller fraction of diactinal oxeas (Arndt, 1935). The morphology of megascleres in demosponges has been investigated and was found to consist of an axial canal around which silica layers are deposited (Uriz et al., 2003). The axial canal harbors the axial filament which is composed of silicatein. This protein had first been studied in *T. aurantium*

(Cha et al., 1999) and subsequently in *S. domuncula* (Krasko et al., 2000). Originally it was described that in the marine demosponge *T. aurantium* three subunits of silicatein exist, –α, – β and –γ (Cha et al., 1999); however, it turned out that only two genes are present in marine demosponges (Krasko et al., 2002), while over four different isotypes have been described in freshwater sponges, e.g. in the endemic Lake Baikal species *Lubomirskia baicalensis* (Müller et al., 2007h). Silicatein is extensively posttranslationally modified, e.g. phosphorylated (Müller et al., 2005a; Müller et al., 2006b). The formation/growth of the spicules was recently elucidated to some detail. The initial synthesis of spicules starts intracellularly (Müller et al., 2005a; Müller et al, 2005a); there the first silica layer is deposited. Subsequently, the immature spicules are extruded from the cells and completed in the extracellular space of the mesohyl by appositional deposition of silica layers, until the 450 µm long and 5 to 7 µm thick spicules have been completed in *S. domuncula* (Müller et al., 2005a, Müller et al., 2006b). Efforts have been undertaken to understand the morphogenetic basis of the size and shape formation of the spicules. In order to approach the question whether it is the axial filament itself, which contributes to the shape formation of the spicules a new, mild extraction procedure was introduced (Schröder et al., 2006). Previously, hydrofluoric acid (HF) had been used to isolate the axial filaments of the spicules; a procedure which is known to cause cleavage of modify phosphate groups of proteins (Kröger et al., 1999; Kröger et al., 2002). For the new, mild extraction procedure, applied here, 4 M urea was used instead of HF to solubilize the axial filament from the silica shell (Schröder et al., 2006). Using this mild extraction procedure, a silicatein preparation was obtained which comprised considerably higher bio-silica formation/condensation activity, compared to samples obtained by HF-extraction. A further progress in the understanding of spiculogenesis, the formation of species-specific spicules with respect to form and size, was achieved by the demonstration that collagen is involved in shaping the size/form of the spicules (Eckert et al., 2006). It remained, however, so far unsolved whether the formation of the collagen fibers around the spicules is the result or the cause of a morphogenetic process during spiculogenesis. Since the cells in demosponges are embedded in a large extracellular matrix within the mesohyl, and there, only loosely attached, it is difficult to conceive how extracellular factors could contribute to the distinct morphology of spicules. We tried to support thoroughly, however without success, the possibility that during the maturation of the spicules cells within the axial filaments of

the spicules exist. Those cells would have given sufficient reason to assume that they are the structure/form-introducing elements during spiculogenesis. Therefore, the recently proposed self-assembly proposition, via fractal intermediates, of silicatein to stabile silicatein filaments became attractive (Murr et al., 2005). The authors proposed that the axial filament self-assembles from silicatein molecules [mono-/oligomers] through the formation of fractally patterned aggregates. In in vitro experiments these authors showed that HF-isolated axial filaments disassemble into oligomeric units in the presence of guanidine or urea and higher pH. In turn, the self-assembly of filaments from those oligomeric units proceeds progressively from an isotropic state via chaotic and fractal states to the ordered state, the filaments. For this process the oligomers must be transferred into conditions which allow a diffusion limited assembly. This interesting model of fractal assembly of filaments from silicatein mono-/oligomers has a series of open issues: (i) the studies were performed with HF-treated silicatein molecules which lack most of the enzymatic activity, (ii) the electron microscopical images presented, suggesting a fractal network (Murr et al., 2005) is not defined with respect to the proposed three silicatein subunits and (iv) the authors proposed that covalently linked monomers [dimers] of silicateins are the nuclei for the fractal intermediates during filament formation. In the present study we compared the selfassembly properties of the silicateins, obtained by the newly introduced mild extraction conditions, using a Tris/glycerol buffer (“TG-Extract”), with the hitherto used HF extraction procedure (“HF Extract”). Applying the HF extraction procedure, axial filaments are obtained which had to be disassembled by urea (“HF-Extract-Urea”) as described (Murr et al., 2005). This is in contrast to the Tris/glycerol extraction procedure which immediately yielded in mono-/dimeric silicateins. Applying these two preparations it could be demonstrated that self-assembly can – under the electrophoretic conditions used here – only be demonstrated if the silicateins from the “TG-Extract” are used. In contrast, the silicateins in the “HF-Extract-Urea” remained in the mono- /dimeric state. In addition, it is shown that the silicateins present in the “TG-Extract” have the ability to form filaments, via dendritic/rectangular branching structures, suggesting fractal intermediates, until the stabile filaments are formed. The silicateins in the “HFExtract- Urea” formed only non-structured aggregates.

2.2 Experimental section

2.2.1 Chemicals, materials and enzymes

Hybond-N+ nylon membrane from Amersham (Little Chalfont, Buckinghamshire; UK); Cy3-conjugated F(ab')2 goat anti-rabbit IgG from Jackson ImmunoResearch (Cambridgshire; UK); proteinase inhibitor cocktail from Roche (Mannheim; Germany); alkaline phosphatase (AP)-labeled anti-rabbit IgG, Z-Phe-Arg-AMC from Calbiochem (San Diego, CA; USA); casein from Sigma (Deisenhofen, Germany) and cathepsin L (specific activity: 6,354 mU / mg protein units/mg) from Calbiochem (San Diego, CA; USA).

2.2.2 Sponges and spicules

Specimens of the marine sponge *Suberites domuncula* (Porifera, Demospongiae, Hadromerida) were collected in the Northern Adriatic near Rovinj (Croatia), and then kept in aquaria in Mainz (Germany).

2.2.3 Spicular extract

Tris-glycerol procedure: Spicular extracts were prepared as follows. Unfrozen sponge tissue was sliced into 2-3 mm^3 cubes and washed several times with distilled water and then incubated in phosphate-buffered-saline [PBS] (pH 7.2; containing 30 mM ethylenediaminetetraacetic acid [EDTA]) while shaking. Then the suspension was washed again with distilled water. The spicules obtained were air-dried and thoroughly pulverized in mortar using the Tris/glycerol buffer (pH 8.8; 50mM Tris-HCl, 15% glycerol [w/v], 1 mM EDTA, 150 mM NaCl, 5 mM DL-dithiothreitol [DTT]). To obtain silicatein, routinely 100 mg of spicules were grinded with 200 µl of Tris/glycerol buffer; the samples were agitated for 1 hr, centrifuged (10 min at 10,000 x g) and the resulting supernatant [fraction: "TG-Extract"] concentrated with Microcon Centrifugal Filter Devices [cutoff: 3 kDa] (Millipore; 3,000 MWCO) and finally frozen at -20°C. All steps were performed on ice or by 4°C.

2.2.4 HF procedure

Fresh material was sliced and washed with PBS. To obtain spicules, the tissue was soaked in HNO_3/H_2SO_4 (1:4 [v/v]) overnight and the acid-insoluble material (siliceous spicules) was rinsed in distilled water until the pH was 6 and then washed with acetone. After air-drying, the spicules (0.3 g) were treated with 100 ml of 1 M HF/4 M NH_4F (pH 5) until the siliceous spicules were completely dissolved (Shimizu et al., 1998). Then the suspension was dialyzed (3-times) against 5 l of distilled water at 4°C for 4 hrs each. Finally, the "Extract" was centrifuged (20 min; 10,000 x g; 4°C) and, the sediment, containing the axial filaments of the spicules was suspended in Milli-Q water and stored at 4°C [fraction: "HF-Extract"]. Following the procedure of Murr and Morse (Murr et al., 2005) the "HF-Extract" was dissolved against 4 M urea (in 50 mM Tris HCl, pH 8.8; 15% [v/v] glycerol, 1 mM EDTA, 150 mM NaCl, 5 mM DTT). After five min the samples were centrifuged (10,000 x g, 10 min, 4°C); and the supernatant containing the mono-/oligomeric silicatein molecules were collected and taken for the further experiments ["HF-Extract-Urea"]. Prior to the transfer the samples were dialyzed against re-assembly buffer (see below) using the Microcon Centrifugal Filter Devices [cutoff: 3 kDa].

2.2.5 Gel electrophoresis and immunoblotting

Protein samples from the axial filament were dissolved in loading buffer (Roti-Load; Roth, Karlsruhe; Germany) and then subjected to 10% polyacrylamide gel electrophoresis, containing sodium dodecyl sulphate ($NaDodSO_4$-PAGE), according to Laemmli (Laemmli, 1970); the $NaDodSO_4$ concentrations used are given with the respective experiments. If not mentioned otherwise, the gel separation has been performed in the presence of 0.1% $NaDodSO_4$ (0.1% $NaDodSO_4$, 1% β-mercaptoethanol concentration and without preheating) or 0.01% $NaDodSO_4$. After separation the gels were washed in 10% methanol (supplemented with 7% acetic acid) for 30 min and then stained in Coomassie brilliant blue. Usually 1.5 µg (gel electrophoresis) or 20 µg of protein (zymogram) per slot were electrophoresed. Where indicated the samples had been preheated for 5 min at 95°C. Western blotting was performed as described (Müller et al., 2005a). The polypeptides were transferred to PVDF membranes and reacted with anti-silicatein antibodies (PoAb-aSILIC; 1:1,000). The membranes were then rinsed in TBS-T (20 mM Tris-HCl [pH 7.6], 137

mM NaCl, 0.1% Tween-20), supplemented with 5% non-fat dry milk and 1.5% bovine serum albumin. The membranes were washed three times in TBS-T and then incubated for 1 hr with AP-labeled anti-rabbit IgG (1:2,000). The immunocomplexes were visualized with the color develop system NBT/BCIP (Roth). In controls adsorbed PoAb-aSILIC (100 µl of antibodies were incubated with 20 µg of recombinant silicatein rSILIC_SUBDO) was used. With this antibody preparation no signal could be seen in Western blots (Schröder et al., 2006). The blots were scanned with a GS-525 Molecular Imager (Bio-Rad; Hercules, CA; USA) to semiquantitatively determine the amount ratio between the two silicatein isoforms (-α and -β).

2.2.6 Determination of proteinase activity

The proteolytic activity of silicatein was measured fluorometrically with the synthetic substrate for cathepsin L, Z-Phe-Arg-AMC. “HF Extract- Urea” or “TG-Extract” were dialyzes against acetate buffer (pH 5.5; 50 mM Na-acetate buffer, 1 mM EDTA and 0.1 M NaCl) and incubated with the silicateins at the following concentrations; 0.3 µg, 2.5 µg, 5 µg or 10 µg / assay. Prior to the activity determination, the silicatein samples had been pre-incubated for 0 to 180 min, as indicated. The activity was assayed as described (Quian et al., 1989; Mort et al., 2002) at 22 °C for 10 min in a final volume of 200 µl. The reaction was stopped by adding 100 mM monochloro-acetic acid in Sodiumacetate buffer. A standard curve was established with 7-amino-4-methyl-coumarin (AMC) under otherwise identical incubation conditions. The fluorescence of the free AMC released was determined using an excitation at 380 nm and an emission at 460 nm in an F-2000 Hitachi fluorescence spectrophotometer. The activity was calculated and given in nmol AMC released/mg protein x min.

2.2.7 Zymogram gel

Proteins in the “HF-Extract-Urea” or “TGExtract” were loaded onto zymogram gels, which contained 0.1% casein [w/v] essentially as described (Jaffe et al., 2003; Nishimura et al., 1995). 20 µg of the silicateins were applied per slot. The samples were separated by $NaDodSO_4$-PAGE (10% gels, containing 0.01% $NaDodSO_4$); following electrophoresis, the gels were washed for 15 min in the acetate buffer, supplemented with 5 mM DTT, over night at room temperature. The areas where

casein had been digested were visualized by staining with Coomassie Brilliant Blue G250. Where indicated, cathepsin L (50 mU) was loaded onto the gel.

2.3 Results

2.3.1 Analysis of spicule extract

The two silicatein samples ("TG-Extract" as well as the "HF-Extract", after treatment with urea and subsequent centrifugation "HF-Extract-Urea") were electrophoresed under native conditions, in the presence of a low concentration of 0.1% $NaDodSO_4$ and in the absence of heat (Fig. 2.1). The samples remained either untreated or were treated with 5% mM β-mercaptoethanol, prior to gel electrophoresis. The protein band from the "TG-Extract", which had not been treated with β-mercaptoethanol, showed an apparent size of 18 kDa (Fig. 2.1A lane a, b and f), while the molecules after β-mercaptoethanol treatment had a size of 24 kDa (Fig. 2.1A lane c). In contrast, the polypeptides in the "HF-Extract" revealed a size of 24 kDa, irrespective of β-mercaptoethanol treatment (Fig. 2.1 A lane d and e). In order to confirm that the protein band corresponds to silicatein, Western blot analysis was performed (Fig. 2.1 B). In the "TG-Extract" the silicatein showed a size of either 18 kDa if they remained untreated (Fig. 2.1 B lane a, b and f), or 24 kDa after treatment with β-mercaptoethanol (Fig. 2.1 B lane c), while the silicateins in the "HF-Extract" showed identical sizes of 24 kDa, without or with β-mercaptoethanol treatment (Fig. 2.1B lane d and e). Based on the $NaDodSO_4$-PAGE (0.1% $NaDodSO_4$) results we suggest that the slower migrating silicatein represents the unfolded protein (24 kDa), while the faster migrating one is the more globular, folded protein (18 kDa). In turn, these data indicate that the silicateins in the "HF-Extract" exist (very likely) in the unfolded structure, irrespective of a pre-treatment with β-mercaptoethanol.

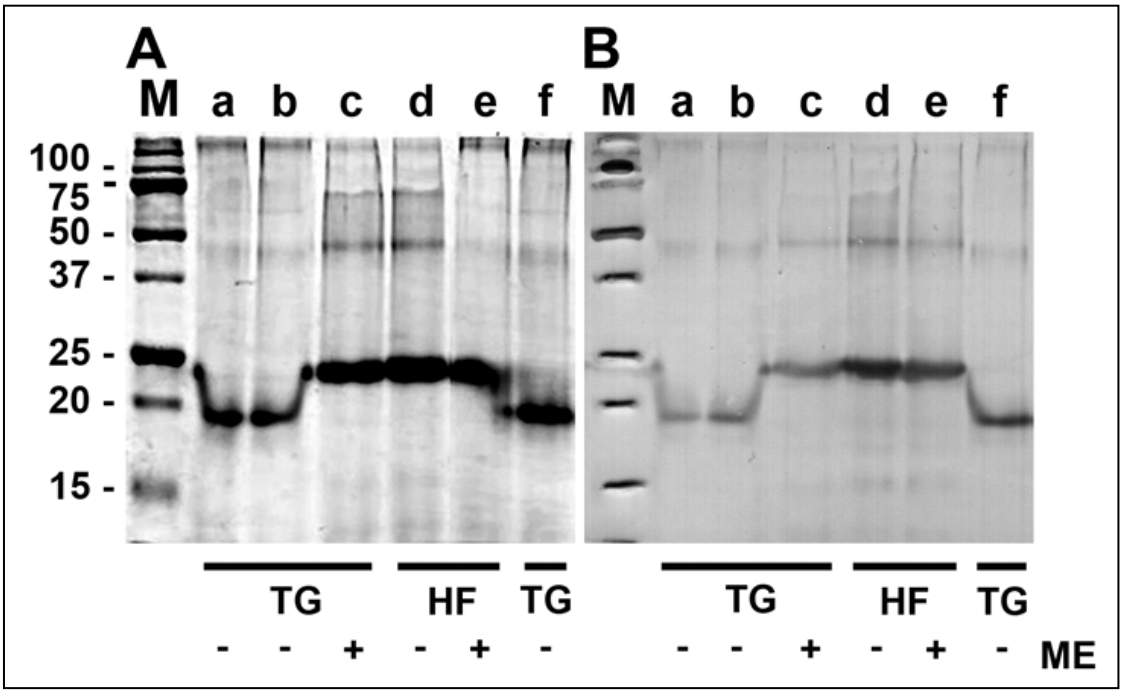

Figure 2.1. Analysis of the silicatein samples ($NaDodSO_4$-PAGE) from‘TG-Extract’’ [TG] and the ‘‘HF-Extract-Urea’’ [HF] after different conditions of sample processing. The samples applied onto the gels remained either without treatment with β-mercaptoethanol [-ME], or were treated with 5% β-mercaptoethanol [+ME] and subjected to $NaDodSO_4$-PAGE (0.1% $NaDodSO_4$; without pre-heating the samples). The samples (1.5 mg/slot) were applied to the gel in the following order. Lanes a and b: ‘‘TG-Extract’’ without β-mercaptoethanol; lane c: ‘‘TG-Extract’’ with β-mercaptoethanol; ‘‘HF-Extract’’ without (lane d) and with β-mercaptoethanol (lane e) and lane f: ‘‘TG-Extract’’ without β-mercaptoethanol. (A) After electrophoresis the gel was stained with Coomassie brilliant blue. (B) Corresponding Western blot; the blot was reacted with PoAb-aSILIC. Size markers are given (M).

2.3.2 Proteinase activity of “HF-Extract-Urea” and “TG-Extract”

The two extracts, “HF-Extract-Urea” and “TG-Extract” were assayed for proteolytic activity using Z-Phe-Arg-AMC as substrate. Incubation conditions were chosen, which had been found to be suitable for the detection of cathepsin L activity (Mort et al., 2002). Taking into account that silicatein has the property to self-assemble, the extracts had been pre-incubated in glycerol-fee buffer for 0 to 180 min, and were subsequently assayed with Z-Phe- Arg-AMC as substrate. The results revealed that both samples showed without pre-incubation only a low proteolytic activity of about 20 nmoles/mg protein x min. However, if the “TG-Extract” samples were pre-

incubated for 60 min or 180 min, a strong increase in the proteolytic activity to 115 nmoles/mg protein x min (60min), and 175 nmoles/mg protein x min (180 min) was measured (Fig. 2.2). In contrast, the activity of the silicatein in the “HF-Extract-Urea” remained unchanged, irrespective of a preincubation treatment (Fig. 2.2).

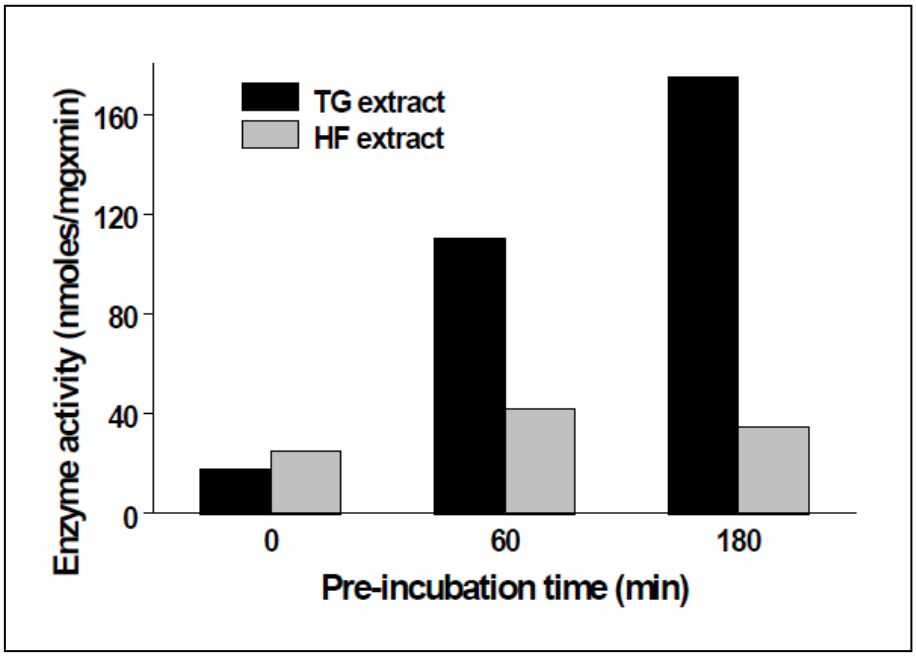

Figure 2.2: Determination of the proteolytic activity displayed by the silicatein samples. Both the ‘‘HF-Extract-Urea’’ [HF] and the ‘‘TG-Extract’’ [TG] were pre-incubated for 0, 60 or to 180 min in the assembly buffer and then assayed in the presence of Z-Phe-Arg-AMC for proteolytic activity, as described under ‘‘Materials and Methods’’. After a 10 min incubation period, the amount of released AMC was determined fluorometrically. The activity is given in nmol AMC released per mg protein x min.

2.3.3 Proteolytic activity (zymogram)

Caseinolytic activities of the silicateins in the “HF-Extract-Urea” or the “TG-Extract” were determined in a zymogram. The samples, containing the disassembled silicateins were incubated in the assembly buffer for 180 min and then applied onto gels for electrophoresis. After overnight incubation at room temperature in acetate buffer with DTT (pH 5.5), the zones of casein digestion had been visualized after staining with Coomassie brilliant blue. The “TG-Extract” showed a pattern of digestion, corresponding to dimers, tetramers and hexamers of silicatein (Fig. 2.3 lane c). Interestingly, on the top of the gel the activity of the polymeric form of silicateins was detectable. In contrast, no caseinolytic activity was seen with a

sample from “HF-Extract-Urea” (Fig. 2.3 lane b). As a standard cathespin L had been separated and found to give a signal at the expected size of 27 kDa (Nishimura et al., 1995); Fig. 2.3 lane a.

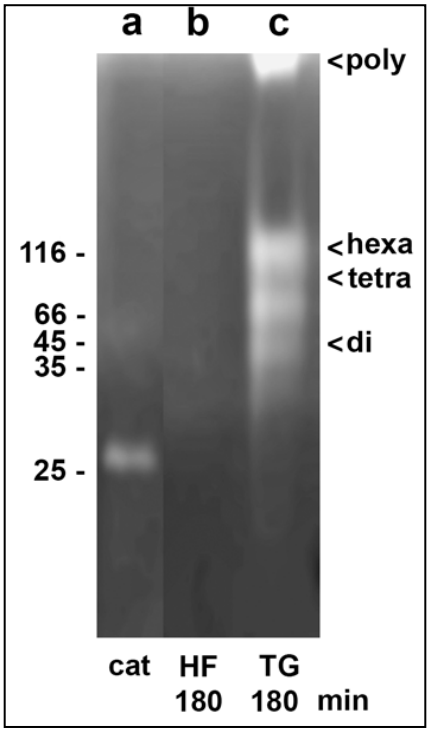

Figure 2.3: Proteolytic activity of protein(s) in ‘‘HF-Extract-Urea’’ (HF; lane b) or ‘‘TG-Extract’’ extracts (TG; lane c); zymogram. In parallel, a sample of cathepsin L (cat; lane a), at a concentration of 0.65 mg/ml, was loaded onto the gel. After size separation the gels were incubated over night at room temperature to identify the zones of proteolytic digestion. The migration distances of dimers (di), tetramers (tetra) and hexamers (hexa) of silicatein are marked; at the top of the gel the proteolytic digestion of polymeric silicatein (poly) is seen.

2.3.4 Filament/aggregate formation from disassembled silicatein

In a first series of experiments ‘‘TG-Extract’’ was transferred to the re-assembly buffer and allowed to form aggregates/filaments during incubation periods of 0, 15, 60 or 120 min (Fig. 2.4 A–D). After reaction with anti-silicatein antibodies and subsequent light microscopic analysis, first filamentous structures were visualized after 60 min with a length of 100–150 mm (Fig. 2.4 C). In contrast, if ‘‘HF-Extract-Urea’’ was processed in the same way, no or only short (<10 µm) filaments were seen; predominantly only random aggregates were seen (Fig. 2.4 E and F).

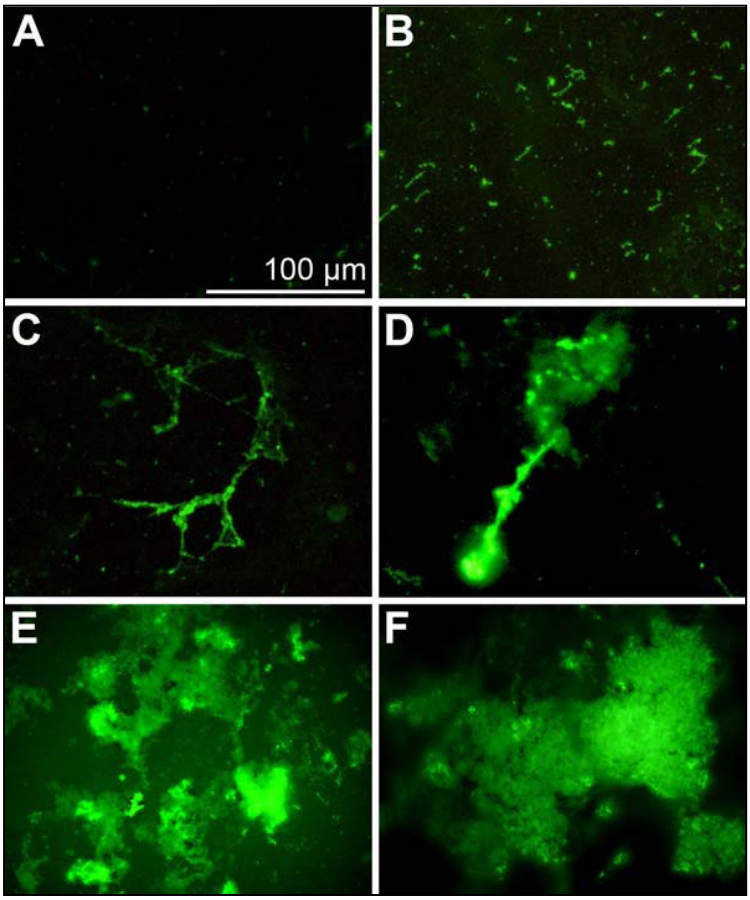

Figure 2.4: Self-assembly of silicatein mono-/dimers present in ‘‘TG-Extract’’ or in ‘‘HF-Extract-Urea’’. Samples of ‘‘TG-Extract’’ or of ‘‘HF-Extract-Urea’’ were incubated in the re-assembly buffer. (A–D) Reassembly products of silicateins from a ‘‘TG-Extract’’ after transfer to the glycerol-free buffer; samples were taken immediately (0 min) (A), after 15 min (B), after 60 min (C) or after 120 min (D). The specimens were reacted with anti-silicatein antibodies PoAb-aSILIC and the immunocomplexes were visualized with labeled secondary antibodies. (E and F) Reassembly of silicateins from ‘‘HF-Extract-Urea’’. Samples were taken 60 min (E) or after 120 min (F) after transfer into the reassembly buffer.

In order to support these light microscopical images, electron microscopical studies (TEM) were performed. Both, the ‘‘TG-Extract’’ and the ‘‘HF-Extract-Urea’’ preparations were allowed to re-assemble during a preincubation period between 0 and 180 min (Fig. 2.5). These analyses revealed that first filamentous structures are formed after an incubation period of 30 min (Fig. 2.5 C) from the mono-/dimeric silicateins (Fig. 2.5 A and B). These filaments increase in size during a prolonged incubation period to about 1.5 µm (60 min; Fig. 2.5 D), 2 µm (120 min; Fig. 2.5 E), or 5 µm (180 min; Fig. 2.5 F) long filaments. The filaments show a characteristic

dendritic/rectangular branching pattern (Fig. 2.6 D–F) No regular filament formation could be detected in silicatein samples, present in the ‘‘HF-Extract-Urea’’ from *S. domuncula*. Under otherwise identical conditions only irregular clumps, which reach sizes of 1–1.5 µm, were seen (Fig. 2.5 G–I).

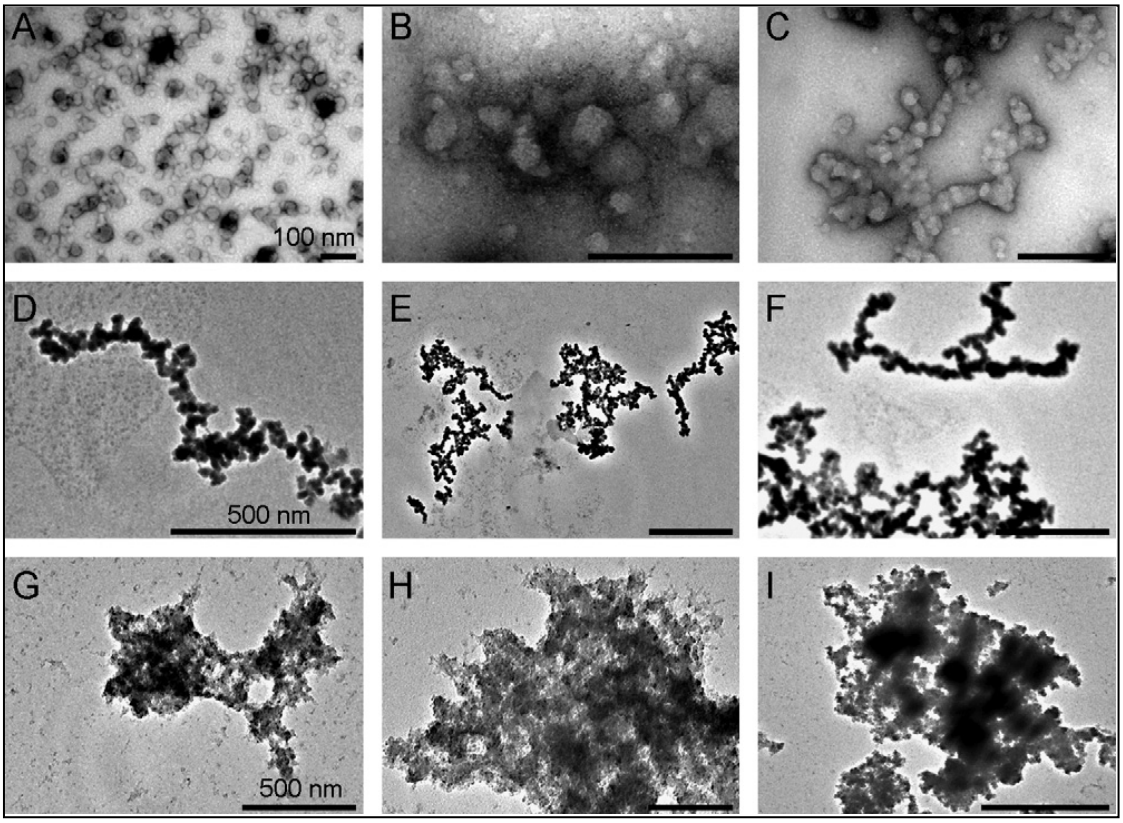

Figure 2.5: Electron microscopical analysis (TEM) of polymerized silicatein from axial filaments. (A–F) ‘‘TG-Extract’’ was prepared and the proteins were transferred into PBS, lacking glycerol (re-assembly buffer). After an incubation period at room temperature for 0–120 min samples were taken and analyzed. (A) Self assembly period: 0 min, (B) 15 min, (C) 30 min, (D) 60 min, (E) 120 min, or (F) 180 min. (G–I) Product of reassembled silicateins from ‘‘HF-Extract-Urea’’. Samples were allowed to remain in the assembly buffer for (G) 60 min, (H) 120 min, or (I) 180 min. Magnification: Bars A–C: 100 nm; D–I: 500 nm.

To determine if the structures formed from the silicateins in the ‘‘TG-Extract’’ can reach the stage of larger filaments, the re-assembly process was extended. The first aggregate formation can be visualized during the first 20 min in the re-assembly buffer (Fig. 2.6 A–C). At 45 min incubation period first filamentous structures are seen (length of 4 µm; Fig. 2.6 D). During the incubation period for 240 min (length of the filaments: approximately 10 µm; Fig. 2.6 E) or 320 min (30 µm; Fig. 2.6 F), long stable filaments are formed. This organized filament formation could not be detected

in ‘‘HF-Extract-Urea’’ samples (not shown). Only amorphous, irregular clumps are formed, as presented already in Fig. 2.5 G–I.

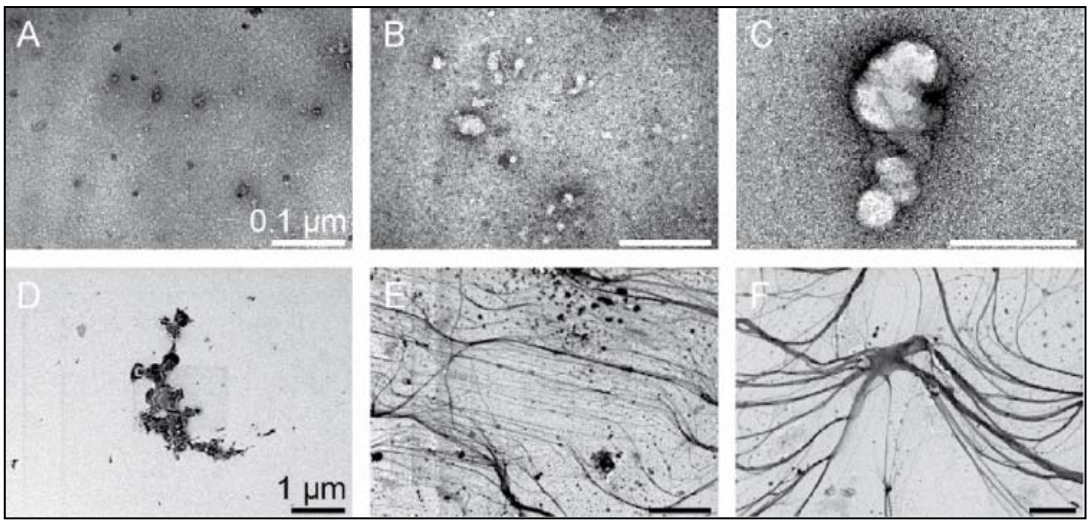

Figure 2.6: Form and shape of filaments/aggregates formed from silicateins, present in the ‘‘TG-Extract’’. Samples were taken and transferred into the reassembly buffer for 5 min (A), 10 min (B), 20 min (C), 45 min (D), 240 min (E), or 320 min (F). After the chosen incubation period the samples were analyzed by TEM.

2.4 Discussion

Morphogenetic events during development in Metazoa are certainly caused, guided and controlled by genomic regulatory systems (Davidson, 2001). Also in sponges, as the earliest phylum that branched off from the common metazoan ancestor, the Urmetazoa (Müller et al., 2004; Müller, 2001), extracellular signaling pathways exist, with myotrophin or the epidermal growth factor [EGF] as examples (Schröder et al., 2000; Perović-Ottstadt et al., 2004). These soluble factors are—like in vertebrates—involved in the differentiation and function of sponge cells; they are released from the cells and act back from the extracellular space on the function of cells, reviewed in (Müller, 2005). As postulated before (Murr and Morse, 2005) and now substantiated in the present study, it is reasonable to assume that self-assembly of silicatein monomers within the axial filament contribute, via fractal intermediates, to a stabile form/organization of the filament. It is proposed that the basic self-assembly of the silicatein-α monomers provides the general platform for the shape and pattern formation of growing spicules. In concert with the silicatein-β, the silicatein-α assemblies might allow the growing/development of the species specific non-rectifiable ‘‘self-similar’’ assembly. We have selected for the present study the axial filaments of the *S. domuncula* spicules [the tylostyles], since they have a simple monaxonial form (Müller et al., 2006b). It is shown, that in contrast to the published data, silicateins composing the axial filament exist in the native state as monomers or as non-covalently linked dimers (see: Fig. 2.1). Previously it had been outlined that the axial filament, obtained by HF treatment from the spicules, might exist as dimers, built of covalently linked monomers (Murr and Morse, 2005). For the studies presented here, a new extraction procedure was introduced, which allowed the preparation of native silicateins ([extraction with Tris/glycerol buffer). This piece of work showed that in the ‘‘TG-Extract’’ the silicatein molecules have a size of 24 kDa, if analyzed by NaDodSO$_4$-PAGE after pre-heating the sample). Interestingly, if the analysis is performed in the absence of b-mercaptoethanol the apparent size of the monomeric molecules is 18 kDa (see: Fig. 2.1). These results imply that b-mercaptoethanol changes the conformation of the silicateins from 18 kDa form (a predicted globular structure) to 24 kDa form (likely to represent more or less unfolded molecules). In order to support this conclusion unequivocally—and to rule out possible species-specific differences—parallel studies with other marine sponge

species are necessary. In contrast to the Tris/glycerol extraction, which revealed already monomeric/dimeric silicateins, the HF-Extracts yielded the axial filaments. In order to dissemble those filaments, they had to be treated with urea (Murr and Morse, 2005). By this procedure, the silicateins migrated at 24 kDa, irrespective of the presence or absence of β-mercaptoethanol. Only one strong protein band could be identified; we might explain this fact by the assumption that silicatein-b in the HF-Extracts underwent some modification, resulting in a co-migration with silicatein-α. This result is taken as a first strong indication that during the HF-extraction procedure the molecules undergo chemical modification(s) (see ‘‘Introduction’’). Additional data, obtained by $NaDodSO_4$-PAGE (in the presence of β-mercaptoethanol and pre-heating the samples) also clearly demonstrate that the silicateins, obtained after HF-extraction, underwent cross-linking with each other to form dimmers (50 kDa), trimers (75 kDa) or tetramers (95 kDa); see: Figs. 2.1 and 2.3. These dimers/multimers do not exist in Tris/ glycerol preparations, if analyzed under identical conditions. Therefore, we conclude that during HF-extraction the silicateins undergo modifications not seen in silicateins from the Tris/glycerol extraction and we propose that the HF-extraction procedure is not suitable for an analysis of the self-assembling property of native silicateins. The latter argument was given already earlier for HF-extracted proteins, e.g. the silica-depositing molecules in diatoms (Kröger et al., 1999, Kröger et al., 2002). As a functional assay for the different preparations (HF- and Tris/glycerol-extracts) polymerization studies were performed in vitro. Using the Tris/glycerol extraction procedure and analyzing the silicateins by PAGE under low $NaDodSO_4$ concentrations (0.01% and absence of heat), the silicateins show a size of 45 kDa, indicative for dimers. If these samples were transferred into a buffer, lacking glycerol, a polymerization to tetramers (95 kDa) and hexamers (135 kDa) takes place, after an incubation period of 120 min. This kind of self-assembly cannot be demonstrated for silicateins, obtained after HF-extraction (‘‘HF-Extract-Urea’’). Silicatein, as a member of the cathepsins, is also known to function besides in synthesizing/condensating orthosilicate to bio-silica, also in hydrolyzing peptide bonds (Cha et al., 1999); hence it acts also as a proteolytic enzyme. Therefore, the proteolytic activity was determined (Quian et al., 1989); see: Fig. 2.2. Intriguingly, it was found that the activity of the native silicatein, isolated under the Tris/glycerol conditions, is much higher than the one seen with samples after HF extraction. In order to support these data further an additional functional (enzymatic) assay was

used, the zymogram. Using this method it was proven that the HF-extracted silicateins (after a pre-incubation period of 180 min) do not show any enzymic activity, while in the Tris/glycerolextracted silicatein fraction distinct hydrolytic activities are identified with an apparent size of 40 kDa (dimer), 80 kDa (tetramer) and 120 kDa (hexamer); see: Fig. 2.3. A further outcome of the $NaDodSO_4$-PAGE studies (in the presence of b-mercaptoethanol and after pre-heating of the sample) was the finding that the two previously identified silicateins (-α and -β (Müller et al., 2007h)) could be clearly separated from each other (see: Fig. 2.1). However, this discrimination could only be obtained from Tris/glycerolextracts but not from HF-Extracts. Furthermore, it became evident that the a-form is more abundant than the b-form; the ratio was determined to be approximately 4:1. Further studies will now be undertaken to support these data, e.g. by applying antibodies raised against silicatein-β. Since however, the sequence similarity between -α and -β is high (Müller et al., 2007h), no pronounced changes are expected. On the basis of a 4:1 ratio between silicatein-α to - β, a computer model for the proposed arrangement between the two isoforms of silicatein is outlined. Ramachandran plots (Ramachandran et al, 1963) of our model proposed, did not reveal any forbidden conformations of the protein backbone (not shown). The B-factor revealed only deviations in outer loop regions of the models but not in the core region (Helliwell, 2005). Only, the C-terminal serine cluster showed a significant deviation (but no energy maximum) in the silicatein-α model from the underlying cathepsin L structure. Previously, Croce et al. (Croce et al., 2004) proposed a planar arrangement of the silicatein molecules under formation of a hexagonal packing. In line with this view and assuming that the orientations of the silicatein molecules within this planar tetramer are the same, we modeled the three possible structural organizations (Fig. 2.7). Three directions of orientation of the active centers can be proposed which had been termed syn-axial (active centers of the enzyme towards the inside of the tetramer; Fig. 2.7 A); anti-axial (active centers on the surface; Fig. 2.7 B); or con-axial (active centers in the plane of the tetrameric silicateins; Fig. 2.7 C). The distance between the active sites of the silicateins has been calculated and found for the syn-axial configuration to be 21.62 nm, for the antiaxial 39.25 nm and for the con-axial arrangement 29.12 nm. Under the assumption that the Ser-clusters are crucial segments in the silicateins (Cha et al., 1999), the con-axial orientation of all silicateins-α is most likely, since only in this arrangement the Ser-clusters of the silicateins are ordered and directed

towards the center of the tetrameric silicateins (see: Fig. 2.7 C). It can be proposed that in this center the tetrameric silicateins-α could interact with one silicatein-β molecule, as proposed in Fig. 2.7 D. A further outcome of this modeling approach was that the silicatein-α molecules, which form the tetrameric platform, are distorted to some extend in order to reach the optimal configurations with the Ser-clusters towards the center (Fig. 2.7 D). The longitudinal growth of the axial filament within the spicules proceeds certainly in an axial direction (Müller et al., 2007b; Schröder et al 2007b; Müller et al., 2003b), and very likely in an uni-directional orientation (Uriz et al., 2003; Müller et al., 2006b). The model, presented here, supports the view that growth of the spicules proceeds towards only one end of the spicules. In a final series of experiments the silicatein samples were subjected to a self-assembly procedure and analyzed by light microscopy (see: Fig. 2.4) and electron microscopy (see: Fig. 2.5). A similar approach had been undertaken with *T. aurantium* (Murr and Morse, 2005). At first, the assembly process was followed by light microscopy. The aggregates as well as the filaments had been visualized by anti-silicatein antibodies. Using the ‘‘TG-Extract’’ which had been transferred to a glycerol-free assembly medium, filaments are formed after 60 min incubation period, which reached sizes of several mm. In contrast, if the HF-extracted silicatein (axial filaments), that had been disassembled with urea was subjected to the assembly buffer only aggregates/clumps, and no filaments, could be seen. These data had been corroborated by application of electron microscopic technique (TEM). This series of analyses revealed that already after a 60 min incubation period of the silicatein mono-/dimers first filaments are seen. The length of the filaments increases with time, reaching sizes of several mm (see: Fig. 2.6). Applying the same incubation procedure, no elongated aggregates or even filaments could be achieved with silicateins present in the ‘‘HF-Extract-Urea’’.

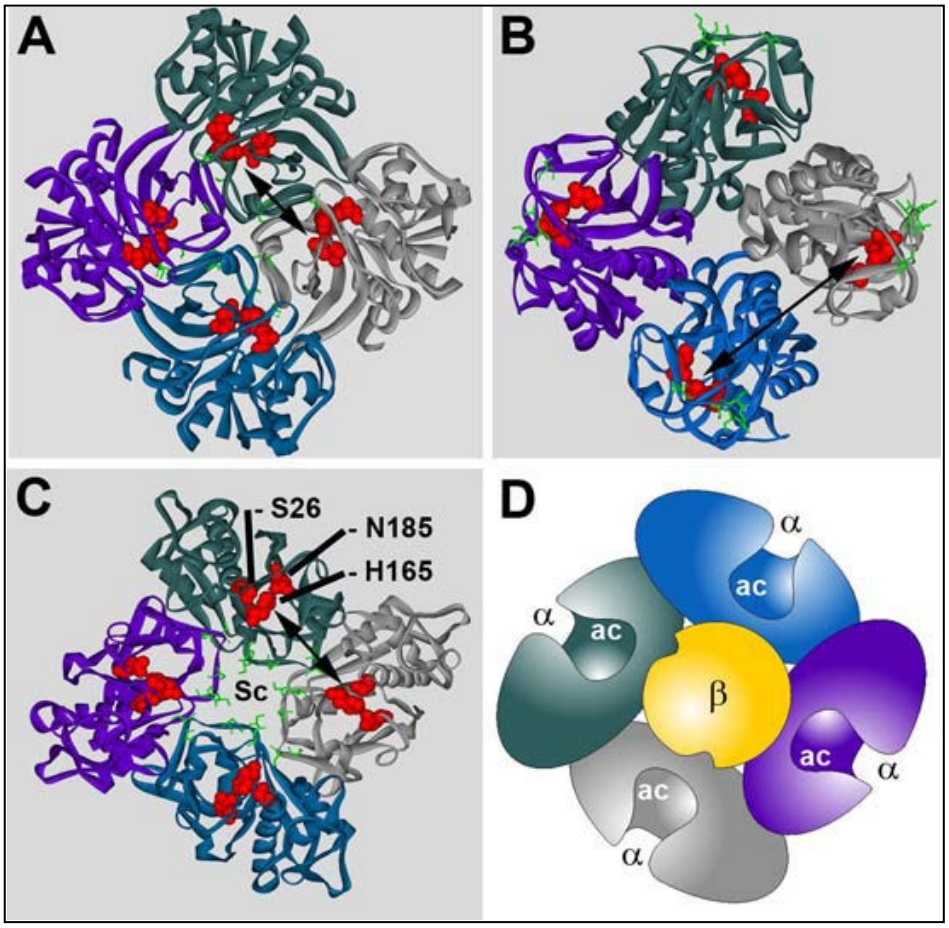

Figure 2.7: Schematic representation of one planar silicatein-α tetramer (α; green-grey-blue-pink); with one silicatein-β (β in the center [yellow]). It is proposed that the orientations of the silicatein units are identical in each of the three configurations. The amino acids involved in the active centers of the silicateins (the amino acids are counted within the mature molecule [Müller et al., 2003b]) are marked; serine (S26), histidine (H165) and asparagine (N185). (A) The silicatein molecules are oriented with their active centers towards the center of the axis (syn-axial), or (B) in the opposite direction of the axis (antiaxial), or, (C) the entrances of the con-active centers are located in the plane of the tetramer (con-axial). Only in the axial-orientation the Ser-rich clusters (Sc) are directed towards the center of tetramer. The double arrow is showing the distance between one pair of histidines between two silicatein-α molecules (H165). (D) Graphical model of the silicatein-α tetramer with the silicatein-β in the center. The active centers in the silicatein-β molecules are marked (ac). .(D and F) The distortion of the silicatein-β molecules within the tetrameric plane is illustrated

Taken together; the data elaborated in the present study demonstrate that silicateins, obtained by Tris/glycerol extraction are very suitable to analyze the biochemical, biophysical properties of the monomeric/dimeric silicatein units. This Tris/glycerol procedure is superior to the hitherto applied HF-extraction. The silicatein molecules in the ‘‘TG-Extract’’ retained the ability to self-assemble and to display enzymic activity.

In addition, they allowed the formation of fractal-like structures, which assembled to filaments. Since bio-silica is also an important material in nano(bio)technology, the understanding of a structure controlled self-assembly of silicatein will surely contribute to further application of bio-silica in industry and medicine, e.g. for the fabrication of biocompatible materials, glasses, ceramics and photonic materials (Tahir et al., 2006); reviewed in: (Müller et al., 2007b; Schröder et al., 2007a). Our results demonstrate that silicatein, a protein of potential importance for the fabrication of biomaterials used in nanobiotechnology, which has been isolated from axial filaments of the demosponge *S. domuncula* using a new extraction procedure is able to polymerize under formation of long filaments.

2.5 References

Adell T., Nefkens I. & Müller W.E.G. (2003). Polarity factor ‘‘Frizzled’’ in the demosponge *Suberites domuncula*: identification, expression and localization of the receptor in the epithelium/pinacoderm. *FEBS Lett* 554, 363–8.

Arndt A.W. (1935). In: Grimpe G, editor. Die Tierwelt der Nord-und Ostsee. Leipzig: *Akademische Verlagsgesellschaft*.

Cha J.N., Shimizu K., Zhou Y., Christianssen S.C., Chmelka B.F., Stucky G.D. & Morse D.E. (1999). Silicatein filaments and subunits from a marine sponge direct the polymerization of silica and silicones in vitro. *Proc Natl Acad Sci USA* 96,361-365.

Compton S. & Jones C.G. (1985). Mechanism of dye response and interference in the Bradford protein assay. *Anal Biochem* 151, 369–74.

Croce G., Frache A., Milanesio M., Marchese L., Causa M. & Viterbo D. (2004). Structural characterization of siliceous spicules from marine sponges. *Biophys J* 86, 526–34.

Davidson E.H. (2001). Genomic regulatory systems: development and evolution. San Diego: *Academic Press*.

Eckert C., Schröder H.C., Brandt D., Perovic-Ottstadt S. & Müller W.E.G. (2006). A histochemical and electron microscopic analysis of the spiculogenesis in the demosponge *Suberites domuncula*. *J Histochem Cytochem* 54, 1031–40.

Guex N. & Peitsch M.C. (1997). SWISS-MODEL and the Swiss-PdbViewer: an environment for comparative protein modeling. *Electrophoresis* 18, 2714–23.

Helliwell J.R. (2005). Macromolecular crystallography with synchrotron radiation. Cambridge: *Cambridge University Press*.

Jaffe C.L. & Dwyer D.M. (2003). Extracellular release of the surface metalloprotease, gp63, from Leishmania and insect trypanosomatids. *Parasitol Res* 91, 229–37.

Krasko A., Batel R., Schröder H.C., Müller I.M. & Müller W.E.G. (2000). Expression of silicatein and collagen genes in the marine sponge *Suberites domuncula* is controlled by silicate and myotrophin. *Eur J Biochem* 267, 4878–4887.

Krasko A., Schröder H.C., Batel R., Grebenjuk V.A., Steffen R. Müller I.M. & Müller W.E.G. (2002). Iron induces proliferation and morphogenesis in primmorphs from the marine sponge *Suberites domuncula. DNA Cell Biol* 21, 67–80.

Kröger N., Deutzmann R. & Sumper M. (1999). Polycationic peptides from diatom biosilica that direct silica nanosphere formation. *Science* 286, 1129–32.

Kröger N., Lorenz S., Brunner E. & Sumper M. (2002). Self-assembly of highly phosphorylated silaffins and their function in biosilica morphogenesis. *Science* 298, 584–6.

Laemmli U.K. (1970). Cleavage of structural proteins during the assembly of the head of bacteriophage T4. *Nature* 227, 680–5.

Mort J.S. (2002). Cathepsin-L. In: Barrett AJ, Rawlings ND, Woessner JF, editors. Handbook of proteolytic enzymes. *Amsterdam: Academic Press* p. 617–24.

Müller W.E.G. (1998 a). Molecular evolution: evidence for monophyly of metazoa. *Progr Molec Subcell Biol*. Berlin, Heidelberg, New York: Springer, p. 19.

Müller W.E.G. (1998 b). Molecular evolution: towards the origin of metazoa. *Progr Molec Subcell Biol*. Berlin, Heidelberg, New York: Springer, p. 21.

Müller W.E.G., Blumbach B. & Müller I.M. (1999). Evolution of the innate and adaptive immune systems: relationships between potential immune molecules in the lowest metazoan phylum [Porifera] and those in vertebrates. *Transplantation* 68, 1215–27.

Müller W.E.G. (2001). How was metazoan threshold crossed: the hypothetical Urmetazoa. *Comp Biochem Physiol* A129, 433–60.

Müller W.E.G., Krasko A., Le Pennec G., Steffen R., Wiens M., Ammar M.S., Müller I.M. & Schröder H.C. (2003b). Molecular mechanism of spicule formation in the demosponge *Suberites domuncula*: silicatein–collagen–myotrophin. *Progr Mol Subcell Biol* 33, 195–221.

Müller W.E.G., Wiens M., Adell T., Gamulin V., Schröder H.C. & Müller I.M. (2004). Bauplan of Urmetazoa: basis for genetic complexity of metazoa. *Intern Rev Cytol* 235, 53–92.

Müller W.E.G., Rothenberger M., Boreiko A., Tremel W., Reiber A. & Schröder H.C. (2005a). Formation of siliceous spicules in the marine demosponge *Suberites domuncula. Cell Tissue Res* 321, 285–97.

Müller W.E.G., Borejko A., Brandt D., Osinga R., Ushijima H., Hamer B., Krasko A., Xupeng C., Müller I.M. & Schröder H.C. (2005b). Selenium affects biosilica formation in the demosponge *Suberites domuncula*: effect on gene expression and spicule formation. *FEBS J* 272, 3838–52.

Müller W.E.G. (2005). Spatial and temporal expression patterns in animals. In: Meyers RA, editor. *Encyclopedia of molecular cell biology and molecular medicine*, vol. 13. Weinheim: WILEY-VCH Press;p. 269–309.

Müller W.E.G., Belikov S.I., Tremel W., Perry C.C., Gieskes W.W.C., Boreiko A. & Schröder H.C. (2006b). Siliceous spicules in marine demosponges (example *Suberites domuncula*). *Micron* 37, 107–20.

Müller W.E.G., Wang X., Belikov S.I., Tremel W., Schlossmacher U., Natoli A., Brandt D., Boreiko A., Tahir M.N., Müller I.M. & Schröder H.C. (2007b). Formation of siliceous spicules in demosponges: example *Suberites domuncula*. In: Bäuerlein E, editor. Handbook of biomineralization. Vol. 1. The biology of biominerals structure formation. Weinheim: *Wiley-VCH* p. 59–82.

Müller W.E.G., Boreiko A., Wang X., Belikov S.I., Wiens M., Grebenjuk V.A., Schlossmacher U. & Schröder H.C. (2007h). Silicateins, the major biosilica forming enzymes present in demosponges: protein analysis and phylogenetic relationship. *Gene* 395, 62–71.

Murr M.M. & Morse D.E. (2005). Fractal intermediates in the self-assembly of silicatein filaments. *Proc Natl Acad Sci USA* 102, 11657–62.

Nishimura Y., Kato G., Furuno K. & Himeno M. (1995). Inhibitory effect of leupeptin on the intracellular maturation of lysosomal cathepsin L in primary cultures of rat hepatocytes. *Biol Pharm Bull* 18, 945–50.

Pancer Z., Kruse M., Müller I. & Müller W.E.G. (1997). On the origin of adhesion receptors of metazoa: cloning of the integrin a subunit cDNA from the sponge *Geodia cydonium. Mol Biol Evol* 14, 391–398.

Perovic´-Ottstadt S., Adell T., Proksch P., Wiens M., Korzhev M., Gamulin V., Müller I.M. & Müller W.E.G. (2004). A (1-3)-b-d-glucan recognition protein from the sponge *Suberites domuncula*: mediated activation of fibrinogen-like protein and epidermal growth factor gene expression. *Eur J Biochem* 271, 1924–37.

Quian F., Bajkowski A.S., Steiner D.F., Chan S.J. & Frankfater A. (1989). Expression of five cathepsins in murine melanomas of varying metastatic potential and normal tissues. *Cancer Res* 49, 4870–5.

Ramachandran G.N., Ramakrishnan C. & Sasisekharan V. (1963). Stereo-chemistry of polypeptide chain configurations. *J Mol Biol* 7, 95–9.

Schröder H.C., Krasko A., Batel R., Skorokhod A., Pahler S., Kruse M., Müller I.M. & Müller W.E.G. (2000). Stimulation of protein (collagen) synthesis in sponge cells by a cardiac myotrophin-related molecule from *Suberites domuncula. FASEB J* 14, 2022–31.

Schröder H.C., Boreiko A., Korzhev M., Tahir M.N., Tremel W., Eckert C., Ushijima H., Müller I.M. & Müller W.E.G. (2006). Co-Expression and functional interaction of silicatein with galectin: matrix-guided formation of siliceous spicules in the marine demosponge *Suberites domuncula. J Biol Chem* 281, 12001–9.

Schröder H.C., Brandt D., Schlossmacher U., Wang X., Tahir M.N., Tremel W., Belikov S.I. & Müller W.E.G. (2007a). Enzymatic production of biosilica-glass using enzymes from sponges: basic aspects and application in nanobiotechnology (material sciences and medicine). *Naturwissenschaften* 94, 339–59.

Schröder H.C., Natalio F., Shukoor I., Tremel W., Schloßmacher U., Wang X. & Müller W.E.G. (2007b). Apposition of silica lamellae during growth of spicules in the demosponge *Suberites domuncula*: biological/biochemical studies and chemical/biomimetical confirmation. *J Struct Biol* 159, 325–334.

Shimizu K., Cha J., Stucky G.D. & Morse D.E. (1998). Silicatein alpha: Cathepsin L-like protein in sponge biosilica. *Proc Natl Acad Sci USA* 95, 6234–8.

Tahir M.N., Eberhardt M., Therese H.A., Kolb U., Theato P., Müller W.E.G., Schröder H.C. & Tremel W. (2006). From single molecules to nanoscopically structured functional materials: Au nanocrystal growth on TiO2 nanowires controlled by surface bound silicatein. *Angew Chem* Int Edit 45, 4803–9.

Uriz M.J., Turon X. & Becerro M.A. (2000). Silica deposition in Demospongiae: spiculogenesis in *Crambe crambe*. *Cell Tissue Res* 301, 299–309.

Uriz M.J., Turon X., Becerro M.A. & Agell G. (2003). Siliceous spicules and skeleton frameworks in sponges: origin, diversity, ultrastructural patterns, and biological functions. *Micr Res Techn* 62, 279–299.

Chapter 3

Identification of a silicatein(-related) protease in the giant spicules of the deep-sea hexactinellid *Monorhaphis chuni*

3.1 Introduction

Silicateins, members of the cathepsin-L family, are enzymes that have been shown to be involved in the biosynthesis/condensation of biosilica in spicules from Demospongiae (phylum Porifera), e.g. *Tethya aurantium* and *Suberites domuncula*. The class Hexactinellida also forms spicules from this inorganic material. This class of sponges includes species that form the largest biogenic silica structures on earth. The giant basal spicules from the hexactinellids *Monorhaphis chuni* and *Monorhaphis intermedia* can reach lengths of up to 3·m and diameters of 10·mm. The phylogenetically oldest metazoans are the sponges (phylum Porifera), which evolved during the Neoproterozoic, Neoproterozoic–Cambrian period (Xiao et al., 2005). Porifera are grouped into three classes, the Hexactinellida and the Demospongiae being both composed of a siliceous skeleton, as well as the class of Calcarea whose skeleton is made of calcium carbonate (Bergquist, 1978). Fossil records (Brasier et al., 1997; Steiner et al., 1993) and 'molecular clock' analyses (Schäcke et al., 1994; Kruse et al., 1998) indicate that the Hexactinellida evolved before to the Demospongiae. So far data indicate that demosponges have the unique ability to synthesize their siliceous skeleton enzymatically (Shimizu et al., 1998; Cha et al., 1999), in contrast to other organisms that deposit bio-silica in a template-controlled manner (reviewed in Perry, 2003). The responsible enzyme, silicatein, was first described by the group of Morse in the marine demosponge *Tethya aurantium* (Cha et al., 1999) and subsequently also identified in other demosponges, most prominently in *Suberites domuncula* (Krasko et al., 2000). The silicateins undergo post-translational modification, primarily phosphorylation (Müller et al., 2005a). The polypeptide sequences of the silicateins share high sequence similarity with cathepsin L (Cha et al., 1999; Krasko et al., 2000); the active centre of silicatein differs from that of cathepsin L by only one amino acid (catalytic triad is Ser-His- Asn in silicatein and Cys-His-Asn in cathepsins). Cathepsins belong to the cysteine proteinases which can be effectively inhibited by E-64 [L-trans-epoxysuccinyl-leucylamido(4- guanidino)butane] (Barrett et al., 1982) (reviewed in Barrett et al.,

2002); The natural cathepsin inhibitor cystatin reduces the activity of cathepsins potently (reviewed in Brage et al., 2005; Laitala-Leinonen et al., 2005). The spicules grow in a lamellar way, through the concentric deposition/formation of silica layers; in the centre of the spicules an organic axial filament is harboured in a rectangular axial canal (reviewed in Schulze, 1904; Schulze, 1925; Reiswig, 1971; Sandford, 2003). The megascleres of *M. chuni* and *M. intermedia* consist of up to 400 lamellae (Levi et al., 1989). We focused especially on the potential existence of silicatein, or silicatein-like molecules in the two types of spicule. We demonstrate for the first time that the protein(s) present in the spicules of *M. chuni* display proteolytic activity, like the silicateins from *S. domuncula*; this indicates/suggests that the spicules in Hexactinellida are also synthesized enzymatically by silicatein-like molecule(s). To further characterize the proteinase, we used the naturally occurring inhibitor E-64 and the sponge inhibitor cystatin. The gene encoding cystatin was obtained from *S. domuncula* and prepared in a recombinant manner. Spicules from the hexactinellids *Monorhaphis chuni* [(Schulze, 1904) Porifera: Hexactinellida: Amphidiscosida: Monorhaphididae] and *Monorhaphis intermedia* [(Li, 1987) Porifera: Hexactinellida: Amphidiscosida: Monorhaphididae] were used. Recently, it has been proposed that *M. chuni* and *M. intermedia* are one species (Tabachnick and Lévi, 2000; Tabachnick, 2002). The *M. chuni* specimens used were provided from the collection of the Museum für Naturkunde Berlin (Germany). They were collected by deep-sea dredging in 1899 at a depth of 1700·m during the ‘Valdivia’ expedition in the Somali basin (ZMB Por 3708, 4253, 12700). M. intermedia was collected during a Chinese expedition in 1981 to the West-Pacific Okinawa Trough at a depth of 900·m (Jinhe Li). Both giant basal spicules and tauactins were used from them. Specimens of the marine demosponge *Suberites domuncula* (Olivi 1792; Porifera: Demospongiae: Hadromerida: Suberitidae) were collected in the Northern Adriatic near Rovinj (Croatia), and then kept in aquaria in Mainz (Germany).

3.2 Experimental section

3.2.1 Spicules and spicule extracts

Spicules were soaked in 2% (w/v) sodium dodecyl sulphate solution overnight to remove cell and tissue remains. The spicules were treated with 50·ml of 2·mol·l^{-1} HF (hydrofluoric acid)/8·mol·l^{-1} NH_4F (pH 5) for only 3·h (Shimizu et al., 1998). Then the suspension was immediately dialysed (3 times) against 5·l of 50·mmol·l^{-1} Tris-HCl buffer (pH 9.0; 100·mmol·l^{-1} NaCl, 10·mmol·l^{-1} EDTA) at 4°C for 4·h each. Subsequently, the extract was concentrated with Microcon centrifugal filter devices (cutoff, 3·kDa, 3000·MW cutoff; Millipore, Schwalbach, Germany) and finally frozen at –20°C until analysis. For the visualization of nanoparticles that make up the giant basal spicules, the cut spicules were etched with HF vapour. For the analysis of the polypeptides within siliceous structures, single lamellae were mechanically separated from the other layers of the giant basal spicules and extracted separately. Spicules from *S. domuncula* were obtained and the axial filaments isolated by the 2·mol·l^{-1} HF/8·mol·l^{-1} NH_4F procedure as described previously (Schröder et al., 2006). The filaments were treated with phosphate-buffered saline (PBS; containing 1% Triton X-100) and used for the determination of the proteinase activity.

3.2.2 Analysis of proteolytic activity: zymogram analysis

Protein samples (axial filaments) were obtained from *S. domuncula*, dissolved in PBS/Triton X-100 (see above), and loaded onto a zymogram gel, containing 0.1% casein (heat denatured) as previously described (Jaffe and Dwyer, 2003). The samples were separated by SDS-PAGE (10% gels). Samples (15·µl) were loaded onto each gel, corresponding approximately to a protein extract from 200·µg of spicules. After protein separation, the gels were incubated in a 50·mmol·l^{-1} Mops buffer (pH 6.8; 5·mmol·l^{-1} $CaCl_2$, 0.1·mmol·l^{-1} $ZnCl_2$, 100·mmol·l^{-1} NaCl, 0.5·mmol·l^{-1} DTT) for 1·h at room temperature. After refreshing this buffer, proteinase activity was allowed to develop overnight at 37°C; then the gels were stained with Coomassie Brilliant Blue in order to visualize the proteinase activity as clear bands on a blue background. Where indicated, the *S. domuncula* spicule extracts were preincubated

(30·min; 20°C) with 1·µmol·l^{-1} E-64 or 5·µg·ml^{-1} of recombinant *S. domuncula* cystatin.

3.2.3 Analysis of proteolytic activity: enzyme activity test

Extracts from spicules of both *M. chuni* and *S. domuncula* were obtained from purified spicules after dissolution of the bio-silica shell with HF/NH_4F as described above. The enzymatic reaction (0.2·ml volume) was performed as described elsewhere (Quian et al., 1989; Mort, 2002) in 96-well plates (Nunc 96 MicrowellTM Plates, Nunc, Wiesbaden, Germany) at room temperature. Cathepsin L was used as a positive control at a final concentration of 10·nmol·l^{-1}. The assay contained 10·µmol·l^{-1} Z-Phe-Arg-AMC as substrate. Incubation was performed for 60·min at room temperature. Then the spicule samples were preincubated either with 1·µmol l^{-1} E-64 or with 5·µg·ml^{-1} of recombinant *S. domuncula* cystatin. A standard curve was established with 7-amino-4-methyl-coumarin (AMC) under otherwise identical incubation conditions. The fluorescence of the free AMC released was determined using excitation at 355·nm and emission at 460·nm in an F-2000 Hitachi fluorescence spectrophotometer as described previously (Dvorak et al., 2005). The activity was calculated and is given in nmol AMC released mg^{-1} protein min^{-1} (Dvorak et al., 2005). Five parallel experiments were performed; the means and the standard deviations were calculated (Sachs, 1984).

3.3 Results

3.3.1 Proteolytic activity of silicatein

One potent broad-spectrum inhibitor of cysteine proteinases is E- 64. The inhibitory activity of E-64 is demonstrated by application of the zymogram technique. Cathepsin L at a concentration of 0.3·µg (2·mU) was loaded onto a gel containing casein. After size separation in the gel, incubation and staining with Coomassie Brilliant Blue, the zone that had been hydrolysed by cathepsin L became clear and visible (not shown here). In parallel, a spicule extract from *S. domuncula* was applied to the gel. After the gel was incubated and developed, a clear band with a size of about 25·kDa could be identified (Fig. 3.1 lane a), corresponding to the silicateins in the extract (Müller et al., 2005a). We attribute the slight difference in the molecular size of the 27·kDa protein band obtained after SDS-PAGE (absence of casein) of extracts and the 25·kDa protein band seen in the zymogram (presence of casein) to the different separation conditions in the gels. If the size-fractionated proteins, obtained after separation by SDS-PAGE (in the presence of casein), were preincubated with E-64, the hydrolytic activity was completely abolished (Fig.·3.1 lane b). Likewise, the recombinant sponge cystatin was able to inhibit the proteolytic activity displayed by the *S. domuncula* spicule extract (Fig.·3.1 lane c). Consequently, we used these two inhibitors to characterize the proteolytic activity, extractable from the *M. chuni* extract.

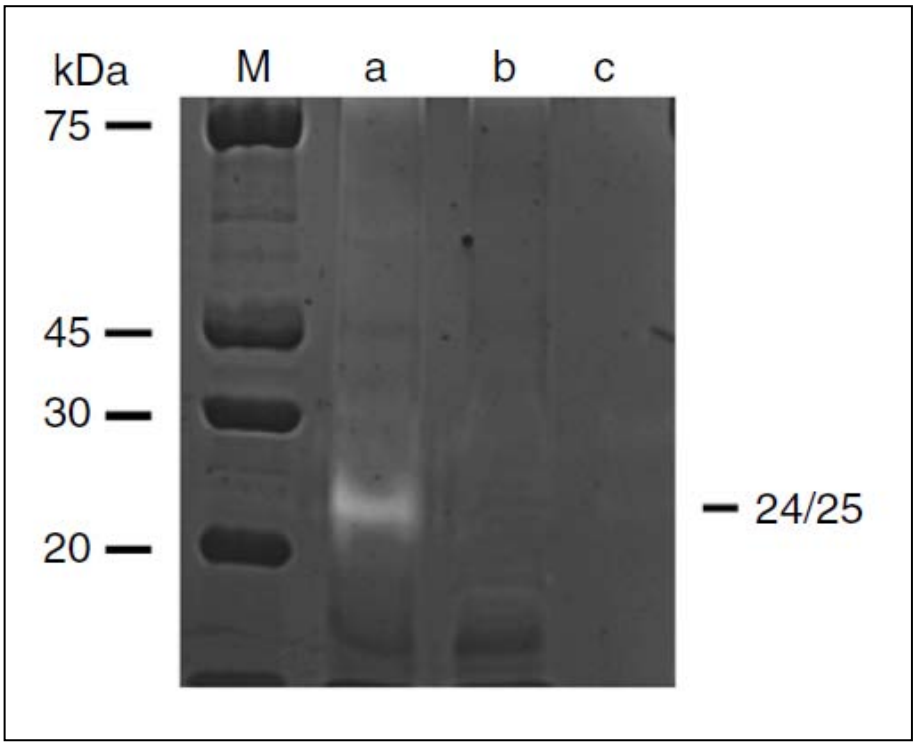

Figure 3.1: Proteolytic activity of silicatein, present in spicule extract from *S. domuncula*. Extracts were prepared and separated by electrophoresis. After size separation the gel was incubated overnight at room temperature to identify the zones of proteolytic digestion as outlined under Materials and methods. The migration distance of the cleared zone (24/25·kDa) is characteristic for silicatein (lane a). If the sample from the spicules had been pre-incubated with E-64 (lane b) or with the recombinant sponge cystatin (lane c), no clearance zone could be seen. Form these data we conclude that silicatein, present in the spicule extract, still retains proteolytic activity. M, size markers.

3.3.2 Cathepsin-like activity in giant basal spicules

Total extracts from giant basal spicules were prepared and assayed for proteinase activity using Z-Phe-Arg-AMC as the substrate. The experiments were performed in parallel with *M. chuni* and *S. domuncula* spicule extracts to determine cathepsin L activity. The results showed that in this assay cathepsin L (concentration 300·ng per assay) had an activity of 12·800·nmol AMC released mg^{-1} protein min^{-1}, under the conditions used. If the inhibitor E-64 (1·µmol·l^{-1}) was added, the activity dropped to values as low as 1400·nmol AMC released mg^{-1} protein min^{-1}; if the sponge cystatin was added (5·µg·ml^{-1}) the activity was likewise only 2450·nmol AMC released mg^{-1} protein min^{-1} (Fig.·3.2). The *S. domuncula* extract showed an activity of 1300·nmol AMC released mg^{-1} protein min^{-1}; the hydrolytic activity was almost totally blocked by

both E-64 and cystatin (Fig.·3.2). The Monorhaphis spicule extract also displayed hydrolytic activity with 144·nmol AMC released mg^{-1} protein min^{-1}. However, the extract from this sponge was only inhibited by E-64 (by 85%), not by cystatin (Fig. 3.2).

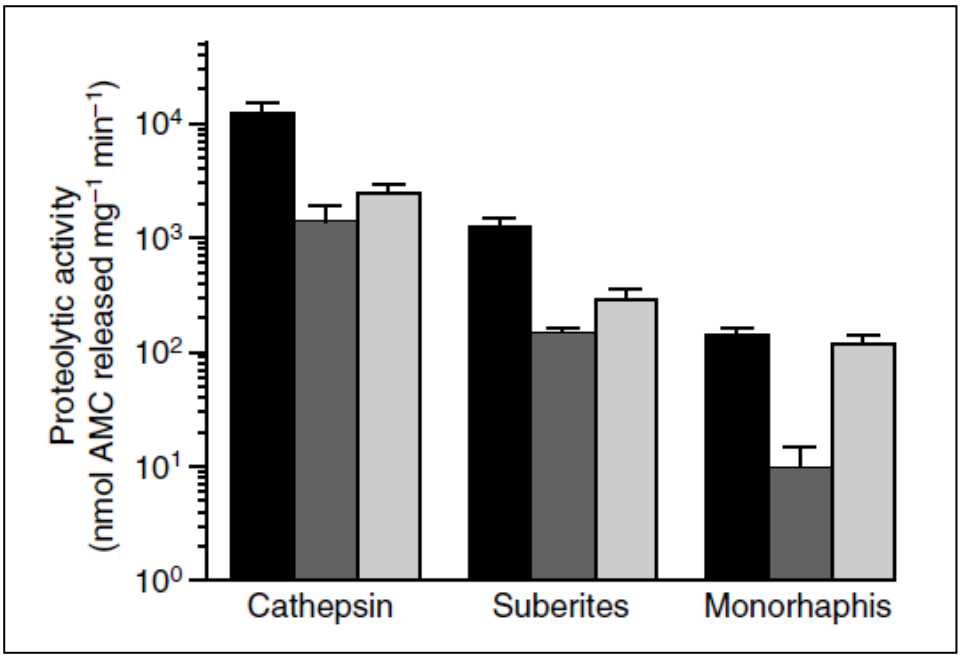

Figure·3.2: Effect of cysteine proteinase inhibitors E-64 and cystatin on the proteolytic activity of cathepsin L (left), as well as spicule extracts from *S. domuncula* (middle) and *M. chuni* (right). The activity of the samples was determined either directly (black columns), or following pretreatment with E- 64 (dark grey columns) or cystatin (light grey columns). The proteolytic activity was measured with the synthetic substrate Z-Phe-Arg-AMC, and is given as nmol AMC released·mg^{-1} protein·min^{-1}. Means (±s.d.) of five independent experiments are given.

3.4 Discussion

M. chuni and *M. intermedia* are deep-sea sponges, which live in a milieu highly under-saturated in silicon (Maldonado et al., 2005). Therefore, it is very surprising that in this habitat these two hexactinellid sponges synthesize the largest bio-silica structures existing on earth. From studies with the demosponge *S. domuncula* it is known that sponges have the potential to actively accumulate silicate, through a silica–bicarbonate {Na^+/HCO_3 – $[Si(OH)_4]$} cotransporter (Schröder et al., 2004). We have recently postulated that all siliceous sponges, including Monorhaphis, are provided with enzymatic machinery to polymerize/condense bio-silica through the enzyme silicatein (Müller et al., 2007d; Wang et al., 2007) to construct/synthesize their spicules, which may be up to 3·m long and 10·mm thick in the case of Monorhaphis. The data presented here support this assumption. For our studies either giant basal spicules or tauactins from Monorhaphis were used.

SDS-PAGE analysis of the fractions revealed that in total extract of *M. chuni /M. intermedia* spicules a 27·kDa protein exists in addition to the 70 kDa molecule(s), while the organic component of the lamellae consists of only protein(s) of 27·kDa. In an earlier study we obtained the first indications that total extract from giant basal spicules contains molecules related to silicatein (Müller et al., 2007d; Wang et al., 2007). In the present study we found that the total extract as well as the extract from separated lamellae of these spicules contains a silicatein(-related) molecule, with respect to size, post-translation modification and enzyme activity. SDS-PAGE showed that characteristic lowmolecular mass protein(s) of 27·kDa exist in the spicules, which match in size with silicateins from demosponges (Cha et al., 1999; Krasko et al., 2000; Müller et al., 2007h) and correspond to the mature enzyme. Since silicateins belong to the class of cathepsin L enzymes, we approached in this study the potential proteolytic activity of the silicateins. In this series of experiments spicule extracts from *S. domuncula* and Monorhaphis were compared. The first hints that extracts from giant basal spicules of Monorhaphis displayproteolytic activity came from a recent study (Müller et al., 2007d). It was shown that spicule proteins of >70·kDa in size show proteolytic activity in both sponges. Considering our findings indicating that the proteolytic activity of spicule extracts as well as the size of the molecules depend on the HF treatment procedure here we applied mild extraction procedures, as outlined above. The extraction conditions had been optimized for the

S. domuncula spicule extract. The results obtained using the zymogram assay system indicated that the 24/25·kDa protein (corresponding to the size of silicatein) displays proteolytic activity. Next, using this technique we determined whether the proteolytic activity in the *S. domuncula* spicule extract can be affected by the inhibitors E-64 and cystatin. E-64, a well-established irreversible cysteine proteinase inhibitor (Barrett et al., 1982; Gour-Salin et al., 1994), interacts with the S2 subsite (binding pocket) of the enzyme and blocks its binding to bulky hydrophobic or aromatic residues of the inhibitor, e.g. to Phe in the P2 position (Gour-Salin et al., 1994).

E-64 was found to be a strong inhibitor of *S. domuncula* silicatein and also of the proteolytic activity measured in the *Monorhaphis* extract. As a substrate to detect the enzyme activity, the cathepsin L-specific synthetic dipeptide derivative Z-Phe-Arg-AMC was used (Mort, 2002). It was demonstrated that the proteolytic activity of the spicule extracts can be blocked by E-64 to over 90% at concentrations as low as $1 \cdot \mu mol \cdot l^{-1}$. As a further potential inhibitor of the (potential) silicateins, cystatin was used. The cystatins are naturally occurring cysteine proteinase inhibitors (see Kopitar-Jerala, 2006). We identified and cloned a cystatin from *S. domuncula*. The only form we could identify was the cDNA encoding the cystatin A/B-related polypeptide. It is interesting to note that these molecules exist only in sponges and the deuterostomian branch, but not in Protostomia. Cystatin A/B polypeptides are strong modulators of bone resorption in mammals, by preferentially inhibiting cathepsin K (Osawa et al., 2003; Laitala-Leinonen et al., 2006). The sponge recombinant cystatin was prepared and found to inhibit the *S. domuncula* silicatein but not the Monorhaphis 24/25·kDa protein (silicatein-like molecule). Now, further studies must be performed to identify specific inhibitors of the silicateins, especially in comparison with the cathepsins (ongoing study), in order to clarify the role of serine, present in the catalytic triad of silicateins (replacing cysteine), during proteinase cleavage. Taken together, the data presented here reveal that the 24·kDa polypeptide in Monorhaphis has a series of characteristics in common with the silicateins found in demosponges; the size, the post-translational modifications and the proteinase activity.

3.5 References

Barrett A.J., Kembhavi A.A., Brown M.A., Kirschke H., Knight C.G., Tama M. & Hanada K. (1982). L-trans-Epoxysuccinyl-leucylamido(4-guanidino)butane and its analogues as inhibitors of cysteine proteinases including cathepsins B, H and L. *Biochem. J*. 201, 189-198.

Barrett A.J., Rawlings N.D. & Woessner J.F. (2002). Cathepsin L. In Handbook of Proteolytic Enzymes, pp. 617-624. *Amsterdam: Academic Press.*

Bergquist P.R. (1978). Sponges. Berkeley, Los Angeles: University of California. Brage M., Abrahamson M., Lindstrom V., Grubb A. & Lerner U.H. (2005). Different cysteine proteinases involved in bone resorption and osteoclast formation. *Calcif. Tissue Int.* 76, 439-447.

Brasier M., Green O. & Shields G. (1997). Ediacarian sponge spicule clusters from southwest Mongolia and the origins of the Cambrian fauna. *Geology* 25, 303- 306.

Cha J.N., Shimizu K., Zhou Y., Christianssen S.C., Chmelka B.F., Stucky G.D. & Morse D. E. (1999). Silicatein filaments and subunits from a marine sponge direct the polymerization of silica and silicones in vitro. *Proc. Natl. Acad. Sci. USA* 96, 361-365.

Gour-Salin B.J., Lachance P., Magny M.C., Plouffe C., Menard R. & Storer A.C. (1994). E-64 [L-trans-epoxysuccinyl-leucylamido(4-guanidino)butane] analogoues as inhibitors of cysteine proteinases: investigation of the S2 subsite interactions. *Biochem. J.* 299, 389-392.

Kopitar-Jerala N. (2006). The role of cystatins in cells of the immune system. *FEBS Lett.* 580, 6295-6301.

Krasko A., Batel R., Schröder H.C., Müller I.M. & Müller W.E.G. (2000). Expression of silicatein and collagen genes in the marine sponge *Suberites domuncula* is controlled by silicate and myotrophin. *Eur. J. Biochem.* 267, 4878-4887.

Kruse M., Leys S.P., Müller I.M. & Müller W.E.G. (1998). Phylogenetic position of the Hexactinellida within the phylum Porifera based on amino acid sequence of the protein kinase C from Rhabdocalyptus dawsoni. *J. Mol. Evol.* 46, 721-728.

Laitala-Leinonen T., Rinne R., Saukko P., Väänänen H.K. & Rinne A. (2006). cystatin B as an intracellular modulator of bone resorption. *Matrix Biol*. 25, 149-157.

Levi C., Barton J.L., Guillemet C., Le Bras E. & Lehuede P. (1989). A remarkably strong natural glassy rod: the anchoring spicule of the Monorhaphis sponge. *J. Mater. Sci. Lett.* 8, 337-339.

Li J. (1987). *Monorhaphis intermedia* – a new species of Hexactinellida. *Oceanol. Limnol. Sin.* 18, 135-137.

Maldonado M., Carmona M.C., Velasquez Z., Puig A., Cruzado A., Lopez A. & Young C.M. (2005). Siliceous sponges as a silicon sink: an overlooked aspect of benthopelagic coupling in the marine silicon cycle. *Limnol. Oceanol.* 50, 799-809.

Mort J.S. (2002). Cathepsin L. In Handbook of Proteolytic Enzymes (ed. A. J. Barrett, N. D. Rawlings and J. F. Woessner), pp. 617-624. *Amsterdam: Academic Press.*

Müller W.E.G., Rothenberger M., Boreiko A., Tremel W., Reiber A. & Schröder H.C. (2005a). Formation of siliceous spicules in the marine demosponge *Suberites domuncula*. *Cell Tissue Res.* 321, 285-297.

Müller W.E.G., Eckert C., Kropf K., Wang X., Schloßmacher U., Seckert C., Wolf S.E., Tremel W. & Schröder H. C. (2007d). Formation of the giant spicules of the deep sea hexactinellid Monorhaphis chuni (Schulze 1904): electron microscopical and biochemical studies. *Cell Tissue Res.* 329, 363-378.

Müller W.E.G., Boreiko A., Wang X., Belikov S.I., Wiens M., Grebenjuk V.A., Schloßmacher U. & Schröder H.C. (2007h). Silicateins, the major biosilica forming enzymes present in demosponges: protein analysis and phylogenetic relationship. *Gene* 395, 62-71.

Osawa M., Kaneko M., Horiuchi H., Kitano T., Kawamoto Y., Saitou N. & Umetsu K. (2003). Evolution of cystatin B: implications for the origin of its variable dodecamer tandem repeat in humans. *Genomics* 81, 78-84.

Perry C.C. (2003). Silicification: the process by which organisms capture and mineralize silica. *Rev. Mineral. Geochem.* 54, 291-327.

Reiswig H.M. (1971). The axial symmetry of sponge spicules and its phylogenetic significance. *Cah. Biol. Mar.* 12, 505-514.

Sandford F. (2003). Physical and chemical analysis of the siliceous skeleton in six sponges of two groups (Demospongiae and Hexactinellida). *Microsc. Res. Tech.* 62, 336-355.

Schäcke H., Müller I.M. & Müller W.E.G. (1994). Tyrosine kinase from the marine sponge *Geodia cydonium*: the oldest member belonging to the receptor tyrosine kinase class II family. In Use of Aquatic Invertebrates as Tools for Monitoring of Environmental Hazards (ed. W. E. G. Müller), pp. 201-211. New York, Stuttgart: *Gustav Fischer Verlag.*

Schröder H.C., Perovic´-Ottstadt S., Rothenberger M., Wiens M., Schwertner H., Batel R., Korzhev M., Müller I.M. & Müller W.E.G. (2004). Silica transport in the demosponge *Suberites domuncula*: fluorescence emission analysis using the PDMPO probe and cloning of a potential transporter. *Biochem. J.* 381, 665-673.

Schulze F.E. (1904). Hexactinellida. Wissenschaftliche Ergebnisse der Deutschen Tiefsee-Expedition auf dem Dampfer “Valdivia” 1898-1899. Stuttgart: *Gustav Fischer Verlag*.

Schulze P. (1925). Zum morphologischen Feinbau der Kieselschwammnadeln. *Z. Morphol. Ökol. Tiere* 4, 615-625.

Shimizu K., Cha J., Stucky G.D. & Morse D.E. (1998). Silicatein alpha: cathepsin L-like protein in sponge biosilica. *Proc. Natl. Acad. Sci. USA* 95, 6234-6238.

Steiner M., Mehl D., Reitner J. & Erdtmann B.D. (1993). Oldest entirely preserved sponges and other fossils from the Lowermost Cambrian and a new facies reconstruction of the Yangtze Platform (China). *Berl. Geowiss. Abh.* E 9, 293- 329.

Tabachnick K.R. (2002). Family Monorhaphididae Ijima, 1927. In Systema Porifera (ed. J. N. A. Hooper and R. W. M. Van Soest), pp. 1264-1266. *New York: Kluwer Academic.*

Tabachnick K.R. & Lévi C. (2000). Porifera: Hexactinellida: Amphidiscophora off New Caledonia. *Mém. Mus. Natl. Hist. Nat*. 184, 53-140.

Wang X., Li J., Qiao L., Schröder H.C., Eckert C., Kropf K. & Müller W.E.G. (2007). The giant spicules of the deep sea hexactinellidan sponges of the genus Monorhaphis (Hexactinellida: Amphidiscosida: Monorhaphididae). *Acta Zool. Sin.* 53, 557-569.

Xiao S., Hu J., Yuan X., Parsley R.L. & Cao R. (2005). Articulated sponges from the Lower Cambrian Hetang Formation in southern Anhui, South China: their age and implications for the early evolution of sponges. *Palaeogeogr. Palaeoclimatol. Palaeoecol.* 220, 89-117.

Chapter 4

Poly(silicate)-metabolizing silicatein in siliceous spicules and silicasomes of demosponges comprises dual enzymatic activities (silica-polymerase and silica-esterase)

4.1 Introduction

Silicon is the second most common element in the Earth's crust (Perry, 2003); it possesses semi-metallic as well as metalloid properties. Silicon exists in nature in combination with oxygen as silicate ions or as silica; silica comprises no negative charge, while silicate anions carry a negative net electrical charge, which is balanced by cations. Free silica/silicate is found both in the crystalline state such as quartz and in the amorphous state such as opal. Silica/silicate is widely used in industry and medicine for the fabrication of poly(silicate), e.g. in amorphous glasses, ceramics, paints, adhesives, catalysts, and photonic materials (reviewed in: Müller et al., 2007b; Schröder et al., 2007a). Furthermore, poly(silicate) is an important new material in nano(bio)technology (Morse, 1999; Wang and Wang, 2006). The latter multidisciplinary research field is concerned with bio- and electronic-engineering at nanometer, molecular and cellular levels (Morse, 1999). The hitherto applied technological production of silica requires usually high temperature conditions and extremes of pH (Stöber et al., 1968). Hydrated amorphous silica, e.g. in the form of opal, has excellent properties like low density and high porosity. In nature, amorphous silica can be produced by diatoms by passive deposition onto an organic matrix. Siliceous sponges (Demospongiae) have the exceptional ability to synthesize silica enzymatically via silicatein (Morse, 2000; Weiner and Dove, 2003). Silicatein is – based on its protein sequence – related to the proteinases of the cathepsin class (Cha et al, 1999).

Silicatein has been isolated from a number of siliceous sponges, e.g. *Tethya aurantium* or *Suberites domuncula* (Cha et al, 1999; Krasko et al., 2000). If the enzyme is isolated from the skeletal elements of these animals, the spicules, it can be used *in vitro* to catalyze polycondensation of a wide variety of alkoxide, as well as ionic and organometallic precursors to the corresponding chalcogens; these processes occur at standard, ambient temperature, pressure and neutral pH (Zhou et al., 1999). By site-directed mutagenesis those amino acids critical to the

condensation of tetraethoxysilane (TEOS) were determined; the catalytic triad is histidine (His), asparagine (Asn) and serine (Ser) (Shimizu et al., 1998). In the active center of silicatein, the hydroxyl group of Ser-26 and the imidazole of His-165 were shown to play key roles in the condensation of TEOS (Zhou et al., 1999). It had been proposed that these functionalities participate in the formation of a transitory pentavalent silicon species, stabilized through a donor bond to the imidazole nitrogen (Zhou et al., 1999). Using a nitrilotriacetic acid-terminated alkanethiol, which had been successfully self-assembled onto gold surfaces, silicatein could be immobilized on matrices; it was found to retain its enzymatic function, allowing the polycondensation of monomeric silicon alkoxides to form silica structures on surfaces (Tahir et al., 2004).

Originally it was shown that silicatein is the main component of the axial filament of the spicules (Cha et al., 1999; Krasko et al., 2000). Later this enzyme was detected also in the extra-spicular space where it contributes to the appositional growth of these skeletal elements (Müller et al., 2005a; Schröder et al., 2006). Silicatein uses either organo-functional silanes (Cha et al., 1999) or orthosilicate for the synthesis of poly(silicate). Since seawater has a low content of silicate (about 5 µM) the sponges have to transport silicate actively into their cells, via a putative $Na^+/HCO_3^-[Si(OH)_4]$ co-transporter (Schröder et al., 2004). Intracellularly silicate is stored in silicasomes, organelles comprising a high content of silicate (Schröder et al., 2007b). These studies were performed with the sponge tissue culture system [termed primmorph system] (Müller et al., 1999a), a special form of 3D-cell aggregates, which are composed of proliferating and differentiating cells. Primmorphs allow the investigation of spicule formation under controlled conditions (Eckert et al., 2006).

The existence of silicatein in silicasomes with high silica levels implies that silicatein might be involved in the storage of silica in these organelles, presumably controlling the gel-sol state of silicate. From diatoms it is known that silicate is deposited in special organelles, the silica deposition vesicles, which contain besides high levels of silicate also organic components of unknown function, e.g. mannose (Li et al., 1989; Vrieling et al., 1999; Bäuerlein, 2003). It can be assumed that these molecules prevent a polycondensation of silicate. Since silicate – at neutral pH – polycondensates at concentrations above 1 mM to poly(silicate) (Iler, 1979), it can be postulated that (organic) molecules, e.g. silicatein, contribute to the stabilization of

the sol state of silica. One mechanism for the gel to sol conversion could be the hydrolysis of the oxygen-bridge of the polymerized/polycondensated silicic acid. The linkage between silicate or tetrahedral silica units in poly(silicate) can be considered as an ester-like bonding. In order to test if silicatein – besides being a poly(silicate) forming enzyme [silica-polymerase] – functions also as an silica-esterase, we studied its hydrolytic function on bis(p-aminophenoxy)-dimethylsilane [BAPD-silane]. This compound comprises two ester-like bonds between silicon and p-aminophenol and two methyl silane linkages (Figure 4.1). In line with a previous study (Cha et al., 1999) we propose that hydrogen-bonding between the imidazole nitrogen of the conserved His and the hydroxyl of the active-site Ser increases the nucleophilicity of the Ser oxygen, facilitating the attack of silicatein on the silicon atom of the substrate. This reaction can be monitored spectroscopically on the basis of the release of p-aminophenol. The experimental data show that silicatein comprises, in addition to its silica-polymerase activity, also a silica-esterase function, thus supporting the concept that silicatein is involved in the stabilization of the sol-state of biogenic silica. The esterase reaction can be completely blocked by Na-hexafluorosilicate and by the cysteine proteinase inhibitor E-64 [L-*trans*-epoxysuccinyl-leucylamido(4-guanidino)butane] (Barrett et al.,1982). For these studies, resulting in the elucidation of the new activity of silicatein to function as a silica-esterase, we used recombinant silicatein-α from the demosponge *S. domuncula* (Krasko et al., 2000).

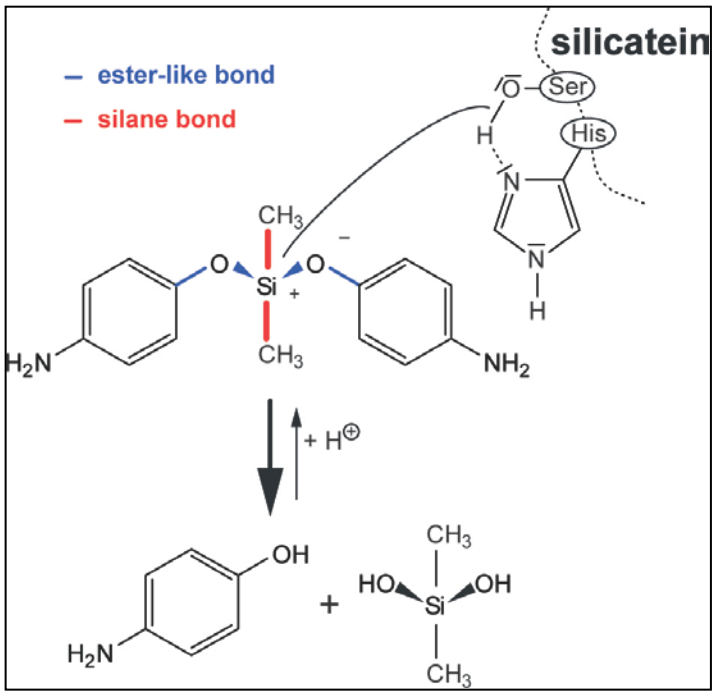

Figure 4.1: Proposed silicatein-α mediated reaction mechanism for hydrolysis of bis(p-aminophenoxy)-dimethylsilane which contains two silicic ester-like (blue) and two silane bonds (red). In the catalytic center of silicatein, the serine (Ser) oxygen makes a nucleophilic attack on the silicon, resulting in displacement of p-aminophenol and formation of a (alkoxyl)-monosilane. This reaction is facilitated by hydrogen bonding between the imidazole nitrogen of the conserved histidine (His) and the hydroxyl of the Ser.

4.2 Experimental section

4.2.1 Chemicals

Dimethyldimethoxysilane ($C_4H_{12}O_2Si$, MW 120.22) and bis(p-aminophenoxy)-dimethylsilane [BAPD-silane] ($C_{14}H_{18}N_2O_2Si$, MW 274.39) were obtained from ABCR (Karlsruhe; Germany); bovine serum albumin (fraction 5) from Roth (Karlsruhe; Germany); Sodiumhexafluorosilicate from Sigma-Aldrich (Taufkirchen; Germany) and p-aminophenol from Riedel de Haën (Seelze; Germany).

4.2.2 Sponges and primmorphs

Specimens of the marine sponge *Suberites domuncula* (Porifera, Demospongiae, Hadromerida) were collected in the Northern Adriatic near Rovinj (Croatia), and then kept in aquaria in Mainz (Germany) at a temperature of 17°C for more than 5 months. From these animals primmorphs, a three-dimensional cell system (Krasko et al., 2000; Müller et al., 1999a; Eckert et al., 2006), were prepared. Tissue of *S. domuncula* was cutted in small pieces of 3 x 3 mm and transferred into calcium- and manganese-free seawater (CMFSW) + EDTA. After 90 minutes incubation at room temperature the sponge tissue was sieved through a net of 20 µm mesh size to separate cells from the spicules. The single cells, which assemble to primmorphs were resuspended and kept at 17°C in natural seawater (enriched with 60 µM of silicate), supplemented with 1% RPMI 1640 medium. Approximately 20 days later the primmorphs were used for analysis (Müller et al., 2005a).

4.2.3 Silicatein-α

Recombinant silicatein-α was prepared in *E. coli* as described (Krasko et al., 2000). The silicatein-α cDNA from *S. domuncula* was inserted into the oligohistidine expression vector pQE30 (Qiagen, Hilden; Germany) and used for transformation of Escherichia coli host strain BL21 (Novagen/Merck, Darmstadt; Germany). After induction of protein expression with isopropyl β-D-1-thiogalactopyranoside, the recombinant silicatein fusion was purified by affinity chromatography, unfolded in 6 M urea / 5 mM imidazole, and subsequently refolded through dialysis against 50 mM Tris-HCl buffer (pH 8.0; 0.5 M L-arginine, glutathion [9 mM GSH/1 mM GSSG]

redox couple, 0.5 M NaCl, 1 mM KCl). The enzyme was stored at a concentration of 2 mg / ml in 20 mM MOPS [3-(N-morpholino) propanesulfonic acid] buffer (pH 7.5; 50 mM Na-acetate, 1 mM EDTA).

4.2.4 Electron immunogold labeling

Polyclonal antibodies (PoAb-aSILIC) against recombinant silicatein-α from *S. domuncula* (Müller et al., 2005a) were used. Primmorph samples were treated with 0.1 % glutaraldehyde / 3% paraformaldehyde in 0.1 M phosphate buffer (pH 7.4). After 2 hrs the material was dehydrated in ethanol and embedded in LR-White Resin (Electron Microscopy Sciences, Hatfield, PA). 60 nm thick slices were cut, transferred onto coated copper grids and blocked with 5 % bovine serum albumin (BSA) in phosphate-buffered-saline (PBS) and then incubated with the primary antibody PoAb-aSILIC (1:1,000) for 12 hours at 4°C. After three washes with PBS / 1 % BSA the sections were incubated with 1:1,000 dilution of the secondary antibody for 2 hours. The second antibody which reacts against rabbit IgG-molecules was labelled with 1, 4 nm nanogold particle. Sections were rinsed in PBS, treated with 1% glutaraldehyde / PBS for 5 min, washed, and dried (Müller et al., 2005a). Subsequently, enhancement of the immunocomplexes was performed with silver as described (Danscher, 1981). The samples were examined by transmission electron microscopy (TEM) with the Tecnai 12 microscope (FEI Electron Optics, Eindhoven; Netherlands). As controls, pre-immune serum or PoAb-aSILIC, adsorbed to recombinant silicatein (Schröder et al., 2006) were used for the studies.

4.2.5 Maldi analysis

The assays were carried out as follows. 4.5 µg / ml Silicatein-α (210 nmol/ml using the size 21,329 Da [Krasko et al., 2000]) in MOPS buffer, was covered with a layer of dimethyl-dimethoxy-silane dissolved in diethyl ether (10 µmol/ml) in a ratio of 10:1 (v/v). After shaking the assays for 1 hr (20°C), samples were taken. For removal of the aqueous layer, containing the decomposition products, silicatein and buffer, the reaction was performed in single-use syringes which can be used like separatory funnels. The organic phase which contained solely the substrate and the siloxane polymer was dried using sodium sulfate to avoid further decomposition. Finally, the products were characterized by means of Matrix assisted laser desorption/ionization-

mass spectrometry (MALDI-MS [Müller et al., 2003b; Bahr et al., 1988]), which was performed in a Finnigan MAT Mass Spectrometer 8230 (Midland; Canada). In a control assay the reaction was performed in the absence of silicatein.

4.2.6 Esterase activity

The assay bases on the concentration-dependent increase of the ultra-violet absorption of the degradation product p-aminophenol (AP) from the hydrolysis of the substrate bis(p-aminophenoxy)-dimethylsilane [BAPD-silane] at a wavelength of 300 nm (Bierbaum, 2001). During continuous stirring of the assays in Suprasil mixing cuvettes (Hellma QS-110, Müllheim; Germany), the reaction was studied at 20°C within the absorbance range of 220 to 800 nm using a Varian Cary 5G UV-Vis-NIR-spectrophotometer (Mulgrave; Australia). Typical reactions of 3.5 ml per assay contained 0.4 µg/ml silicatein-α in the 20 mM MOPS buffer. First silicatein-α was mixed with the buffer and the baseline was measured. After addition of the substrate (30 sec) the kinetic determinations were started. From a 2 mM stock solution of BAPD-silane in diethyl ether the substrate concentrations from 20 µM to 200 µM were prepared. Where indicated sodium hexafluorosilicate (1 mM) or E64 (10 µM) was added to the reaction mixture, containing BAPD-silane (20 µM or 200 µM) and silicatein. In controls silicatein-α was replaced by BSA (4.5 µg / ml assay).

4.3 Results

4.3.1 Presence of silicatein in spicules and in cell organelles, the silicasomes

In *S. domuncula* the formation of spicules is a rapid process and surely proceeds more frequently in embryos or in primmorphs than in adult specimens. Because of this 60 nm sections through primmorphs were reacted with gold-labelled antibodies to silicatein-α and analyzed by TEM inspection.

Figure 4.2 A shows a cross-section through a spicule (sp). As expected strong signals are seen in the axial filament (af) within the sponge spicule. Hitherto this is the place proposed for major occurrence of the enzyme (Müller et al., 2005a; Müller et al., 2006b). A closer view of the axial canal (ac) in the center of the spicule reveals a localization of silicatein in the axial filament as well as within the silica shell surrounding the spicule (Fig. 4.2 C).

Not just within the spicule the antibodies react but the images also show a likewise dense accumulation of gold grains in the extra-spicular space, reflecting a dense package of silicatein molecules also there. The silicatein molecules are arranged around the spicules in concentric rings (ri) (Fig. 4.2 B). Strong reactions of PoAb-aSILIC are seen also in vesicles of the sclerocytes, the cells surrounding the spicules (Fig. 4.2 E and 4.2 F). These intracellular vesicles, termed silicasomes (sis), are rich in silica (Schröder et al., 2007b) and as the gold grains show they are additionally densely filled with the enzyme. Extracellular (Fig. 4.2 G) the silica-vesicles (siv) fuse with the concentric ring structures around the spicule (Fig. 4.2 H). Often these silica-vesicles remain as intact entities within the rings/cylinders, reacting positively to anti-silicatein (Fig. 4.2 H). Controls show that pre-immune serum does not react with structures within or around the spicules (Fig. 4.2 D); also PoAb-aSILIC, adsorbed to recombinant silicatein, did not react (not shown).

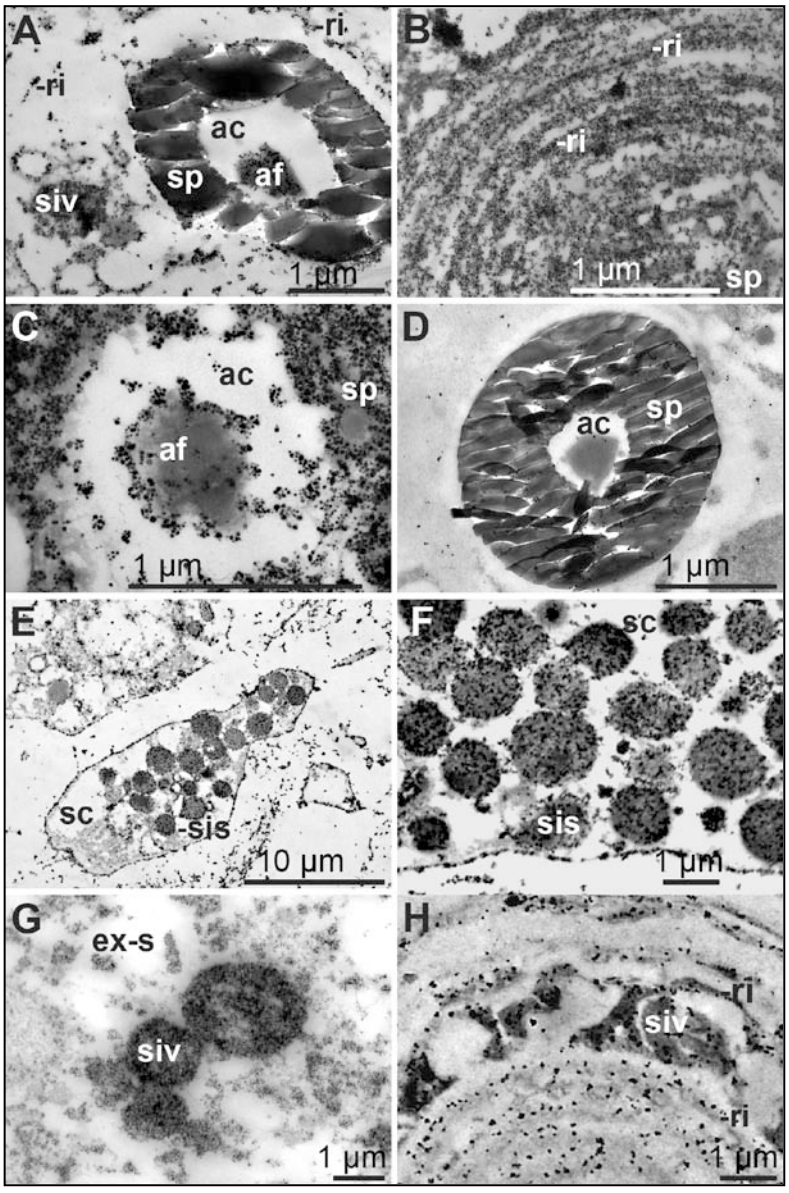

Figure 4.2: Localization of silicatein in spicules and in intra- and extracellular vesicles by TEM immunogold labeling. (i) Association of silicatein with spicules. (A) Strong antibody reactions are seen within the axial canal (ac) in the axial filament (af), which is surrounded by the spicule (sp); in addition, a silica vesicle (siv) within one concentric ring (ri) is present. (B) Strong antigen–antibody reactions are also seen on the concentric rings (ri) surrounding a spicule (sp). (C) In the axial canal (ac), high levels of signals are seen in and on the axial filament (af), as well as the inner rim of the silica spicule (sp). (D) Control: incubation of a section with pre-immune serum; no reaction is seen within the axial canal (ac) and around the spicule (sp). (ii) Intracellular localization of silicatein in vesicles. (E,F) The cells around the spicules, the sclerocytes (sc), are filled with vesicles, which strongly react with antibodies. These vesicles are termed silicasomes (sis). (iii) Extracellular localization of silicatein in vesicles. (G) In the extracellular space (ex-s), the silica vesicles (siv) can still be seen. (H) These silica vesicles (siv) frequently remain intact within rings/cylinders (ri).

4.3.2 Catalytic function of silicatein: silica-polymerase

The synthesis of polymerized derivates of silicic acid, poly(silicate), in terms of siloxanes, was performed with recombinant silicatein-α and dimethyl-dimethoxy-silane as substrate. After an incubation period of 1 hr the organic phase of the sample with the polymer was dried with sodium sulphate and then analyzed by MALDI-MS. If the sample was incubated without silicatein-α no signals above a mass of 500 Da are seen (Fig. 4.3 A).As shown in Figure 3B a stepwise 74 to 75 dalton increase in mass is recorded above an m/z of 500 which is due to a stepwise polymerization of -Si(Me)2-O- units to the starter silane-substrate. Under the incubation conditions which were used the synthesis of oligomers with 11 Si(Me)2-O-units could be resolved. This result demonstrates for the first time that silicatein-α, with its silica-polymerase activity, causes polymerization/condensation via a successive addition of monomeric silica units.

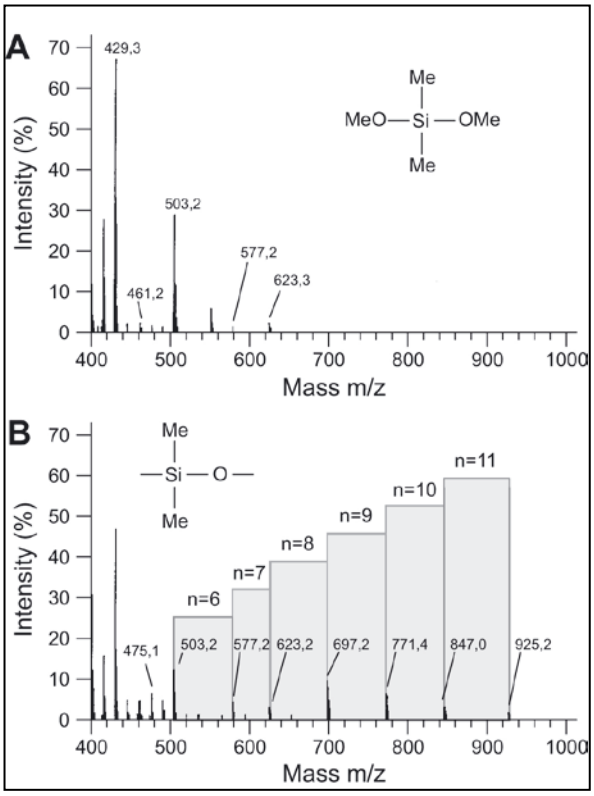

Figure 4.3: MALDI-MS spectrum of the products formed from dimethyldimethoxysilane in the absence (A) or presence of silicatein (B). The mass distributions differ significantly. In presence of silicatein (B) a distinct increase in chain length can be observed. The distance of 74 to 75 Da between each individual peak corresponds to the mass of a single -Si(Me)2-O unit; oligomeric polymerization of 11 units can be resolved. In contrast, (A), in the absence of silicatein no polymerization products can be observed.

4.3.3 Catalytic function of silicatein: silica-esterase activity

The silica-esterase activity of the recombinant silicatein-α was shown by the cleavage of bis(p-aminophenoxy)-dimethylsilane (BAPD-silane) as a substrate. The temperature optimum was found to be in the range of 20°C to 25°C. The silica-esterase was routinely determined at 20°C using a substrate range between 20 µM and 250 µM of BAPD-silane. After cleavage of one of the silica-ester bonds the concentration of the released product p-aminophenol (AP) was determined at a wavelength of 300 nm. Under the used conditions 300 nm is in the trailing edge of the main absorption bands. Another maximum is recorded at 230 nm (Fig. 4.4).

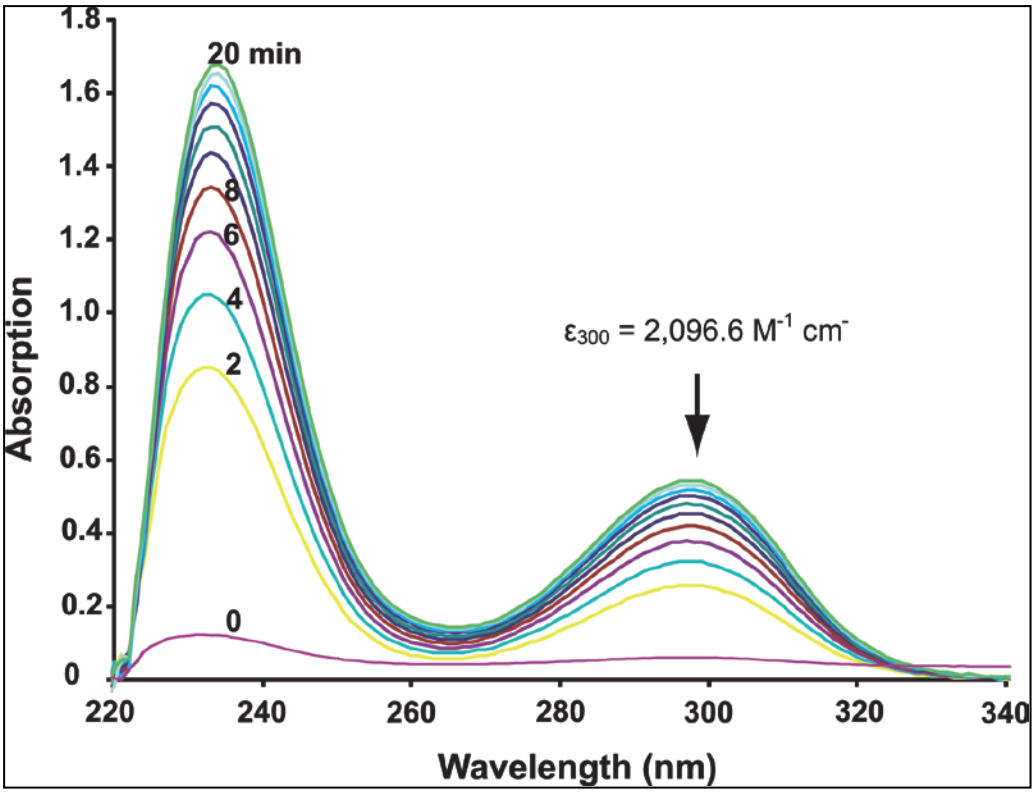

Figure 4.4: Change of absorption spectra during incubation of silicatein in the presence of 140 µM bis(p-aminophenoxy)-dimethylsilane substrate. At time zero min of the reaction, the absorbance at λ 300 nm is very low. The absorbance increase steadily during the consequitive 20 min of incubation. The molar absorption coefficient (ε) at 300 nm is indicated.

The molar absorption coefficient (ε at λ 300 nm) was determined (Pace et al., 1995) to be 2096.6 $L \bullet mol^{-1} \bullet cm^{-1}$ in enzyme reactions with BAPD-silane (20 µM, 100 µM and 200 µM).

Using this value the Michaelis constant (K_m) was determined (Michaelis and Menten, 1913) and calculated to be 22.7 µmol/l. In comparison, the K_m-value of the human recombinant cathepsin L (EC Number 3.4.22.15), the enzyme closest related to silicatein, expressed in *E. coli* was 1.1 µmol/l, using the substrate benzyloxycarbonyl-Phe-Arg-4-methylcoumarin-7-amide (Nomura et al., 1996). The turnover number (molecules of converted substrate per one enzyme molecule per sec) of the silicatein in the silica-esterase assay was determined to be 5.2. Human cathepsin L shows a slightly higher value of 20 using the substrate benzyloxycarbonyl-Phe-Arg-4-methylcoumarin-7-amide (Mason 1986).

In two series of experiments the specificity of the reaction was determined. At first, silicatein was replaced in the assay by the same amount of BSA. Under otherwise identical conditions, no significant increase in the absorbance at both 300 nm and 230 nm was seen during 2 min to 60 min incubation periods (20°C). Second, a direct interaction between the ester-like substrate BAPD-silane (50 µM) and a silicate monomer sodium hexafluorosilicate (1 mM) was studied in the reaction with silicatein. Sodium hexafluorosilicate was proven in earlier studies to induce growth of sponge cells in culture and to cause a differential gene expression *in vivo* and *in vitro* (Krasko et al., 2000; Osinga et al., 1999). After addition of a 20-fold molar excess of sodium hexafluorosilicate with respect to the ester-like substrate BAPD-silane a complete suppression of the ester-like activity of the enzyme was determined in the photometric test used here. Finally, the serine proteinase inhibitor E-64 was added to the reaction; at a concentration of 10 µM a > 95% inhibition of the esterase activity was determined.

4.4 Discussion

Sponges have to cope with an energetically highly expensive chain of reactions to form their siliceous spicules. The first barrier is the uptake of dissolved silicic acid from the surrounding aqueous milieu; usually only low concentrations of silicic acid, of approximately 5 µM, exist in the water (Maldonaldo et al., 2005). The uptake of silicic acid is very likely mediated by an ATP-consuming pump/transporter (Schröder et al., 2004). It is unknown whether the inorganic silicic acid monomers are converted intracellularly to organosilicate units. The subsequent process requires an intracellular transport of the silicic acid, or derivatives of it, to the organelles in which the initial formation of the spicules proceeds. It had been described that in the spicule-forming cells, the sclerocytes, the first layers of the silica shell of the spicules are formed around the silicatein-based axial filament in specific organelles (Müller et al., 2005a).

The prerequisite for the intracellular initiation of spicule synthesis is an accumulation of the silicic acid preferentially in special organelles. Recently such vesicles with high silica content, the silicasomes, have been identified in sclerocytes (Schröder et al., 2007b). It should be expected that in silicasomes where the silicic acid content is high, self-polymerization- or self-condensation processes are facilitated. Polymerization/condensation of monomeric silicic acid to poly(silicate) is a random process (Iler, 1979) which results in the formation three-dimensional condensed silica polymers or nuclei. In the present study experimental results have been provided which show that in these silicasomes silicic acid co-exists with silicatein. Hence, based on these microscopic analyses we asked further whether silicatein could function as a silica-esterase allowing a hydrolysis of the silicate ester bonds, under simultaneous dislocation of water. The data summarized here demonstrate that indeed silicatein has such a property; it mediates the cleavage of silicate ester bonds in the BAPD-silane substrate. Furthermore, it is documented that silicatein exhibits, as initially proposed (Cha et al., 1999), also silica polymerizing activity. We demonstrate that the polymerizing growth of the silica chains, mediated by the silica-polymerase activity of silicatein, involves a step-wise addition of single silica monomeric units. This finding implies that silicatein holds two different enzymatic properties, a silica-esterase activity and a polymerizing/polycondensating activity (silica-polymerase). At present, we work on the elucidation of the molecular

switch controlling these dual enzymatic functions; first data indicate that low molecular weight compound(s) direct silicatein to either the catabolic or the anabolic reaction. Enzymatic parameters of the silica-esterase activity were determined. The Michaelis constant (K_m: 22.7 µmol/l) and the turnover number (5.2 molecules of converted substrate per one enzyme molecule per sec) for the silica-esterase catalytic reaction of silicatein is similar to those that have been determined for the related hydrolytic enzyme cathepsin L (Nomura et al., 1996; Mason 1986).

The content of the silicasomes is released into the extracellular space (Schröder et al., 2007b), and transported from there to the spicules. As shown here, the extracellular silica-vesicles which contain silicatein, fuse with the appositionally growing spicules in the diametral direction, and very likely also in the axial direction (Müller et al., 2007b). These data show that silicatein is transported in silicasomes into the extracellular space; there, these silica-vesicles contribute to the appositionally growing spicules. Furthermore, our data allow to develop a functional model which contributes to the understanding of the, apparently template/matrix-lacking, growth of the siliceous spicules. The simultaneous release of silicic acid and silicatein into the concentric rings around the growing spicules, which gives rise to lamellar formation of the spicules (Osinga et al., 1999), allows a controlled polymerization/condensation process of silicic acid by silicatein along galectin strings/nets (Müller et al., 2006b). Very likely the shape of the poly(silicate) product is additionally tailored by a collagen sheathing (Eckert et al., 2006). A schematic outline of the localization and the transport of silicatein in the extra-spicular space is given in Fig.4.5.

The data summarized here provide for the first time enzyme kinetic data of silicatein, which will render a future rational- and aim-oriented application of silicatein in fabrication of (new) biomaterials, based on layered silica, titania and zirconia possible (Tahir et al., 2005). This new view is based on the finding of the dual role of silicatein, to act as an anabolic- (silica-polymerase) and a catabolic enzyme (silica-esterase), allowing the formation of controlled silica structures. In addition, patterning of poly(silicate) is modulated by self-assembly of silicatein molecules in an organized, fractal manner (Murr and Morse, 2005; Müller et al., 2007b); the fractal pattern very likely imprints the initial shape of the spicules (Müller et al., 2007c). The finding that silicatein catalyzes two reactions, acting as silica polymerase and silica esterase, provides this enzyme with advantageous properties, e.g. for production of a flexible

shell around organisms after bioencapsulation with silica. Recently, this feature has been utilized to encapsulate bacteria (Müller et al., 2008e): *E. coli* were transformed with the silicatein gene, and, after expression of silicatein and subsequent incubation with silicic acid, the bacteria had been encapsulated with bio-silica, a viscous cover, which did not reduce their growth properties (Müller et al., 2008e).

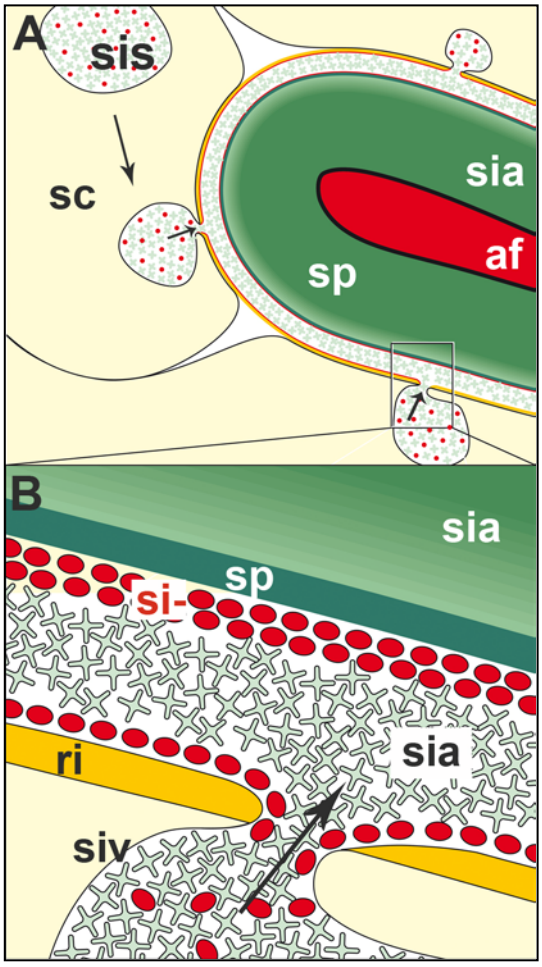

Figure 4.5: Localization of silicatein in the extra-spicular space. (A) The spicules (sp), formed from poly(silicate) (sia) are surrounded by sclerocytes (sc) which harbor the special organelles, the silicasomes (sis), that are rich in silicatein (red circles) and silicic acid (bluish circles). In the center of the spicules runs the axial filament (af), which is built from silicatein molecules. (B) The silicasomes are released from the sclerocytes and transported into the extracellular space from where these silica-vesicles (siv) are translocated to the ring structures surrounding the growing spicules (sp). The content of the silica-vesicles, harboring silicatein and monomeric silicic acid, fuse with the concentric rings (ri) present around the spicules. There the silicatein molecules are associated with the ring sheet, while the poly(silicate) (sia) remains in the siliceous lamellae, which are formed within the rings.

4.5 References

Bahr U., Deppe A., Karas M. & Hillekamp F. (1988). Mass spectrometry of synthetic polymers by UV-matrix-assisted laser desorption/ionization. *Anal Chem* 64, 2866 – 2869.

Barrett A.J., Kembhavi A.A., Brown M.A., Kirschke H., Knight C.G., Tama M. & Hanada K. (1982). L-*trans*-Epoxysuccinyl-leucylamido(4-guanidino)butane and its analogues as inhibitors of cysteine proteinases including cathepsins B, H and L. *Biochem J* 201, 189-198.

Bäuerlein E. (2003). Biomineralization of unicellular organisms: an unusual membrane biochemistry for the production of inorganic nano- and microstructures. *Angew Chem Int Ed* 42, 614-641.

Bierbaum V. (2001). Frontiers in Mass Spectrometry. *Chem Rev* 101, 209-606.

Cha J.N., Shimizu K., Zhou Y., Christianssen S.C., Chmelka B.F., Stucky G.D. & Morse D.E. (1999). Silicatein filaments and subunits from a marine sponge direct the polymerization of silica and silicones *in vitro*. *Proc Natl Acad Sci USA* 96, 361-365.

Chatterjee S., Pramanik S. & Bhattacharya S.C. (2005). Spectroscopic study of some photographic developing agents in reverse micelles of AOT in heptane. *J Molec Liquids* 116, 131– 137.

Danscher G. (1981). Histochemical demonstration of heavy metals. A revised version of the sulphide silver method suitable for both light and electronmicroscopy. *Histochemistry* 71, 1-16.

Eckert C., Schröder H.C., Brandt D., Perovic-Ottstadt S. & Müller W.E.G. (2006). A histochemical and electron microscopic analysis of the spiculogenesis in the demosponge *Suberites domuncula*. *J Histochem Cytochem* 54, 1031-1040.

Iler K.K. (1979). The Chemistry of Silica. Wiley & Sons, New York.

Krasko A., Batel R., Schröder H.C., Müller I.M. & Müller W.E.G. (2000). Expression of silicatein and collagen genes in the marine sponge *Suberites domuncula* is controlled by silicate and myotrophin. *Europ J Biochem* 267, 4878-4887.

Li C.W., Chu S. & Lee M. (1989). Characterizing the silica deposition vesicle of diatoms. *Protoplasma* 151, 158-163.

Maldonado M., Carmona M.C., Velasquez Z., Puig A., Cruzado A., Lopez A. & Young C.M. (2005). Siliceous sponges as a silicon sink: An overlooked aspect of benthopelagic coupling in the marine silicon cycle. *Limnol Oceanogr* 50, 799–809.

Mason R.W. (1986). Species variants of cathepsin L and their immunological identification. *Biochem J* 240, 285-288.

Michaelis L. & Menten M. (1913). Die Kinetik der Invertinwirkung. *Biochem Z* 49, 333-369.

Morse D.E. (1999). Silicon biotechnology: Harnessing biological silica production to make new materials. *Trends in Biotechnology* 17, 230-232.

Morse D.E. (2000). Silicon biotechnology: Proteins, genes and molecular mechanisms controlling biosilica nanofabrication offer new routes to polysiloxane synthesis. In *Organosilicon Chemistry IV: from Molecules to Materials* (Auner N, Weis J, eds), pp. 5-16. Wiley-VCH, New York.

Müller W.E.G., Wiens M., Batel R., Steffen R., Borojevic R. & Custodio R.M. (1999a). Establishment of a primary cell culture from a sponge: primmorphs from *Suberites domuncula*. *Marine Ecol Progr Ser* 178, 205-219.

Müller W.E.G., Krasko A., Le Pennec G., Steffen R., Ammar M.S.A., Wiens M., Müller I.M. & Schröder H.C. (2003b). Molecular mechanism of spicule formation in the demosponge *Suberites domuncula*: silicatein - collagen - myotrophin. *Progress Molec Subcell Biol* 33, 195-222.

Müller W.E.G., Rothenberger M., Boreiko A., Tremel W., Reiber A. & Schröder H.C. (2005a). Formation of siliceous spicules in the marine demosponge *Suberites domuncula. Cell Tissue Res* 321, 285-297.

Müller W.E.G., Belikov S.I., Tremel W., Perry C.C., Gieskes W.W.C., Boreiko A. & Schröder H.C. (2006b). Siliceous spicules in marine demosponges (example *Suberites domuncula*). *Micron* 37, 107-120.

Müller W.E.G., Wang X., Belikov S.I., Tremel W., Schloßmacher U., Natoli A., Brandt D., Boreiko A., Tahir M.N., Müller I.M. & Schröder H.C. (2007b). Formation of siliceous spicules in demosponges: example *Suberites domuncula*. In Handbook of Biomineralization; Vol. 1: Biological Aspects and Structure Formation (Bäuerlein E, ed), pp. 59-82. Wiley-VCH, Weinheim.

Müller W.E.G., Schloßmacher U., Eckert C., Krasko A., Boreiko A., Ushijima H., Wolf S.E., Tremel W. & Schröder H.C. (2007c). Analysis of the axial filament in spicules of the demosponge *Geodia cydonium*: different silicatein composition in microscleres [asters] and megascleres [oxeas and triaenes]. *Europ J Cell Biol* 86, 473-487.

Müller W.E.G., Engel S., Wang X.H., Wolf S.E., Tremel W., Thakur N.L., Krasko A., Divekar M. & Schröder H.C. (2008e) Bioencapsulation of living bacteria (Escherichia coli) with poly(silicate) after transformation with silicatein-α gene. *Biomaterials* 29, 771-779.

Murr M.M. & Morse D.E. (2005). Fractal intermediates in the self-assembly of silicatein filaments. *Proc Natl Acad Sci USA* 102, 11657–11662.

Nomura T., Fujishima A. & Fujisawa Y. (1996). Characterization and crystallization of recombinant human cathepsin L. *Biochem Biophys Res Commun* 228, 792-796.

Osinga R., Tramper J. & Wijffels R.H. (1999). Cultivation of marine sponges. *Mar Biotechnol* 1, 509-532.

Pace C.N., Vajdos F., Fee L., Grimsley G. & Gray T. (1995). How to measure and predict the molar absorption coefficient of a protein. Protein Sci 4, 2411-2423.

Perry C.C. (2003). Silicification: the process by which organisms capture and mineralize silica. *Rev Mineralog. Geochem* 54, 291-327.

Schröder H.C., Perović-Ottstadt S., Rothenberger M., Wiens M., Schwertner H., Batel R., Korzhev M., Müller I.M. & Müller W.E.G. (2004). Silica transport in the demosponge *Suberites domuncula*: fluorescence emission analysis using the PDMPO probe and cloning of a potential transporter. *Biochem J* 381, 665-673.

Schröder H.C., Boreiko A., Korzhev M., Tahir M.N., Tremel W., Eckert C., Ushijima H., Müller I.M. & Müller W.E.G. (2006). Co-Expression and functional interaction of silicatein with galectin: matrix-guided formation of siliceous spicules in the marine demosponge *Suberites domuncula*. *J Biol Chem* 281, 12001–12009.

Schröder H.C., Brandt D., Schloßmacher U., Wang X., Tahir M.N., Tremel W., Belikov S.I. & Müller W.E.G. (2007a). Enzymatic production of biosilica-glass using enzymes from sponges: Basic aspects and application in nanobiotechnology (material sciences and medicine). Naturwissenschaften 94, 39-359.

Schröder H.C., Natalio F., Shukoor I., Tremel W., Schloßmacher U., Wang X. & Müller W.E.G. (2007b). Apposition of silica lamellae during growth of spicules in the demosponge *Suberites domuncula*: biological/biochemical studies and chemical/biomimetical confirmation. *J Struct Biol* 159, 325–334.

Shimizu K., Cha J., Stucky G.D. & Morse D.E. (1998). Silicatein alpha: cathepsin L-like protein in sponge biosilica. *Proc Natl Acad Sci USA* 95, 6234-6238.

Stöber W., Fink A. & Bohn E. (1968). Controlled growth of monodisperse silica spheres in the micron size range. *J Colloid Interface Sci* 26, 62-69.

Tahir M.N., Théato P., Müller W.E.G., Schröder H.C., Janshoff A., Zhang J., Huth J. & Tremel W. (2004). Monitoring the formation of biosilica catalysed by histidin-tagged silicatein. *ChemComm*. 24, 2848-2849.

Tahir M.N., Théato P., Müller W.E.G., Schröder H.C., Boreiko A., Faiß S., Janshoff A., Huth J. & Tremel W. (2005). Formation of layered titania and zirconia catalysed by surface-bound silicatein. *ChemComm* 44, 5533-5535.

Vrieling E.G., Poort L., Beelen T.P.M. & Gieskes W.W.C. (1999). Growth and silica content of the diatoms *Thalassiosira weissflogii* and *Navicula salinarum* at different salinities and enrichments with aluminium. *Europ J Phycology* 34, 307-316.

Wang X. & Wang Y. (2006). An introduction to the study on natural characteristics of sponge spicules and bionic applications. *Advances in Earth Science* 21, 37-42.

Weiner S. & Dove P.M. (2003). An overview of biomineralization processes and the problem of the vital effect. I*n Biomineralization. Reviews in Mineralogy & Geochemistry* (Dove PM, DeYoreo JJ, Weiner S, eds), pp. 54, 1-29.

Zhou Y., Shimizu K., Cha J.N., Stucky G.D. & Morse D.E. (1999). Efficient catalysis of polysiloxane synthesis by silicatein α requires specific hydroxy and imidazole functionalities. *Angew Chem Int Ed Engl* 38, 780–782.

Chapter 5

Silintaphin-1: Interaction with silicatein during structure guiding biosilica formation

5.1 Introduction

The skeleton of siliceous sponges is constructed of an interwoven meshwork of skeletal elements (spicules), which are made of biosilica (Uriz et al., 2003; Sandford, 2003). Size and shape of spicules are genetically controlled and represent a species-specific morphology often used for phylogenetic and taxonomic purposes. Spicules are classified into the larger megascleres (> 30 µm; Fig. 1A to C) and the smaller microscleres (< 30 µm; Fig. 1D to G). They display a high variety of symmetries, from monaxons (one axis symmetry) with two rays (oxea/styles; Fig. 1A) or three rays (triactinal scleres; Fig. 1B) to triaxons (consisting of six rays intersecting at right angles) or tetraxons (Fig. 1C). Microscleres are even more ornate. Such scleres are found in both demosponges, e.g. *Geodia cydonium* (Fig. 1D and E) and hexactinellids, e.g. *Monorhaphis chuni* (Fig. 1F) or *Euplectella marshalli* (Fig. 1G). Basically, spiculogenesis follows the same pattern in both demosponges and hexactinellids. It starts with the formation a proteinaceous axial filament around which a silica shell is formed. The axial filament is located within a central canal of spicules and also in their rays. If the spicules are spherical, e.g. in the sterrasters of G. cydonium, the axial filaments within the centrally oriented rays reach the surfaces and form cone-like tips, often sticking out from the tips (Fig. 1E). Following this intracellular phase and as outlined in the earliest description by Lieberkühn (1856) (Fig. 1B), the growing spicules are extruded from the cells and completed extracellularly within the mesohyl (Müller et al., 2005a).

In Demospongiae and Hexactinellida, the siliceous matrix of spicules is formed enzymatically by cathepsin-related silicatein(s) (Shimizu et al., 1998; Cha et al., 1999; Krasko et al., 2000; Müller et al., 2008c). These enzyme(s) catalyze the synthesis of the inorganic polymer from monomeric silica building blocks (Müller et al., 2008b; Schröder et al., 2010). Two isoforms of silicateins have been described previously, silicatein-α and silicatein-β (Shimizu et al., 1998; Krasko et al., 2000). Unique to the silicateins is that they carry out two functions, (i) to catalyze biosilica formation and (ii) to provide the initial blueprint for spicular morphogenesis (Müller et

al., 2009b). Silicatein molecules strongly interact with each other and form oligomers composed of the different isoforms, silicatein-α and silicatein-β (Müller et al., 2005a). The self-assembly of silicateins has been studied in *Tethya aurantium* and described as diffusion limited, fractally patterned aggregates finally forming filaments (Murr and Morse, 2005). If spicular proteins are isolated not by hydrofluoric acid [HF] treatment, a solvent which might chemically modify the enzyme, but in a glycerol-containing Tris buffer under mild conditions, as first described for *S. domuncula* spicules (Müller et al., 2007a), the dimer-tetramer-oligomer transitions can be followed even by sodium dodecyl sulfate polyacrylamide gel electrophoresis. Similar to the *T. aurantium* silicateins (Murr and Morse, 2005), the *S. domuncula* enzymes assemble via fractal intermediates and form long, highly flexible filaments. In contrast to *T. aurantium*, *S. domuncula* silicateins never covalently link to form filaments (Murr and Morse, 2005; Müller et al., 2007a). Based on electrophoretic analyses, a model has been proposed to describe the assembly process in the following three steps: (i) initial stoichiometric assembly of four silicatein-α monomers to a tetramer, which enfolds one central silicatein-β monomer, (ii) individual pentamers assemble to fractal-like structures, (iii) fractal-like structures undergo filament formation.

The axial filaments of siliceous sponges appear as rather rigid rods (Uriz, 2006). Combination of several techniques, including synchrotron radiation, scanning electron microscopy [SEM], thermogravimetric analysis, spectroscopy, and molecular modeling propose that the axial filaments of demosponges and hexactinellids are hexagonally packed into units which are stacked by hydrogen bonds (Croce et al., 2004). Furthermore, the axial filament is thought to provide the basic shape/morphology of spicules (Wang et al., 2010).

Recently, another protein involved in poriferan biosilicification has been identified: Silintaphin-1 (43 kDa) was discovered during a yeast two-hybrid library screening as strong interactor of silicatein (Wiens et al., 2009). Silintaphin-1 bears a protein-interaction domain (PH domain) that is required for binding of silicatein. Both recombinant proteins (silicatein and silintaphin-1) assemble in vitro to microscale filaments and facilitate the formation of synthetic spicules in the presence of Fe_2O_3 (Wiens et al., 2009) or silica nanoparticles (Müller et al., 2009b).

The present study aims to analyze the effect of self-assembled complexes of recombinant silicatein and silintaphin-1 on biosilica synthesis, as compared to the activity of recombinant silicatein or isolated axial filaments. For all studies, the

S. domuncula system was used. Only here, the most comprehensive biological and developmental data are available (Müller, 2006a) as well as biochemical (Müller et al., 2005a) and molecular biological data (Harcet et al., 2010), which are required for understanding of poriferan spiculogenesis and bodyplan formation. The data presented in this study shows that silintaphin-1 significantly enhances the activity of silicatein and, consequently, is crucially involved in the organization of the fractal-like biosilica structures.

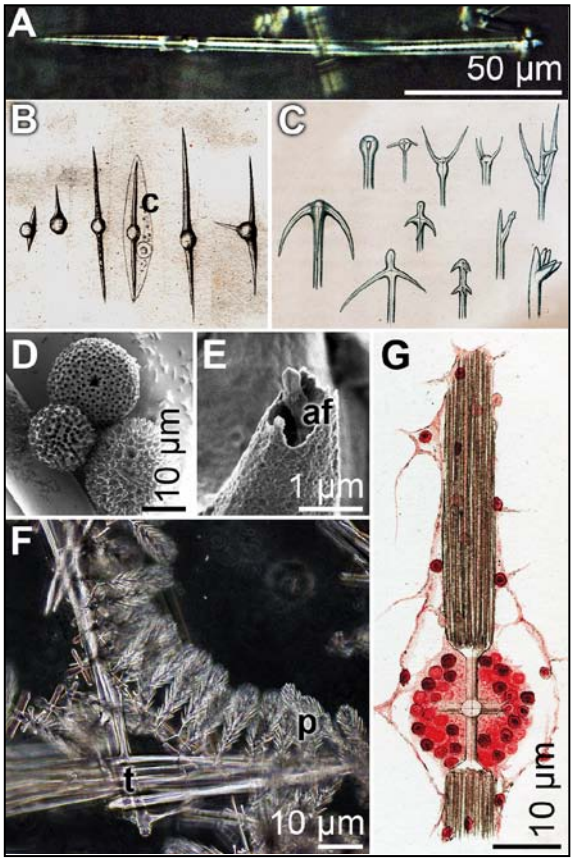

Fig. 5.1. Morphology of siliceous sponge spicules. (A to C): megascleres; (D to G): microscleres. (A) Monaxonal spicules, having one axis but two (different) rays, with the example of a *S. domuncula* (demosponge) tylostyle. (B) The earliest drawing of spicule formation in tissue of the freshwater sponge *Spongilla sp.* (Lieberkühn 1856), outlining the intracellular initiation of spicule synthesis; c: cell. This sponge forms monaxonal, triactinal (three rays) scleres. (C) Tetraxonal spicules, growing along four axes. Here, different spicular shapes of the demosponges *Tetilla grandis, Craniella simillima*, and *Craniella cranium* are shown; reproduced from Sollas (1888). (D) As example of microscleres, the spherical sterraster of *Geodia cydonium* (demosponge) are shown. The centrally oriented rays are reaching the surface and end in cone-like tips. (E) Open tips show the axial filament (af) embedded within the rays. (F) Especially in hexactinellids, an excessive branching of microscleres exists. In the hexactinellid *M. chuni*, microscleres (pinular pentactines, p) are associated with megascleres (tauactines, t). (G) Drawing from Ijima (1901) of an *Euplectella marshalli* microsclere.

5.2 Experimental section

5.2.1 Production of recombinant proteins and antibodies:

Recombinant silicatein-α was prepared as described (Krasko et al., 2000). In brief, the silicatein-α cDNA from *S. domuncula* was inserted into the oligohistidine expression vector pQE30 (Qiagen, Hilden; Germany) and used for transformation of Escherichia coli host strain BL21 (Novagen/Merck, Darmstadt; Germany). After induction of protein expression with isopropyl β-D-1-thiogalactopyranoside, the recombinant silicatein-fusion was purified by affinity chromatography, unfolded in 6 M urea / 5 mM imidazole, and subsequently refolded through dialysis against 50 mM Tris-HCl buffer (pH 8.5; 0.5 M L-arginine, glutathion [9 mM GSH / 1 mM GSSG] redox couple, 0.3 M NaCl, 1 mM KCl). The final protein concentration was adjusted to 250 µg/ml.

Recombinant silintaphin-1 cDNA was cloned into the expression vector pTrcHis2-TOPO (Invitrogen, Karlsruhe; Germany) in frame with a C-terminal 6xHis-tag and transferred into BL21 cells (Wiens et al., 2009). The recombinant fusion protein was purified by affinity chromatography and stored in 50 mM Tris-HCl (pH 7.4; 150 mM NaCl) at a concentration of 85 µg/ml.

Polyclonal antibodies [pAb] against the recombinant proteins were raised in rabbits (silicatein-α and silicatein-β; Müller et al., 2005a) or in Balbc/An mice (silintaphin-1; Wiens et al., 2009). For immunodetection, pAb directed against silicatein-α (aSilic-α 387) was diluted 1:1,500 (immunohistology) or 1: 2,000 (Western blotting). pAb directed against silicatein-β (aSilic-β 389) was diluted 1:1,000 (immunohistology or Western blotting). Finally, pAB directed against silintaphin-1 (aSiphn-1-01) was diluted 1,500 or 1:3,000. Where indicated, 100 µl of the antibody sample were adsorbed (30 min, 20°C) with 50 µg/ml of recombinant protein (recombinant silicatein-α, silicatein-β, or silintaphin-1) prior to use. Secondary antibodies were obtained from Invitrogen and Dianova (Hamburg; Germany).

5.2.2 Animals

Specimens of the marine sponge *Suberites domuncula* (Porifera, Demospongiae, Hadromerida) were collected in the Northern Adriatic near Rovinj (Croatia) and then kept in aquaria in Mainz (Germany) at a temperature of 17°C for more than 5 months.

5.2.3 Spicules and spicular extracts

Tissue samples of the sponge *S. domuncula* were cutted into 1 x 1 mm pieces and were treated on ice with a 4:1 (v/v) sulfuric acid/nitric acid solution to obtain clean spicules. They were washed with distilled water until the spicules were free of acid and reached pH 6. To ensure that their surface did not contain any contaminating proteins the spicules were treated with n-butanol/water/SDS overnight.

For Western blot analysis the axial filaments of the spicules were extracted with buffered HF (1M HF/ 4M NH_4F; pH 5.5) overnight at room temperature. After complete removal of the spicules silica the extracts were dialyzed against distilled water and the proteins were pelleted by centrifugation (40,000 x g; 4°C; 24 hrs), according to Shimizu et al. (1998). This sample was termed “HF-extract”.

For the second isolation procedure the axial proteins of *S. domuncula* spicules were obtained using a mild Tris/glycerol extraction buffer system (pH 8.8; 50mM Tris-HCl, 15% glycerol [w/v], 1mM EDTA, 150mM NaCl, 5mM DL-dithiothreitol [DTT]), according to Müller et al. (2007a). The spicules were homogenized in 200 ml of Tris/glycerol buffer in a motar and were agitated on a shaker at 25°C for 1 h. The supernatant was concentrated with Microcon Centrifugal Filter Devices (3000 MWCO Millipore, Schwalbach; Germany) for 10 minutes at 10,000 x g. The resulting extracts were termed “glycerol-extract”. The protein concentration was determined by application of the Bradford method (Kruger, 2002), using Coomassie blue (Roti®-Quant, Roth, Karlsruhe, Germany). The results were statistically evaluated using the paired Student’s *t*-test (Sachs, 1984).

Prior to activity testing, the samples were diluted to 30 µg/ml using 50 mM Tris-HCl (pH 7.4; 150 mM NaCl).

5.2.4 Determination of enzymatic activity

For the determination of enzymatic activity either 6 µg of purified recombinant silicatein-α or 6 µg of axial filament extract ("glycerol-extract") were prepared in 1 ml of 50 mM Tris-HCl (pH 7.4; 150 mM NaCl). In some experiments the recombinant silicatein-α sample was mixed prior activity test for 10 min with recombinant silintaphin-1 at a stoichiometric ratio of 1:1, 4:1, or 10:1 [wt:wt].

In a second series of experiments the "glycerol-extract" was supplemented with one of the three antibodies (aSilic-α, aSilic-β, or aSiphn-1-01) prior to testing.

Silicatein activity was assayed as described (Cha et al., 1999; Krasko et al., 2000). Hydrolysis of TEOS [tetraethyl orthosilicate silicate; Sigma-Aldrich, Taufkirchen; Germany] was performed as described (Tong et al., 2002). In short, using a 1:5 molar ratio of TEOS:H_2O in 10 mM HCl at a pH 2.5 for 10 min. For activity tests, 200 µM of prehydrolyzed TEOS was added as the last component. The enzymatic reactions were performed at 22°C for 1 hr while agitating. After incubation the samples were centrifuged (10,000 x g, 30 min, 4°C) and washed 3 times with ethanol. The sedimented silica particles were treated with 2 M NaOH for 30 min (30°C) to hydrolyze biosilica. The quantification soluble silicic acid was determined by the classical molybdenum blue colorimetric method (Shimizu et al., 1998), using the Silicon Test colorimetric assay kit (Merck #1.14794, Darmstadt; Germany). Based on the absorbance values at 795 nm, absolute amounts of silicic acid were calculated according to a calibration curve of a silicon standard (Merck #1.09947). As controls heat denatured protein solution were used in parallel. The experiments were performed in duplicate and were statistically evaluated using the paired Student`s t-test

For determination of the enzymatic activity of the axial filaments isolated by HF treatment they were transferred into the reaction mixture and incubated with 380 µM of prehydrolyzed TEOS. After incubation at 22°C for 24 hrs the samples were mounted on carbon coated copper grids, washed three times with water and analyzed by TEM.

Similarly, aggregates of recombinant silicatein-α or silicatein-α/silintaphin-1 (in a 4 to 1 molar stoichiometric ratio) were supplemented with 200 µM of prehydrolyzed TEOS and were allowed to re-assemble for 240 min in the 50 mM Tris-HCl buffer (pH 7.4; 150 mM NaCl). After incubation at 22°C for 24 hrs, the reaction product was mounted

on carbon coated copper grids, washed three times with water and analyzed by TEM. The final protein concentration in the assays was 6 µg.

5.2.4 Immunohistology

Frozen cryosections (8 µm thickness) through sponge tissue samples were fixed with paraformaldehyde and reacted with polyclonal antibodies against silicatein-α (aSilic-α), silicatein-β (aSilic-β), and silintaphin-1 (aSiphn-1-01) at the dilutions of 1:1500. After blocking with 1% milkpowder the specimens were incubated with the corresponding secondary species-specific antibody, i.e. Cy3-conjugated $F(ab')_2$ goat anti-rabbit IgG, Cy3-conjugated goat anti-mouse IgG (Jackson ImmunoResearch, Cambridgshire; UK), or with Alexa Fluor 488-conjugated $F(ab')_2$ goat anti-rabbit IgG (Invitrogen). Immunofluorescence was assessed with an Olympus AHBT3 light microscope, together with an AH3-RFC reflected light fluorescence attachment.

5.2.5 TEM fixation

Sponge tissue samples were fixed in fixation buffer 1 (2,5 % (v/V) Glutaraldehyd, (0,82 % (m/v) NaCl, 0,1 M phosphate buffer, pH 7,3-7,4) for 1 hour at room temperature. After washing with 0, 1 M phosphate buffer (1,75 % (m/V) NaCl, pH 7,4) 4 times for 15 minutes the samples are fixed in fixation buffer 2 (0,1 M phosphate puffer, 25 % (m/v) $NaHCO_3$, 2,0 % (v/v) OsO_4, 1,0 % (m/v) NaCl, pH 7,3-7,4) for 1 hour at room temperature. Then the samples were washed with distilled water for 6 x 10 minutes. Before embedding the samples into Araldite CY 212 they were dehydrated with increasing ethanol solutions (0 %, 50 %, 70 %, 80 %, 96 %, 100 %) for 2 x 10 minutes each concentration. The araldite solution (51 % (m/v) Araldite CY 212, 47 % (m/v) Araldite hardener HY 964, 2 % (m/v) 2,4,6, Tris(dimethylaminomethyl)phenol) was diluted 1:1 (v/v) with propylene oxide and the samples were incubated for 1 day at room temperature. For hardening the samples were transferred into pure araldite solution at 60°C for 2 days. They were cut (Ultracut S, Leica, Nussloch) into 60 nm sections and transfered onto copper grids (75 square per inch)

5.2.6 SDS-PAGE and Western blotting analyses

The protein samples ("HF-extract") were subjected to 14% polyacrylamide gel electrophoresis containing 0.01% SDS. Sodium dodecyl sulfate polyacrylamide gel electrophoresis (SDS-PAGE) was essentially as described (Müller et al., 2007a). After size separation the proteins were stained with Coomassie brilliant blue. In parallel gels proteins were transferred to PVDF membranes (Millipore-Roth, Karlsruhe; Germany) via semi-dry blotting (1mA / 1cm^2). The membranes were blocked with 1% milk powder overnight at 4°C and after washing with 1xTBS (10 mM Tris-HCl, 150 mM NaCl, pH 8,0) they were reacted with the three polyclonal antibodies against aSilic-α, aSilic-β, and aSiphn-1-01 at dilutions of 1:2000. Subsequently, the membranes were washed three times with 1xTBST (10 mM Tris-HCl, 150 mM NaCl, 0, 05 % Tween®20 (v/v), pH 8,0) and incubated with anti-rabbit IgG, or anti-mouse IgG (alkaline phosphatase-conjugated; 1:2,000 dilution; Sigma). After equilibration in P3 buffer 100 mM Tris, 100 mM NaCl, pH 9,5) the immunocomplexes were visualized with the substrate system NBT/BCIP [nitro blue tetrazolium chloride/5-bromo-4-chloro-3-indolyl phosphate, toluidine salt] (Roth).

5.2.7 Electron microscopic analysis of biosilica products

The biosilica products formed by axial filaments in vitro were incubated with prehydrolyzed TEOS for 1h at 25°C on a shaker. The samples were washed several times with water and were applied onto carbon coated copper grids (Plano, Wetzlar, Germany), air-dried and inspected using a Philips EM-420:120 kV transmission electron microscope (TEM) equipped with a CCD camera.

The samples for High-resolution scanning electron microscopy (SEM) were mounted on stubs (carbon adhesive Leit-Tabs No.: G 3347 [Plano, Wetzlar; Germany]) and were analyzed with a Gemini Leo 1530 high-resolution field emission scanning electron microscope (Zeiss, Oberkochen; Germany).

5.2.8 Filament assembly with silicatein-α and silintaphin-1

Recombinant silicatein-α was incubated (at 22°C) alone or at stoichiometric molar concentrations with silintaphin-1 in the 50 mM Tris-HCl buffer (pH 7.4; 150 mM NaCl), lacking glycerol. If only silicatein-α was added the 500 µl assay, 6 µg of

silicatein-α [equivalent to 480 nM] protein was subjected. Protein samples were taken after incubation steps between 1 min and 120 min. The samples were prepared based on the “on-grid” droplet procedure described by Huxley (1960), modified by Harris (1991). 10 µl droplets of the samples were dropped on 300-mesh copper grids coated with a formvar polymer (Plano, Wetzlar). After 20 seconds the droplet was soaked with a filter paper, leaving a thin aqueous film on the grid. The aqueous layer was allowed to dry at room temperature for 2 hours. To remove the buffer crystals the grids were washed three times with Millipore ultrapure water and were tried overnight at room temperature. Transmission electron microscopy (TEM) was carried out on a Philips EM 420 instrument at an accelerating voltage of 120 kV.

5.3 Results

5.3.1 Biosilica formation by axial filaments in vitro

Spicules, the siliceous skeletal elements of siliceous sponges comprise at their centers an axial canal which harbors the triangular (Demosponges) or hexagonal (Hexactinellids) axial filament. Cross-sections through *S. domuncula* tissue showed the axial canal (ac), which harbors the triangular axial filaments (af) (Fig. 5.2).

Characteristical for the species *S. domuncula* are the two forms of monoaxonal spicules. The oxeas have pointed tips at both ends and the more abundantly tylostyles have a pointed tip on one end and a knob at the other end (Arndt, 1935). The terminal knob is resting on a sub-terminal collar (Fig. 5.2 B)

Routinely for the isolation of the axial filaments the spicules were extracted from the tissue with sulfuric acid/nitric acid-solution. Afterwards the spicules were treated with buffered HF to release the axial filaments (Fig. 5.2 C). Terminally dissolved samples (almost) completely consisted of axial filaments with a diameter of 600 to 900 nm (Fig. 5.2 D). These filaments mainly consist of silicateins and silintaphin-1 (Wiens et al., 2009). To analyze the axial filaments activity of forming biosilica they were incubated in a reaction mixture, supplemented with 200 µM of prehydrolyzed TEOS (22°C for 24 hrs). Ultimately, the filaments were washed with distilled water and analyzed by SEM.

Figure 5.2 E shows axial filaments which are heavily decorated with slabs (Fig. 5.1 E), having an average size of 90 nm (Fig. 5.2 F). Concurrent energy-dispersive X-ray spectroscopy (EDX) revealed that the slabs consisted of silica (not shown).

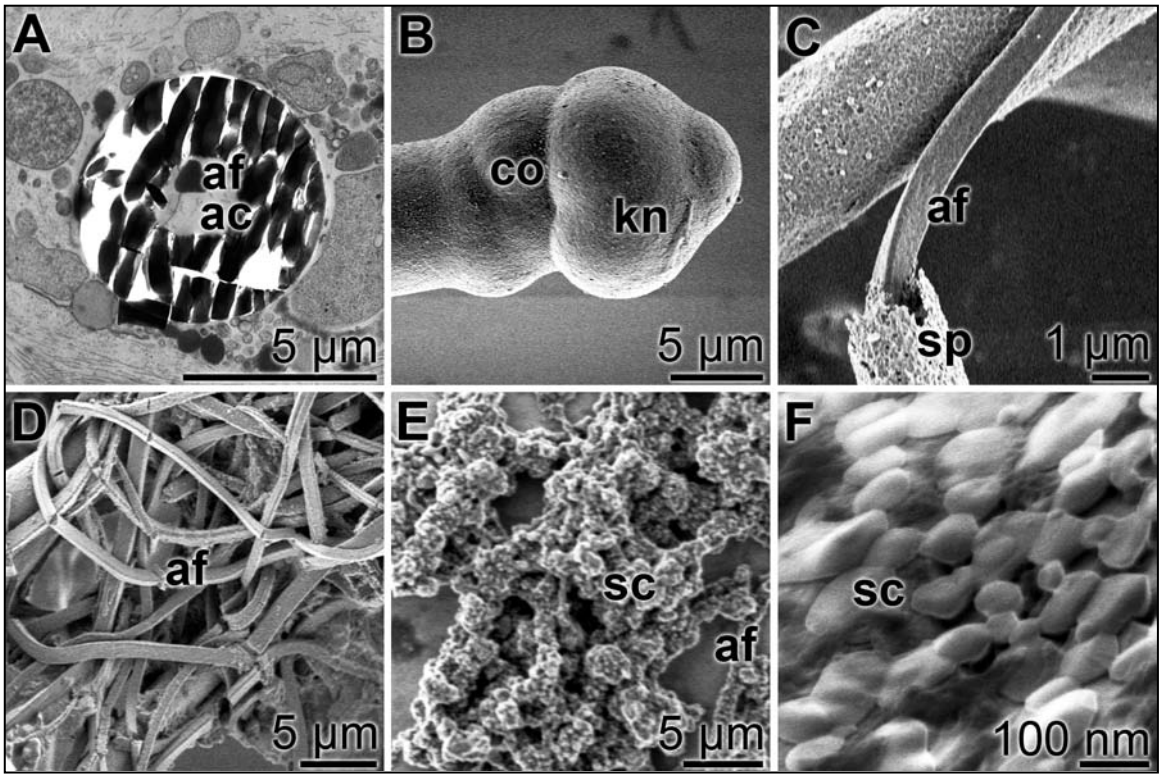

Figure 5.2: Localization of the axial filament in spicules of *S. domuncula*. (A) Cross-section through tissue showing a spicule that comprises in its center the axial canal (ac), harboring the axial filament (af); TEM. (B) SEM analysis of one terminus of a *S. domuncula* tylostyle with its terminal knob (kn) and the sub-terminal collar (co). (C) Partially HF-dissolved spicule (sp), showing the protruding axial filament; SEM. (D) A pile of axial filaments (af) from terminally HF-dissolved spicules; SEM. (E) Axial filaments of HF-dissolved spicules were incubated with 200 µM of prehydrolyzed TEOS (24 hrs) and subsequently inspected by SEM. The bio-silica clusters formed (sc) are abundant and associated with the filaments. (F) Higher magnification of bio-silica clusters formed on the surface of the axial filaments; TEM.

5.3.2 Co-localization of silicatein-α, silicatein-β, and silintaphin-1 in spicules

Immunochemistry in combination with tissue cuts was used to determine the exact location of silicatein-α, silicatein-β and silintaphin-1. For this purpose frozen cryosections of *S. domuncula* were fixed with paraformaldehyde and blocked with blocking solution (1% w/v milk powder in 1xTBS buffer) to prevent antibodies to react unspecifically. Then the cuts were reacted with polyclonal antibodies raised against silicatein-α (aSilic-α), silicatein-β (aSilic-β), and silintaphin-1 (aSiphn-1-01) (1:1500

dilution, 1% w/v blocking solution). Afterwards the slices were incubated with the corresponding secondary species-specific antibody labeled with the chromophor Cy 3 or Alexa Fluor 488. The resulting immunocomplexes were analyzed microscopically.

Figure 5.3 shows the co-localization of silicatein-α, silicatein-β, and silintaphin-1. As control the slices were incubated with the adsorbed primary antibodies and the fluorescent images show the complete absence of a fluorescent signal, indicating that the first antibodies do not react unspecifically (Fig. 5.3 Ab, Bb).

In contrast, the cuts treated with αSilic-α, αSilic-β and αSiphn-1-01 antibody show an intense signal along the spicules, indicating the presence of silicatein-α, silicatein-β and silintaphin-1 at this specific location. αSilic-a, Fig. 5.3 C; αSiphn-1-01, Fig. 5.3 D),

Both αSilic-α (Fig. 5.3 Aa) and αSilic-β (Fig. 5.3 Ba) recognized the same structures within the same slice irrespective of whether the section was performed in an axial or a transverse direction. In controls, with adsorbed antibodies, no signals were seen, indicating the specific binding of the antibodies (Fig. 5.3 Ab, 5.3 Bb). Similarly, antibodies raised against silicatein-α and silintaphin-1 elicited colocalizing signals along the spicules (aSilic-a, Fig. 5.3 C; aSiphn-1-01, Fig. 5.3 D), and again, in controls with adsorbed antibodies, no immunodetection was observed (data not shown).

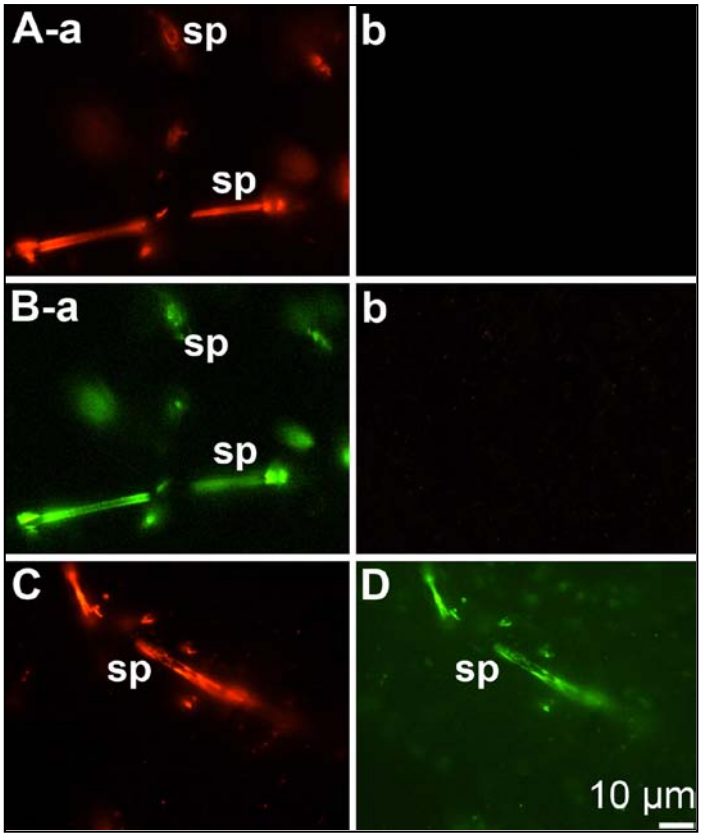

Figure 5.3: Co-localization of silicatein-α, silicatein-β, and silintaphin-1 in spicules. (A to D) Immunohistological analyses. A *S. domuncula* tissue cryosection was co-incubated with pAb against silicatein-α (aSilic-α) and silicatein-β (aSilic-β). Immunocomplexes were visualized with Cy3-labeled (A; silicatein-α) or FITC-labeled (B; silicatein-β) secondary antibodies. Non-adsorbed (a) or adsorbed (b) primary antibodies were used in parallel. In a further series, one section was co-incubated with pAb against silicatein-α (C; Cy3) and silintaphin-1 (aSiphn-1-01; FITC; D). sp, spicule.

Proteins were size-separated by SDS-PAGE and then stained with Coomassie brilliant blue. After size-separation, proteins were detected on Western blots using the following antibodies: αSilic-α directed against silicatein-α [Silic-α], αSilic-β against silicatein-α [Silic-β], and αSiphn-1-01 against silintaphin-1 [Siphn-1]. Where indicated, the membranes were incubated with antibodies that had been adsorbed with the corresponding recombinant protein [ads].

In a further approach, to demonstrate the presence of silicatein-α, silicatein-β and silintaphin-1 in spicules, protein extracts of HF-cleaned spicules were prepared, size-separated by SDS-PAGE, and analyzed by western blotting (Fig. 5.4 E). The protein pattern obtained by SDS-PAGE revealed, besides bands of very high molecular

mass (> 250 kDa), two major bands of 25 kDa and 26 kDa (Fig. 5.4 Ea; M: size marker). By application of the before mentioned antibodies, the former band was identified as silicatein-α, and the latter band as silicatein-β (Fig. 5.4 Eb). Even though silintaphin-1 was not visible on Coomassie Brilliant Blue-stained SDS gels (Fig. 5.4 Ea), αSiphn-1-01 detected the protein at its expected size of 43 kDa on the blots.

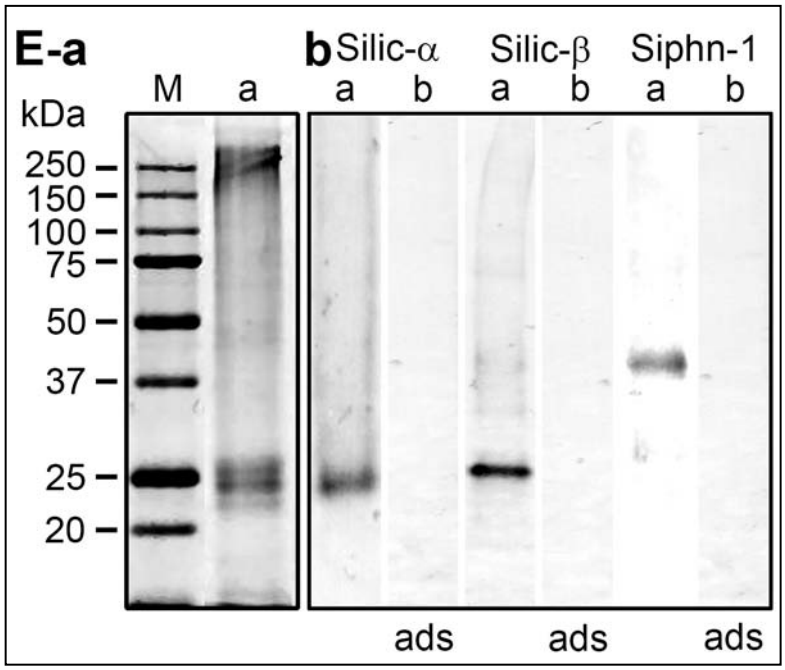

Figure 5.4: Western blot analysis of the spicular protein extracts. (E-a) Proteins were size-separated by SDS-PAGE and then stained with Coomassie brilliant blue; M, size-marker. (E-b) After size-separation, proteins were detected on Western blots using the following antibodies: αSilic-α directed against silicatein-α [Silic-α], αSilic-β against silicatein-α [Silic-β], and αSiphn-1-01 against silintaphin-1 [Siphn-1]. Where indicated, the membranes were incubated with antibodies that had been adsorbed with the corresponding recombinant protein [ads].

5.3.3 Enzymatic activity of silicatein and axial filament proteins in vitro

Following incubation of recombinant silicatein-α with TEOS for 1 hr at 22°C, the biosilica product of the enzymatic reaction was hydrolyzed by NaOH. Then, the soluble silicic acid concentration was determined colorimetrically, revealing 77±23 µg of biosilica per ml assay that had contained 6 µg enzyme (Fig. 5.5). The biosilica forming activity of recombinant silintaphin-1 was significantly lower (28±12 µg/assay). Conversely, if both proteins were allowed to interact prior to the addition of TEOS, the extent of biosilica formation was substantially higher. At a silicatein-α/silintaphin-1

stoichiometric molar ratio of 1:1 (4:1), both proteins elicited 201±46 (415±46) µg/assay. However, further increase of the ratio resulted in a lowered activity, with 165±31 µg/assay. In control assays, which contained prehydrolyzed TEOS but no protein, the poly(silicate)-forming activity was negligible with 15±14 µg/assay (Fig. 5.5).

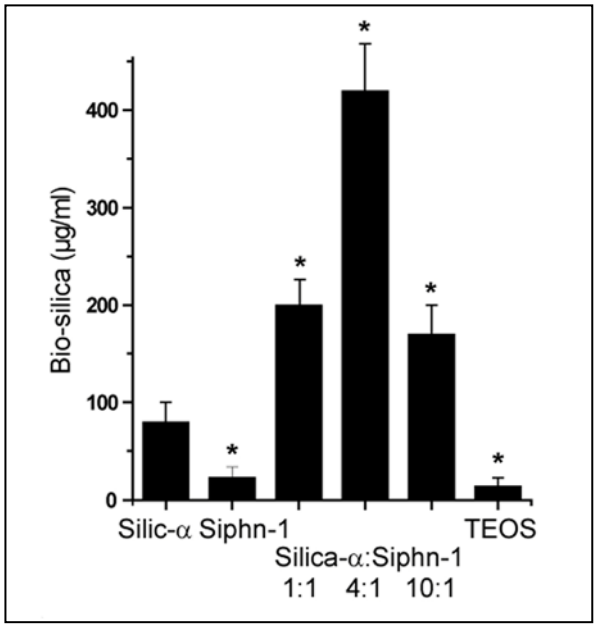

Figure 5.5: Silicatein-mediated synthesis of bio-silica in vitro. (A) Using prehydrolyzed TEOS as substrate, the activity of recombinant silicatein-α, silintaphin-1, or silicatein-α:silintaphin-1 (in a stoichiometric ratio of 1:1, 4:1, or 10:1) was assessed by using the molybdenum blue colorimetric method. In parallel control experiments, the deposition of poly(silicate) was determined in the absence of protein.

Similarly, the activity of isolated spicule proteins [“spicular extract”] was assayed, following incubation with prehydrolyzed TEOS. Hence, 6 µg proteins elicited a comparably high activity with 321±18 µg/assay (Fig. 5.6). The activity could be significantly reduced after blocking of the proteins with antibodies (aSilic-α, aSilic-β, or aSiphn-1-01). In particular aSilic-α pre-incubation considerably lowered the activity to 15±3 µg/assay. In contrast, the effects of aSilic-β or aSiphn-1-01 were less pronounced, with 134±6 µg/assay or 238±15 µg/assay, respectively.

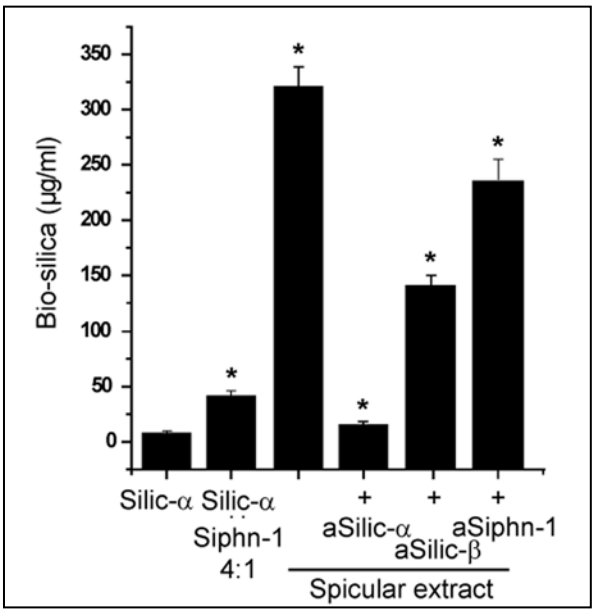

Figure 5.6: Using prehydrolyzed TEOS as substrate, the activity of spicular protein extracts in a glycerol-based Tris buffer system was determined. The activity of the extracts "spicular extract", was analyzed in the absence of antibodies or after preincubation with aSilic-α, aSilic-β, or aSiphn-1-01. For comparison, the activity of silicatein-α and silicatein-α:silintaphin-1 (4:1) are given in parallel. The results are expressed as means (n=10 experiments each) ± SEM; *P < 0.01.

5.3.4 Self-assembly of recombinant silicatein-α and silintaphin-1

The axial filaments mainly consist of silicateins and silintaphin-1 (Wiens et al., 2009). To analyze the selfassembly of the recombinant Silicatein-α with or without the recombinant Silintaphin the experiments were carried out in a Tris buffer (lacking glycerol) and investigated by TEM and SEM analysis (Fig. 5.7, Fig. 5.8). In preceding experiments it had been found that glycerol inhibits an *in vitro* self-association of silicateins into oligomers and further on to filaments (Müller et al., 2007a).

Native silicatein extracts form spicules were prepared from axial filament and allowed to polymerize in the absence of glycerol for 15 min to 180 min (Fig. 5.7 A 15-180 min). Those samples show fractal-like assembly pattern. In contrast, if a spicular extract was prepared with hydrofluoric acid, no distinct pattern formation could be observed (Fig. 5.7 B). Silicatein-α was added at a concentration of 50 µg/ml [2 µM] to the reaction mix. Self-assembly of recombinant silicatein-α revealed no distinct fractals and only ruffled aggregates could be visualized. After 1 min of incubation no

structures could be resolved by TEM. However, after 15 min randomly organized aggregates became visible (Fig. 5.7 A), which increased in size and compactness of packing after 30 min (Fig. 5.7 C 1 to 120 min). With increasing time, the aggregates continued to grow (60 min; 120 min). In comparison, co-incubation of recombinant silicatein-α and silintaphin-1 in a stoichiometric ratio of 4 to 1 elicited a drastically changed self-assembly (Fig. 5.7 1 to 120 min) with fractal-like patterns. Again, no aggregation was seen after 1 min of incubation. However, already after 15 min, 30 nm large spherical assemblies were formed that re-organized into > 100 nm large aggregates. After 30 and 60 min total incubation time, size and compactness of the assemblies increased until finally, filament-like structures were formed after > 120 min. The length of the filaments exceeded 5 µm but the diameter remained almost constant with 20 nm (Fig. 5.7 D 120 min).

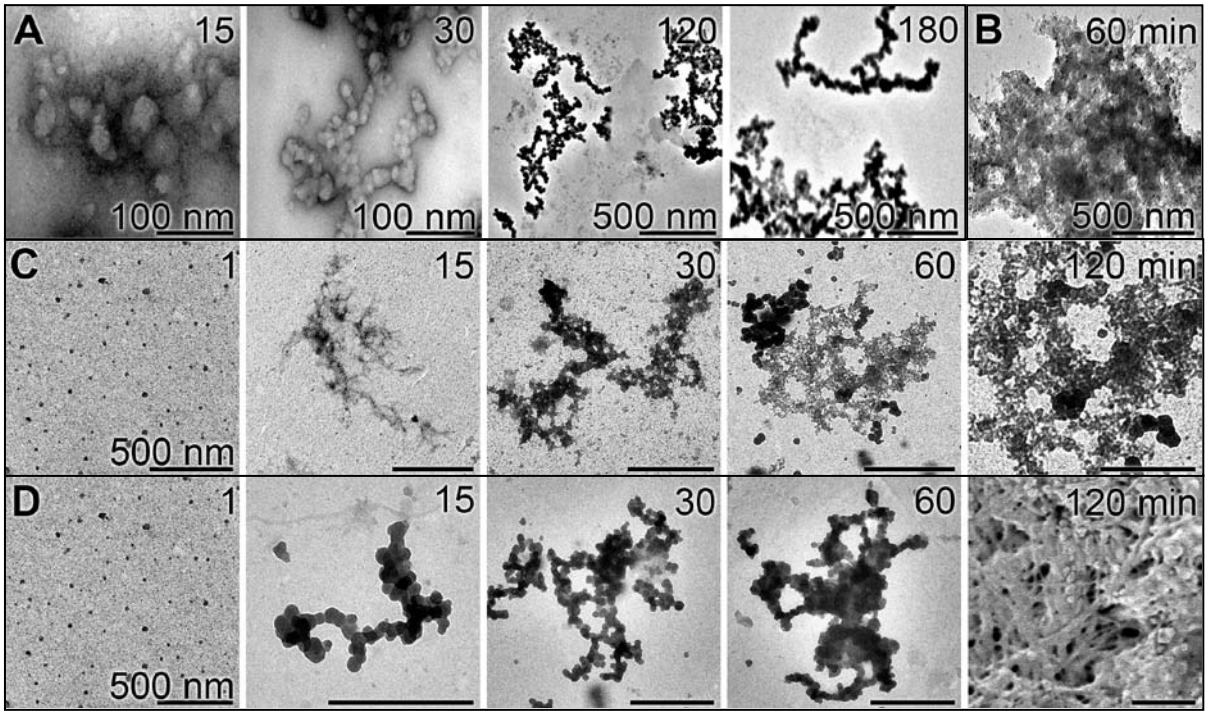

Figure 5.7: Self-assembly of silicatein-α and silintaphin-1 *in vitro*. (A) Native silicatein extracts form spicules were prepared from axial filament and allowed to polymerize in the absence of glycerol for 15 min to 180 min; TEM. Those samples show fractal-like assembly pattern. (B) In contrast, if an extract was prepared after dissolution of the spicules with hydrofluoric acid, no distinct pattern formation could be observed; TEM. Transmission electron micrographs of recombinant silicatein-α (C), which produces ordered dendritic growth pattern and of recombinant silicatein-α:silintaphin-1 in a molar ratio of 4:1 (D). Both samples were allowed to assemble in Tris-HCl buffer, lacking glycerol, for 1 min, 15 min, 30 min, 60 min, and 120 min. Then, the samples were inspected by TEM. All size bars in (C) and (D) measure 500 nm.

5.3.5 Biosilica formation of self-assembled recombinant silicatein-α and silintaphin-1

Protein aggregates of assembled recombinant silicatein-α (after 240 min incubation time) were exposed to prehydrolyzed TEOS for 24 hrs (22°C) and then inspected by SEM (Fig. 5.8 F). The micrographs showed particles, with an average size of about 30 nm, which were densely packed and deposited in a rod-shaped form. A similar arrangement of rod-shaped particles was also observed following co-incubation of silicatein-α/silintaphin-1. However, only in the presence of silicatein-α/silintaphin-1 a filamentous backbone structure could be visualized (Fig. 5.8 L), unless the accumulation of the particles around the backbone was too dense. In addition, the length of the rod-shaped structures in the silicatein-α/silintaphin-1 assays (Fig. 5.8 M) exceeded those that had assembled exclusively via silicatein-α (4 µm vs. < 2 µm). Concurrent EDX revealed the predominant presence of Si, whereas in control assays without prehydrolyzed TEOS, Si could not be detected (data not shown).

In the above mentioned experiment, a stoichiometric ratio of 4:1 was applied (silicatein-α:silintaphin-1). Other ratios of 10:1 or 1:10 did not result in differently shaped aggregates than those formed in the presence of silicatein-α.

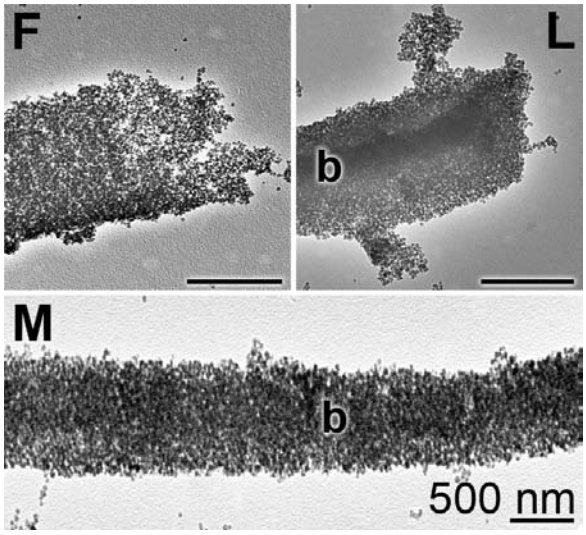

Figure 5.8: Self-assembly of silicatein-α and silintaphin-1 with TEOS in vitro. After a total incubation period for 240 min, protein assemblies were supplemented with prehydrolyzed TEOS for an additional 24 hrs (22°C). During that time, clusters of silica particles were formed. While in the presence of silicatein-α (Silic-α) the clusters appeared homogeneous (F), the clusters formed in the presence of silicatein-α:/silintaphin-1 (Silic-α/Siphn-1; L) frequently showed a backbone-like structure (b). (M) The length of the silica deposits in the assays with silicatein-α:silintaphin-1 often exceeded 4 µm. Size bars in all images, 500 nm.

5.4 Discussion

Biosilica of poriferan spicules consists of 2.8 nm large siliceous building blocks (Woesz et al., 2006). These nanospheres, which are most likely the product of the enzyme silicatein (Morse et al., 1999), are assembled to larger silica particles and to appositionally layered lamellae (reviewed in: Wang et al., 2010). Fully-grown spicules can have a size of several meters (Müller et al., 2009c) and still carry silicatein and other proteins embedded within the biosilica. Hence, silicatein was identified both between and within individual siliceous layers of spicules (Woesz et al., 2006; Müller et al., 2008a). In particular a combination of SEM and NanoSIMS spectroscopy has been helpful to substantiate the latter result (Müller et al., 2010b). Based on these data, it has been hypothesized that the fusion of silica nanospheres in spicules occurs during a sintering-like process, which consequently has been termed bio-sintering (Müller et al., 2009c). This assumption is supported by the observation that during maturation of demosponge spicules, individual silica layers fuse under formation of a solid rod (Müller et al., 2009).

In previous studies, it was shown that proteins, isolated of axial filaments, re-assemble in a fractal-related manner (Murr and Morse, 2005; Müller et al., 2007a). Similarly, recombinant silicatein-α assembles in vitro to nano-structures that, however, do not have defined shape and morphology. Nevertheless, they retained enzymatic activity and formed silica particles after addition of prehydrolyzed TEOS. As shown here, coincubation of recombinant silicateina and silintaphin-1 (4 : 1) resulted in a change in the shape／morphology of the biosilica product. The physical interaction between these two molecules (silicatein-a and silintaphin-1) has been proven through the technique of yeast two-hybrid library screening (Wiens et al., 2009); furthermore, silintaphin-1 contains a putative interaction PH domain (Wiens et al., 2009), also supporting such a physical interaction between the two molecules. Finally, the immunofluorescence data reported earlier (Müller et al., 2009b; Wiens et al., 2009) strongly indicated this interaction as well. At present, no quantitative data on the presence of silintaphin-1 in the axial filament can be given, as western blotting analysis only faintly failed to detect silintaphin-1 in extracts from the axial filament, as shown here. We attribute this finding to a failure of the antibodies to detect the silintaphin-1 antigen after the processing procedure during size separation and blot transfer, and／or to a modification of the protein that might have occurred during the

HF treatment required for the isolation of the axial filament. On the basis of the qualitative assessment of the staining intensities recorded with immunohistology, we suppose that silintaphin-1 exists in the axial filament at concentrations above 5–10%. The characterization of the silicatein aggregates as fractals has been documented by microscopic analysis (Müller et al., 2009b, Murr and Morse, 2005), physical–chemical determinations (Müller et al., 2009b), and mathematical calculations (Murr and Morse, 2005).

After incubation with the monomeric silica substrate, they remained as a protein backbone embedded in the resulting silica nanospheres. Conversely, these nanoparticles remained smaller (ca. 20 nm in size) than the biosilica slabs formed on the surfaces of native axial filaments (ca. 90 nm). Hence, it must be concluded that additional components, hitherto unknown, are required for full growth and morphogenesis of spicules.

In parallel to the structural analyses, the enzymatic activity of the silicatein-α/silintaphin-1 assembly was assessed and compared to the activity of randomly packed silicatein-α aggregates. Generally it must be stressed that the silica-forming activity, mediated by silicateins, is high in sponge tissue and causes a considerable spicular growth rate. Thus, growth rates of 1 to 10 µm/hr have been calculated for spicules of the demosponge *Ephydatia fluviatilis*, which have an average length of 200 to 350 µm and a thickness of 15 µm (Imsiecke et al., 1995). Consequently, the total weight of one spicule amounts to approximately 88.3 x 10^{-9} g, equivalent to roughly 4.4 x 10^{13} molecules of biosilica that is formed per hr in one spicule. Taking into account the amount of 5% of protein in a spicule, as measured for *M. chuni* spicules (Müller et al., 2008a), it follows that 2.2 x 10^{-10} g of protein (mainly silicatein-α) catalyze the synthesis of 4.4 x 10^{-9} g biosilica per hr. Since the molecular mass of mature silicatein is 25 kDa, it follows that 8.8 x 10^{-15} moles silicatein (= 5.3 x 10^{9} molecules) synthesize 4.4 x 10^{-9} g (= 7.33 x 10^{-11} moles [4.4 x 10^{13} molecules]) of biosilica per hr.

In turn and referring to native silicatein, the turnover number of silicate per silicatein on a molar basis is 12 x 10^{3} molecules of converted substrate per silicatein molecule per hr in spicules. With respect to recombinant silicatein-α, it has been determined that the enzyme catalyzes the conversion of the synthetic substrate bis(p-aminophenoxy)-dimethylsilane with a turnover rate of 18.7 x 10^{3} per hr (Müller et al., 2008b). In the present study, we found a very similar activity for recombinant

silicatein-α with a turnover rate of 5.4 x 10^3 molecules (on the basis of 77 µg biosilicate formed per 6 µg protein) per molecule silicatein-α and per hr. Interestingly, if the enzyme was allowed to re-associate with silintaphin-1 in a 4:1 molar stoichiometric ratio, the enzymatic activity strongly increased (i.e. 5.3-fold; 28.8 x 10^3 of polymerized silicate). In comparison, the activity of native proteins, isolated of spicules by using the glycerol/Tris based extraction puffer system, was substantially higher with 343 x 10^3 molecules of polymerized silicate per molecule silicatein per hr. Nevertheless, due to the combined application of silicatein-α and silintaphin-1, the values for in vitro and in vivo synthesis of biosilica differ by roughly one order of magnitude. Addition of antibodies directed against silicatein-α, silicatein-β, and silintaphin-1 significantly changed the outcome of the enzyme reaction. Thus, addition of silicatein-α antibodies (and to a lower extent of silicatein-β or silintaphin-1 antibodies) considerably reduced the amount of biosilica formed. From these data we conclude that silicatein-α has the highest impact on biosilica synthesis in the axial filament of spicules. Nevertheless, the significant inhibitory effects of aSilic-β and aSiphn-1-01 are indicative that the presence of all three proteins is required for maximal biosilicification activity. These results, in combination with the microscopic analyses, indicate that silicatein-α-mediated biosilica synthesis depends on the presence of silintaphin-1. Recently it was proposed that silicatein mediates initial formation of highly reactive cyclic silicic acid species which facilitate, in a second phase, silica polycondensation in the absence of the enzyme (Schröder et al., 2010). Consequently, these studies suggest a dual effect of the proteinaceous polymeric substrate/matrix formed of silicateins and silintaphin-1; it (i) facilitates the enzymatic activity of silicatein-α (DelCardayré and Raines, 1994) and (ii) accelerates the subsequent non-enzymatic polycondensation before releasing the fully synthesized inorganic polymer (biosilica). Binding studies of silicatein to silica particles are in progress to evaluate this hypothesis.

In summary, our results demonstrate the cooperative effect of silintaphin-1 and silicatein on biosilica formation. Hence, silintaphin-1 is not only important for the assembly of silicatein to filaments but also enhances the enzymatic activity.

5.5 References

Arndt W. (1935). Porifera, Die Tierwelt der Nord- und Ostsee. Series: 3a (27), *Becker & Erler*, Leipzig, 1935, pp. 1–140.

Cha J.N., Shimizu K., Zhou Y., Christianssen S.C., Chmelka B.F., Stucky G.D. & Morse D.E. (1999). Silicatein filaments and subunits from a marine sponge direct the polymerization of silica and silicones *in vitro*. *Proc Natl Acad Sci USA* 96, 361-365.

Croce G., Frache A., Milanesio M., Marchese L., Causà M., Viterbo D. Barbaglia A., Bolis V., Bavestrello G., Cerrano C., Benatti U., Pozzolini M., Giovine M. & Amenitsch H. (2004). Structural characterization of siliceous spicules from marine sponges. *Biophysical J* 86, 526-534.

DelCardayré S.B. & Raines R.T. (1994). Structural determinants of enzymatic processivity. *Biochemistry* 33, 6031-6037.

Harcet M., Roller M., Cetkovic H., Perina D., Wiens M., Müller W.E.G. & Vlahovicek K. (2010). Demosponge EST sequencing reveals a complex genetic toolkit of the simplest metazoans. *Mol Biol Evol*, 27, 2747-56

Harris J.R. (Editor). Electron Microscopy in Biology: A practical approach. Oxford, UK: *Oxford University Press*, 1991, 210pp (The practical approach series)

Huxley, H.E. & Zubay G. (1960). *Journal of Molecular Biology*, 2, 10-18

Ijima I. (1901). Studies on the Hexactinellida. Contribution I. (Euplectellidae). *J Coll Sci Imp Univ Tokyo* 15, 1-299.

Imsiecke G., Steffen R., Custodio M., Borojevic R. & Müller W.E.G. (1995). Formation of spicules by sclerocytes from the freshwater sponge Ephydatia muelleri in short-term cultures in vitro. *In Vitro Cell Dev Biol* 31, 528-535.

Krasko A., Batel R., Schröder H.C., Müller I.M. & Müller W.E.G. (2000). Expression of silicatein and collagen genes in the marine sponge *Suberites domuncula* is controlled by silicate and myotrophin. *Eur J Biochem* 267, 4878-4887.

Kruger N.J. (2002). The Bradford method for protein quantification. In: Walker, JM *The Protein Protocols Handbook*; 2nd Edition. Humana Press: Totowa.

Lieberkühn N. (1856). Zur Entwicklungsgeschichte der Spongilliden. *Arch Anat Physiol*., 399-414.

Morse D.E. (1999). Silicon biotechnology: harnessing biological silica production to construct new materials. *Trends Biotechnol*;17, 230-232.

Müller W.E.G., Rothenberger M., Boreiko A., Tremel W., Reiber A. & Schröder H.C. (2005a). Formation of siliceous spicules in the marine demosponge *Suberites domuncula. Cell Tissue Res* 321, 285-297.

Müller W.E.G. (2006a). The stem cell concept in sponges (Porifera): metazoan traits. *Semin Cell Dev Biol* 17, 481-491.

Müller W.E.G., Boreiko A., Schloßmacher U., Wang X.H., Tahir M.N., Tremel W., Brandt D., Kaandorp J.A. & Schröder H.C. (2007a). Fractal-related assembly of the axial filament in the demosponge *Suberites domuncula*: relevance to biomineralization and the formation of biogenic silica. *Biomaterials* 28, 4501-4511.

Müller W.E.G., Jochum K., Stoll B. & Wang X.H. (2008a). Formation of giant spicule from quartz glass by the deep sea sponge Monorhaphis. *Chem Mater* 20, 4703-4711.

Müller W.E.G., Schloßmacher U., Wang X.H., Boreiko A., Brandt D., Wolf S.E., Tremel W. & Schröder H.C. (2008b). Poly(silicate)-metabolizing silicatein in siliceous spicules and silicasomes of demosponges comprises dual enzymatic activities (silica-polymerase and silica-esterase). *FEBS J* 275, 362-370.

Müller W.E.G., Wang X.H., Kropf K., Boreiko A., Schloßmacher U., Brandt D., Schröder H.C. & Wiens M. (2008c). Silicatein expression in the hexactinellid *Crateromorpha meyeri*: the lead marker gene restricted to siliceous sponges. *Cell Tissue Res* 333, 339-351.

Müller W.E.G., Kasueske M., Wang X.H., Schröder H.C., Wang Y., Pisignano D. & Wiens M. (2009a). Luciferase a light source for the silica-based optical waveguides (spicules) in the demosponge *Suberites domuncula. Cell Mol Life Sci* 66, 537-552.

Müller W.E.G., Wang X.H., Cui F.Z., Jochum K.P., Tremel W., Bill J., Schröder H.C., Natalio F., Schloßmacher U. & Wiens M. (2009b). Sponge spicules as blueprints for the biofabrication of inorganic-organic composites and biomaterials. *Appl Microbiol Biotechnol* 83, 397-413.

Müller W.E.G., Wang X.H., Burghard Z., Bill J., Krasko A., Boreiko A., Schloßmacher U., Schröder H.C. & Wiens M. (2009c). Bio-sintering processes in hexactinellid sponges: Fusion of bio-silica in giant basal spicules from Monorhaphis chuni. *J Struct Biol* 168, 548-561.

Müller W.E.G., Wang X., Schröder H.C., Korzhev M., Grebenjuk V.A., Markl J.S., Jochum K.P., Pisignano D. & Wiens M. (2010a). A cryptochrome-based photosensory system in the siliceous sponge *Suberites domuncula* (Demospongiae). *FEBS J* 277, 1182-1201.

Müller W.E.G., Wang X., Sinha B., Wiens M., Schröder H.C. & Jochum K.P. (2010b). NanoSIMS: Insights into the organization of the proteinaceous scaffold within hexactinellid sponge spicules. *ChemBioChem* 11, 1077-1082.

Murr M.M. & Morse D.E. (2005). Fractal intermediates in the self-assembly of silicatein filaments. *Proc Natl Acad Sci USA* 102, 11657-11662.

Sachs L. (1984). *Angewandte Statistik*; Springer: Berlin; p 242.

Sandford F. (2003). Physical and chemical analysis of the siliceous skeleton in six sponges of two groups (Demospongiae and Hexactinellida). *Microsc Res Tech* 62, 336-355.

Schröder H.C., Wiens M., Schloßmacher U., Brandt D. & Müller W.E.G. (2010). Silicatein-mediated polycondensation of orthosilicic acid: Modeling of catalytic mechanism involving ring formation. *Silicon*; DOI: 10.1007/s12633-010-9057-4

Shimizu K., Cha J., Stucky G.D. & Morse D.E. (1998). Silicatein alpha: cathepsin L-like protein in sponge biosilica. *Proc Natl Acad Sci USA* 95, 6234-6238.

Sollas W.J. (1888). Report on the Tetractinellida collected by H. M. S. "Challenger", during the years 1873-1876. - Rep. Scient. *Results Voyage HMS Challenger*. (Zool.) 25, 1-458.

Tong X., Tang T., Feng Z. & Huang B. (2002). Preparation of polymer/silica nanoscale hybrids through sol-gel method involving emulsion polymers. II. Poly(ethyl acrylate)/SiO2. J *Appl Polym Sci* 86, 3532-3536.

Uriz M.J., Turon X., Becerro M.A. & Agell G. (2003). Siliceous spicules and skeletons frameworks in sponges: origin, diversity, ultrastructural patterns, and biological functions. *Microsc Res Tech* 62, 279-299.

Uriz M.J. (2006). Mineral spiculogenesis in sponges. *Can J Zool* 84, 322-356.

Wang X., Wiens M., Schröder H.C., Hu S., Mugnaioli E., Kolb U., Tremel W., Pisignano D. & Müller W.E.G. (2010). Morphology of sponge spicules: silicatein a structural protein for bio-silica formation. *Advanced Biomat/Advanced Engin Mat* 12, B422- B437.

Wiens M., Bausen M., Natalio F., Link T., Schlossmacher U. & Müller W.E.G. (2009). The role of the silicatein-a interactor silintaphin-1 in biomimetic biomineralization. *Biomaterials* 30, 1648-1656.

Woesz A., Weaver J.C., Kazanci M., Dauphin Y., Aizenberg J., Morse D.E. & Fratzl P. (2006). Micromechanical properties of biological silica in skeletons of deep-sea sponges. *J Mater Res* 21, 2068-2078.

Extended summary

Industrial production of silica requires usually high temperature conditions and extreme pH (Stöber et al., 1968). In nature, biosilicification is an evolutionarily old and widespread type of biomineralization both in unicellular and multicellular organisms which requires organic surfaces and matrices. These organisms form an astonishing variety of siliceous structures that cannot yet be achieved by synthetic chemical methods. Organic guiding macromolecules control the initiation, growth and morphology of the biomineral and the speed of the mineralization process; e.g. like it occurs in diatoms (Kröger et al., 1999). Siliceous sponges have the exceptional ability to synthesize their siliceous skeleton enzymatically via the protein silicatein (Morse 2000; Weiner and Dove, 2003). Size and shape of spicules are genetically controlled and represent a species-specific morphology often used for phylogenetic and taxonomic purposes. They constitute the chief supporting framework of these animals and function as a protection against predators.

Basically, spiculogenesis follows the same pattern in both demosponges and hexactinellids. Spiculogenesis starts intracellularly (Müller et al., 2005a; Müller et al, 2005b) with the formation of a proteinaceous axial filament around which a silica shell is formed. Subsequently, the immature spicules are extruded from the cells and completed in the extracellular space of the mesohyl by appositional deposition of silica layers (Müller et al., 2005a, Müller et al., 2006b). The axial filament, which is composed of silicatein, is located within the central canal of spicules and also in their concentric layers (Uriz et al., 2003). This protein was first studied in *Tethya aurantium* (Cha et al., 1999) and subsequently in *Suberites domuncula* (Krasko et al., 2000). Each sponge species synthesizes at least two silicateins, which are termed silicatein-α and silicatein-β. The isolated enzyme from spicules is used *in vitro* to catalyze polycondensation of a wide variety of alkoxide, ionic and organometallic precursors at standard, ambient temperature, pressure and neutral pH (Zhou et al., 1999).

For all studies, the *S. domuncula* system is used. Only here, the most comprehensive biological and developmental data is available (Müller, 2006a) as well as biochemical (Müller et al., 2005) and molecular biological data (Harcet et al., 2010), which are required for the understanding of poriferan spiculogenesis and bodyplan formation.

In order to approach the question whether it is the axial filament itself, which contributes to the shape formation of the spicules a new, mild extraction procedure is introduced (Schröder et al., 2006). Previously, hydrofluoric acid (HF) has been used to isolate the axial filaments of the spicules; a procedure which is known to cause cleavage of modify phosphate groups of proteins (Kröger et al., 1999; Kröger et al., 2002). As a functional assay for the different preparations, polymerization studies are performed *in vitro*. Comparing the self-assembly properties of the silicateins obtained by the mild extraction with the HF extraction procedure it could be demonstrated that self-assembly – under the used electrophoretic conditions – only occurs with the silicateins obtain with the mild extraction method. It could be shown that the silicateins, obtained after HF-extraction, underwent cross-linking to form dimers (50 kDa), trimers (75 kDa) or tetramers (95 kDa). To achieve silicatein monomers, the silicatein multimers had to be disassembled by urea (Murr and Morse 2005). These dimers/multimers are not present in the mild extraction preparations, when these are analyzed under identical conditions. In contrast the new extraction procedure allowes the solubilization of native silicateins from the silica shell without HF (Schröder et al., 2006) and immediately yield monomeric (24kDa) protein which readily forms dimers through non-covalent linkages. Furthermore polymerization to tetramers (95 kDa) and hexamers (135 kDa) takes place. This indicates that, in contrast to previously published data, silicateins composing the axial filament exist in the native state as monomers or as non-covalently linked dimmers. The silicateins obtained with the mild extraction method form initially rectangular branching structures, suggesting fractal intermediates, which further evolve to stabile filaments. On the other hand, the HF-extracted silicateins form only non-structured aggregates. One may conclude from this that during HF-extraction the silicateins undergo modifications not seen in the proteins obtained with the mild extraction method, which indicates that the HF-extraction procedure is not suitable for an analysis of the self-assembling properties of native silicateins. As postulated before (Murr and Morse, 2005) and now substantiated, it is reasonable to assume that self-assembly of silicatein monomers within the axial filament contribute, via fractal intermediates, to a stabile form/organization of the filament. It is proposed that the basic self-assembly of the silicatein-α monomers provides the general platform for the shape and pattern formation of growing spicules.

Silicatein, as a member of the cathepsins, is also known to catalyze the hydrolysis of peptide bonds [Cha et al., 1999]; hence it acts also as a proteolytic enzyme. Therefore, the proteolytic activity was determined [Quian et al., 1989]. Intriguingly, it is found that using the mild extraction procedure, a silicatein preparation is obtained which comprises considerably higher biosilica formation/condensation activity, compared to samples obtained by HF-extraction. The samples show a considerable proteolytic activity that increases during the polymerization phase of the protein. Using the zymogram method it is proven that the HF-extracted silicateins do not show any enzymatic activity, while in the mild extracted silicatein fraction distinct hydrolytic activities are identified with an apparent size of 40 kDa (dimer), 80 kDa (tetramer) and 120 kDa (hexamer). Starting from monomeric silicateins a stoichiometric association of the silicateins occurs. Furthermore, it becomes evident that in *S. domuncula* silicatein-α is four times more abundant in the axial filament than silicatein-β. With these results as a basis a computer model for the proposed arrangement between the two isoforms of silicatein is calculated. It is proposed that monomeric silicatein-α molecules form dimers and then tetramers into which one silicatein-β molecule is inserted into the central cleft. The model prediction revealed that the serine clusters of four silicatein-α molecules are exposed to the center of the tetrade. Based on these data it is plausible that a planar tetramer composition is formed where the active sites of the enzymes are oriented con-axial (active centers on the outer surface of the assembly) while the Ser-clusters are oriented towards the center of the tetrameric silicatein complex. Those cluster are likely to allow binding of the oligo(silicate) product. The longitudinal growth of the axial filament within the spicules proceeds certainly in an axial direction (Müller et al., 2007b; Schröder et al 2007a; Müller et al., 2003b), and very likely in an uni-directional orientation (Uriz et al., 2003; Müller et al., 2006b). The model, presented here, supports the view that growth of the spicules proceeds towards only one end of the spicules. It is concluded that initially the silicateins re-assemble randomly, and in the second phase order themselves to fractal-like structures, which subsequently form the filaments.

Taken together these results demonstrate that silicateins, obtained by the mild extraction method are very suitable to analyze the biochemical, biophysical properties of the monomeric/dimeric silicatein units. In addition, they allowed the formation of fractal-like structures, which assembled to filaments. Since biosilica is also an important material in nano(bio)technology, the understanding of a structure

controlled self-assembly of silicatein will surely contribute to further develop applications of biosilica in industry and medicine, e.g. for the fabrication of biocompatible materials, glasses, ceramics and photonic materials (Tahir et al., 2006b); reviewed in: (Müller et al., 2007b; Schröder et al., 2007a).

The class Hexactinellida (porifera) also forms silicious spicules and includes species that form the largest biogenic silica structures on earth. The giant basal spicules from the hexactinellids *Monorhaphis chuni* and *Monorhaphis intermedia* can reach lengths of up to 3·m and diameters of 10·mm. The giant spicules consist of a biosilica shell that surrounds the axial canal, which harbors the axial filament, in regular concentric, lamellar layers, suggesting an appositional growth of the spicules. The megascleres of *M. chuni* and *M. intermedia* consist of up to 400 lamellae (Levi et al., 1989). In chapter 3, spicule extracts from *S. domuncula* and *M. chuni* are compared and the potential existence of silicatein, or silicatein-like molecules and the potential proteolytic activity of the silicateins are approached. Indicating that the proteolytic activity of spicule extracts as well as the size of the molecules depend on the HF treatment procedure here a mild extraction procedure is applied. In total protein extracts of *M. chuni* spicules, a 27·kDa protein and additional 70·kDa proteins exist, while the organic component of a single lamellae consists of only protein(s) of 27·kDa. Western Blot analysis shows the cross-reaction with anti-silicatein antibodies. By using the zymogram assay system it is demonstrated for the first time that the protein(s) present in the spicules of *M. chuni* display proteolytic activity, like the silicateins from *S. domuncula*. This suggests that the spicules in Hexactinellida are also synthesized enzymatically by silicatein-like molecules. To further characterize the proteolytic activity, the inhibitor E-64 for cysteine-proteinases is used. E-64 is found to be a strong inhibitor of *S. domuncula* silicatein and also of the proteolytic activity measured in the *M. chuni* extract. As a substrate to detect the enzyme activity, the cathepsin L-specific synthetic dipeptide derivative Z-Phe-Arg-AMC is used (Mort, 2002). It is demonstrated that the proteolytic activity of the spicule extracts can be blocked by E-64 to over 90% at concentrations as low as $1 \cdot \mu mol \cdot l^{-1}$. These results indicate that the 24·kDa polypeptide in Monorhaphis has several characteristics in common with the silicateins found in demosponges like the size, the post-translational modifications and the proteinase activity.

Since seawater has a low content of silicate (about 5 µM) the sponges have to transport silicate actively into their cells, via an ATP-consuming $Na^+/HCO_3^-[Si(OH)_4]$ co-transporter (Schröder et al., 2004). In sclerocytes, spicule-forming cells, silicate is stored intracellularly in special organelles, the silicasomes, which comprise a high content of silicate (Schröder et al., 2007a). It should be expected that the high silicic acid content in silicasomes faciliates self-polymerization or self-condensation processes. In chapter 4 experimental results have been provided which show that silicic acid co-exists with silicatein in these silicasomes. It can be assumed that these molecules prevent a polycondensation of silicate. Since silicate – at neutral pH – polycondensates at concentrations above 1 mM to poly(silicate) (Iler, 1979), it can be postulated that (organic) molecules, e.g. silicatein, contribute to the stabilization of the sol state of silica. In a first approach, to determine the Michaelis constant (K_m) of silicatein activity, an optical test is developed which allowed to measure and quantify the kinetic parameters, describing the silicatein product formation. For this study the recombinant silicatein-α is used. Based on the observation that silicatein is a reversible enzyme, and functions as a silica polymerase as well as a silica esterase the reaction parameters have been determined spectroscopically with the substrate BAPD silane [bis(p-aminophenoxy)-dimethylsilane (Müller et al., 2008g). In this study the temperature optimum was found to be in the range 20–25°C. Using this substrate the Michaelis constant (K_m) was calculated to be 22.7 µM. In comparison, the K_m value for human recombinant cathepsin L, one of the enzymes closest related to the silicatein is determined to be 1.1 µM, using the substrate benzyloxycarbonyl-Phe-Arg-4-methylcoumarin-7-amide (Nomura et al., 1996). Such a value is by far below the critical concentration required for silica polycondensation (Perry, 2003), or for non-enzymatic (collagen-mediated) silica polycondensation, which is around 4.5 mM Na-silicate (Ehrlich et al., 2010). The turnover value for silicatein in this silica esterase assay was found to be 5.2 molecules of converted substrate per enzyme molecule per second. The reaction is completely blocked by sodium hexafluorosilicate and E-64. It is documented that silicatein exhibits, as initially proposed (Cha et al., 1999), also silica polymerizing activity. It is demonstrated that the polymerizing growth of the silica chains, mediated by the silica-polymerase activity of silicatein, involves a step-wise addition of single silica monomeric units. This finding implies that silicatein holds two different enzymatic properties, a silica-esterase activity and a polymerizing activity (silica-polymerase). Electron microscopy

data show that silicatein is transported in silicasomes into the extracellular space; there, these silica-vesicles contribute to the appositionally growing spicules. With the findings it is possible to develop a functional model which contributes to the understanding of the growth of the siliceous spicules. The simultaneous release of silicic acid and silicatein into the concentric rings around the growing spicules, which gives rise to lamellar formation of the spicules (Osinga et al., 1999), allows a controlled polymerization process of silicic acid by silicatein along galectin strings/nets (Müller et al., 2006b). Very likely the shape of the product is additionally tailored by a collagen sheathing (Eckert et al., 2006).

Recently, another protein involved in poriferan biosilicification has been identified: Silintaphin-1 (43 kDa) was discovered during a yeast two-hybrid library screening as strong interactor of silicatein (Wiens et al., 2009). Silintaphin-1 bears a protein-interaction domain (PH domain) that is required for binding of silicatein. It guides silica deposition and subsequent spicular morphogenesis. Both recombinant proteins (silicatein and silintaphin-1) assemble in vitro to microscale filaments and facilitate the formation of synthetic spicules in the presence of γ-Fe_2O_3 (Wiens et al., 2009) or silica nanoparticles (Müller et al., 2009b). In chapter 5 the role of silintaphin-1 during the aggregation process is clarified. The re-assembly experiments are performed with recombinant silicatein-α and recombinant silintaphin-1 at different stoichiometric ratios (Schloßmacher et al., 2011). Self-assembly of recombinant silicatein-α reveales no distinct fractal pattern and only ruffled aggregates could be visualized. Nevertheless, they retain enzymatic activity and form silica particles after addition of pre-hydrolyzed TEOS. However, if the recombinant silicatein-α sample is supplemented with recombinant silintaphin-1 (molecular ratio 4 : 1) organized aggregates are formed. The length of the filaments exceeds 5 µm, but the diameters remains almost constant, at 20 nm. In order to elucidate if during biosilica formation, mediated by silicatein, the structural pattern is changed, the silicatein-α filaments and the silicatein-α/silintaphin-1 fibers are incubated with orthosilicate [pre-hydrolyzed TEOS]. During the 24 h incubation period the silicatein-α fibers organize with the 30 nm silica particles to densely packed rods. A similar arrangement of the silica particles is observed following co-incubation of silicatein-α/silintaphin-1. However, in contrast to the fibers formed with silicatein-α alone, the silicatein-α/silintaphin-1 fibers show a filamentous backbone structure that is surrounded by the nanoparticles.

Conversely, these nanoparticles remain smaller (ca. 20 nm in size) than the biosilica slabs formed on the surfaces of native axial filaments (ca. 90 nm). Hence, it must be concluded that additional components, so far unknown, are required for full growth and morphogenesis of spicules.

In parallel to the structural analysis, the enzymatic activity of the silicatein-α/silintaphin-1 assembly is assessed and compared to the activity of randomly packed silicatein-α aggregates. Generally it must be stressed that the spicular growth rate is high in sponge tissue. For example, the spicule growth rates of 1 - 10 µm/hr are measured in the primmorph system (Imsiecke et al., 1995) of the freshwater demosponge *Ephydatia fluviatilis.* The spicules have an average length of 200 – 350 µm and a thickness of 15 µm (Imsiecke et al., 1995). Consequently, the total weight of one spicule is approximately 88.3 x 10^{-9} g, equivalent to roughly 4.4 x 10^{13} molecules of SiO_2 being formed per hr in one spicule. Taking into account the amount of 5% of protein in a spicule, as measured for *M. chuni* spicules (Müller et al., 2008a), it follows that 2.2 x 10^{-10} g of protein (mainly silicatein-α) catalyze the synthesis of 4.4 x 10^{-9} g SiO_2 per hr. Since the molecular mass of mature silicatein is 25 kDa, it follows that 8.8 x 10^{-15} mol of silicatein (= 5.3 x 10^{9} molecules) in the spicules *in vivo* are synthesizing 4.4 x 10^{-9} g [7.33 x 10^{-11} mol (4.4 x 10^{13} molecules)] of biosilica per hour. These values are compared with the *in vitro* values, using recombinant silicatein. The calculations reveal that the turnover rate for silicatein-α is 5.4 x 10^{3} molecules (on the basis of 77 µg of biosilicate formed per 6 µg of protein) per molecule of silicatein-α and per hour.

In frame of the finding that in sponge tissue silicatein co-exists with silintaphin-1 and silintaphin-2 it is pressing to study the enzyme activity of silicatein activity in the presence of the interacting protein, primarily of silintaphin-1 (Schloßmacher et al., 2011). Importantly, if the enzyme is allowed to re-associate with silintaphin-1 prior to the addition of orthosilicate, the extent of biosilica formation is substantially higher. At a silicatein-α/silintaphin-1 stoichiometric molar ratio of 4:1, the enzymatic activity strongly increases (i.e. 5.3-fold; 28.8 x 10^{3} molecules of polymerized silicate). In comparison, the activity of native proteins, isolated from spicules with a mild extraction buffer system, is in the same range (20.5 x 10^{3} molecules of polymerized silicate being formed per molecule of silicatein per hour). Nevertheless, due to the combined application of silicatein-α and silintaphin-1, the values for *in vitro* and *in vivo* synthesis of biosilica differ by roughly one order of magnitude.

Since in the axial filament extract not only the silicateins are present but also silintaphin-1, antibody inhibition experiments are performed to neutralize/inactivate one or both components. From these data it could be concluded that silicatein-α has the highest impact on biosilica synthesis in the axial filament of spicules. Nevertheless, the significant inhibitory effects of anti-silicatein-β and anti-silintaphin-1 are indicative that the presence of all three proteins is required for maximal biosilicification activity. This comparison between the biosilica formation in the intact cell organization and the biosilica synthesis *in vitro* indicates that the silicateins are the causative enzymes that mediate biosilica formation in the sponges, at least in the demosponges. In summary, these results demonstrate the cooperative effect of silintaphin-1 and silicatein on biosilica formation.

In combination with the microscopic analysis, these results indicate that silicatein-α-mediated biosilica synthesis depends on the presence of silintaphin-1, which is not only important for the assembly of silicatein into filaments but also enhances the enzymatic activity. Recently it is proposed that silicatein mediates initial formation of highly reactive cyclic silicic acid species which facilitate, in a second phase, silica polycondensation in the absence of the enzyme (Schröder et al., 2010). Consequently, these studies suggest a dual effect of the proteinaceous polymeric substrate/matrix formed of silicateins and silintaphin-1; it (i) facilitates the enzymatic activity of silicatein-α (DelCardayré and Raines, 1994) and (ii) accelerates the subsequent non-enzymatic polycondensation before releasing the fully synthesized inorganic polymer (biosilica). Binding studies of silicatein to silica particles are in progress to evaluate this hypothesis.

References

Cha J.N., Shimizu K., Zhou Y., Christianssen S.C., Chmelka B.F., Stucky G.D. & Morse D.E. (1999). Silicatein filaments and subunits from a marine sponge direct the polymerization of silica and silicones *in vitro*. *Proc Natl Acad Sci USA* 96, 361-365.

DelCardayré S.B. & Raines R.T. (1994). Structural determinants of enzymatic processivity. *Biochemistry* 33, 6031-6037.

Eckert C., Schröder H.C., Brandt D., Perovic-Ottstadt S. & Müller W.E.G. (2006). A histochemical and electron microscopic analysis of the spiculogenesis in the demosponge *Suberites domuncula*. *J Histochem Cytochem* 54, 1031-1040.

Ehrlich H., Deutzmann R., Brunner E., Cappellini E., Koon H., Solazzo C., Yang Y, Ashford D., Thomas-Oates J., Lubeck M., Baessmann C., Langrock T., Hoffmann R., Wörheide G., Reitner J., Simon P., Tsurkan M., Ereskovsky A.V., Kurek D., Bazhenov V.V., Hunoldt S., Mertig M., Vyalikh D.V., Molodtsov S.L., Kummer K., Worch H., Smetacek V. & Collins M.J. (2010). Mineralization of the meter-long biosilica structures of glass sponges is templated on hydroxylated collagen. *Nature Chem* 2, 1084-1088.

Harcet M., Roller M., Cetkovic H., Perina D., Wiens M., Müller W.E.G. & Vlahovicek K. (2010). Demosponge EST sequencing reveals a complex genetic toolkit of the simplest metazoans. *Mol Biol Evol*, 27, 2747-56

Iler K.K. (1979). The Chemistry of Silica. Wiley & Sons, New York.

Imsiecke G., Steffen R., Custodio M., Borojevic R. & Müller W.E.G. (1995). Formation of spicules by sclerocytes from the freshwater sponge Ephydatia muelleri in short-term cultures in vitro. *In Vitro Cell Dev Biol* 31, 528-535.

Krasko A., Batel R., Schröder H.C., Müller I.M. & Müller W.E.G. (2000). Expression of silicatein and collagen genes in the marine sponge *Suberites domuncula* is controlled by silicate and myotrophin. *Eur J Biochem* 267, 4878-4887.

Kröger N., Deutzmann R. & Sumper M. (1999). Polycationic peptides from diatom biosilica that direct silica nanosphere formation. *Science* 286, 1129–32.

Kröger N., Lorenz S., Brunner E. & Sumper M. (2002). Self-assembly of highly phosphorylated silaffins and their function in biosilica morphogenesis. *Science* 298,, 584–6.

Morse D.E. (2000). Silicon biotechnology: Proteins, genes and molecular mechanisms controlling biosilica nanofabrication offer new routes to polysiloxane synthesis. In *Organosilicon Chemistry IV: from Molecules to Materials* (Auner N, Weis J, eds), pp. 5-16. Wiley-VCH, New York.

Mort J.S. (2002). Cathepsin-L. In: Barrett AJ, Rawlings ND, Woessner JF, editors. Handbook of proteolytic enzymes. *Amsterdam: Academic Press* p. 617–24.

Müller W.E.G., Krasko A., Le Pennec G., Steffen R., Wiens M., Ammar M.S., Müller I.M. & Schröder H.C. (2003b). Molecular mechanism of spicule formation in the demosponge *Suberites domuncula*: silicatein–collagen–myotrophin. *Progr Mol Subcell Biol* 33, 195–221.

Müller W.E.G., Rothenberger M., Boreiko A., Tremel W., Reiber A. & Schröder H.C. (2005a). Formation of siliceous spicules in the marine demosponge *Suberites domuncula. Cell Tissue Res* 321, 285–97.

Müller W.E.G. (2006a). The stem cell concept in sponges (Porifera): metazoan traits. *Semin Cell Dev Biol* 17, 481-491.

Müller W.E.G., Belikov S.I., Tremel W., Perry C.C., Gieskes W.W.C., Boreiko A. & Schröder H.C. (2006b). Siliceous spicules in marine demosponges (example *Suberites domuncula*). *Micron* 37, 107–20.

Müller W.E.G., Boreiko A., Schloßmacher U., Wang X.H., Tahir M.N., Tremel W., Brandt D., Kaandorp J.A. & Schröder H.C. (2007a). Fractal-related assembly of the axial filament in the demosponge *Suberites domuncula*: relevance to biomineralization and the formation of biogenic silica. *Biomaterials* 28, 4501-4511.

Müller W.E.G., Wang X., Belikov S.I., Tremel W., Schlossmacher U., Natoli A., Brandt D., Boreiko A., Tahir M.N., Müller I.M. & Schröder H.C. (2007b). Formation of siliceous spicules in demosponges: example *Suberites domuncula*. In: Bäuerlein E, editor. Handbook of biomineralization. Vol. 1. The biology of biominerals structure formation. Weinheim: *Wiley-VCH* p. 59–82.

Müller W.E.G., Jochum K., Stoll B. & Wang X.H. (2008a). Formation of giant spicule from quartz glass by the deep sea sponge Monorhaphis. *Chem Mater* 20, 4703-4711.

Müller W.E.G., Schloßmacher U., Wang X.H., Boreiko A., Brandt D., Wolf S.E., Tremel W. & Schröder H.C. (2008g). Poly(silicate)-metabolizing silicatein in siliceous spicules and silicasomes of demosponges comprises dual enzymatic activities (silica-polymerase and silica-esterase). *FEBS J* 275, 362–370.

Müller W.E.G., Wang X.H., Cui F.Z., Jochum K.P., Tremel W., Bill J., Schröder H.C., Natalio F., Schloßmacher U. & Wiens M. (2009b). Sponge spicules as blueprints for the biofabrication of inorganic-organic composites and biomaterials. *Appl Microbiol Biotechnol* 83, 397-413.

Murr M.M. & Morse D.E. (2005). Fractal intermediates in the self-assembly of silicatein filaments. *Proc Natl Acad Sci USA* 102, 11657-11662.

Osinga R., Tramper J. & Wijffels R.H. (1999). Cultivation of marine sponges. *Mar Biotechnol* 1, 509-532.

Perry C.C. (2003). Silicification: the process by which organisms capture and mineralize silica. *Rev Mineralog. Geochem* 54, 291-327

Quian F., Bajkowski A.S., Steiner D.F., Chan S.J. & Frankfater A. (1989). Expression of five cathepsins in murine melanomas of varying metastatic potential and normal tissues. *Cancer Res* 49, 4870–5.

Schloßmacher U., Wiens M., Schröder H.C., Wang X.H., Jochum K.P. & Müller W.E.G. (2011). Silintaphin-1: Interaction with silicatein during structure guiding biosilica formation. *FEBS J* 278, 1145-1155.

Schröder H.C., Perović-Ottstadt S., Rothenberger M., Wiens M., Schwertner H., Batel R., Korzhev M., Müller I.M. & Müller W.E.G. (2004). Silica transport in the demosponge *Suberites domuncula*: fluorescence emission analysis using the PDMPO probe and cloning of a potential transporter. *Biochem J* 381, 665-673.

Schröder H.C., Boreiko A., Korzhev M., Tahir M.N., Tremel W., Eckert C., Ushijima H., Müller I.M. & Müller W.E.G. (2006). Co-Expression and functional interaction of silicatein with galectin: matrix-guided formation of siliceous spicules in the marine demosponge *Suberites domuncula*. *J Biol Chem* 281, 12001–12009.

Schröder H.C., Brandt D., Schloßmacher U., Wang X., Tahir M.N., Tremel W., Belikov S.I. & Müller W.E.G. (2007a). Enzymatic production of biosilica-glass using enzymes from sponges: Basic aspects and application in nanobiotechnology (material sciences and medicine). *Naturwissenschaften* 94, 39-359.

Schröder H.C., Wiens M., Schloßmacher U., Brandt D. & Müller W.E.G. (2010). Silicatein-mediated polycondensation of orthosilicic acid: Modeling of catalytic mechanism involving ring formation. *Silicon*; DOI: 10.1007/s12633-010-9057-4

Tahir M.N., Eberhardt M., Therese H.A., Kolb U., Theato P., Müller W.E.G., Schröder H.C. & Tremel W. (2006). From single molecules to nanoscopically structured functional materials: Au nanocrystal growth on TiO2 nanowires controlled by surface bound silicatein. *Angew Chem* Int Edit 45, 4803–9.

Uriz M.J., Turon X., Becerro M.A. & Agell G. (2003). Siliceous spicules and skeletons frameworks in sponges: origin, diversity, ultrastructural patterns, and biological functions. *Microsc Res Tech* 62, 279-299.

Wiens M., Bausen M., Natalio F., Link T., Schlossmacher U. & Müller W.E.G. (2009). The role of the silicatein-a interactor silintaphin-1 in biomimetic biomineralization. *Biomaterials* 30, 1648-1656.

Zhou Y., Shimizu K., Cha J.N., Stucky G.D. & Morse D.E. (1999). Efficient catalysis of polysiloxane synthesis by silicatein α requires specific hydroxy and imidazole functionalities. *Angew Chem Int Ed Engl* 38, 780–782.

List of figures

Publications

Müller W.E.G., Boreiko A., Schloßmacher U., Wang X.H., Tahir M.N., Tremel W., Brandt D., Kaandorp J.A. & Schröder H.C. (2007a). Fractal-related assembly of the axial filament in the demosponge *Suberites domuncula*: relevance to biomineralization and the formation of biogenic silica. *Biomaterials* 28, 4501-4511.

Schröder H.C., Natalio F., Shukoor I., Tremel W., Schloßmacher U., Wang X.H. & Müller W.E.G. (2007b). Apposition of silica lamellae during growth of spicules in the demosponge *Suberites domuncula*: biological/biochemical studies and chemical/biomimetical confirmation. *J Struct Biol* 159, 325-334.

Müller W.E.G., Boreiko A, Schloßmacher U, Wang XH, Eckert C, Kropf K, Li J & Schröder HC (2008b). Identification of a silicatein(-related) protease in the giant spicules of the deep-sea hexactinellid Monorhaphis chuni. *J Exp Biol* 211, 300-309.

Müller W.E.G., Schloßmacher U., Wang X.H., Boreiko A., Brandt D., Wolf S.E., Tremel W. & Schröder H.C. (2008g). Poly(silicate)-metabolizing silicatein in siliceous spicules and silicasomes of demosponges comprises dual enzymatic activities (silica-polymerase and silica-esterase). *FEBS J* 275, 362–370.

Wang X.H., Boreiko A., Schloßmacher U., Brandt D., Schröder H.C., Li J., Kaandorp J.A., Götz H., Duschner H. & Müller W.E.G. (2008c). Axial growth of hexactinellid spicules: formation of cone-like structural units in the giant basal spicules of the hexactinellid *Monorhaphis. J Struct Biol* 164, 270–280.

Wiens M., Bausen M., Natalio F., Link T., Schlossmacher U. & Müller W.E.G. (2009b). The role of the silicatein-α interactor silintaphin-1 in biomimetic biomineralization. *Biomaterials*. 30, 1648-56

Wolf S.E., Schloßmacher U., Pietuch A., Mathiasch B., Schröder H.C., Müller W.E.G & Tremel W. (2010). Formation of silicones mediated by the sponge enzyme silicatein-α. *Dalton Trans* 39, 9245–9249.

Müller W.E.G., Wang X.H., Wiens M., Schloßmacher U., Jochum K.P. & Schröder H.C. (2011g). Hardening of bio-silica in sponge spicules involves an aging process after its enzymatic polycondensation: Evidence for an aquaporin-mediated water absorption. *Biochim. Biophys. Acta [General Subjects]* 1810, 713–726.

Schloßmacher U., Wiens M., Schröder H.C., Wang X.H., Jochum K.P. & Müller W.E.G. (2011). Silintaphin-1: Interaction with silicatein during structure guiding biosilica formation. *FEBS J* 278, 1145-1155.

Wang X.H., Wiens M., Schröder H.C., Schloßmacher U., Pisignano D., Jochum K.P. & Müller W.E.G. (2011). Evagination of cells controls bio-silica formation and maturation during spicule formation in sponges. *PLoS ONE* 6, e20523.

Schröder H.C., Wang X., Manfrin A., Yu S.H., Grebenjuk V.A., Korzhev M., Wiens M., Schlossmacher U. & Müller W.E.G. (2012). Silicatein: acquisition of structure-guiding and structure-forming properties during maturation from the pro-silicatein to the silicatein form; *J Biol Chem* DOI: 10.1074/jbc.M112.351486

Wang X, Schloßmacher U, Wiens M, Batel R, Schröder HC, Müller WE (2012). Silicateins, silicatein interactors and cellular interplay in sponge skeletogenesis: formation of glass fiber-like spicules. *FEBS J*. 279,1721-36